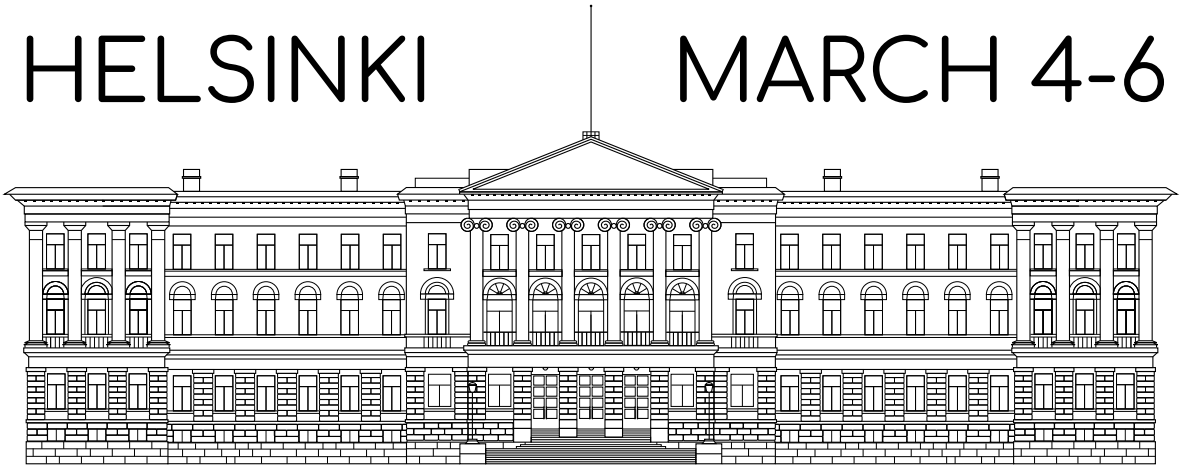


HELSINKI

MARCH 4-6



PHYSICS DAYS 2024

CONFERENCE ABSTRACTS

Table of contents

Abidi, Kameyab Raza: Two-dimensional metals are nanoscale amoeba	1
Aden, Philson-Amanda: Air purifiers as collectors of aerosol particles containing radioactive substances in radiation hazard situations	2
Aikebaier, Faluke: Machine learning the Kondo entanglement cloud from local measurements	3
Amoroso, Pejk: Point Defects in Ga-doped Ge	4
Ansas, Lotta: Determining the swimming dynamics of a mesoscale living organism	5
Antão, Tiago: Designing frustrated moiré order with twisted van der Waals multiferroics	6
Arjas, Kristian: Multimode Lasing in Supercell Plasmonic Nanoparticle Arrays	7
Ashraf, Aqsa: Development of Medium Energy Ion Scattering Technique	8
Asvestari, Eleanna: Quantifying modelling limitations in reconstructing the magnetic field of the solar corona	9
Auranen, Kalle: Probing triaxiality beyond the proton drip line: Spectroscopy of ^{147}Tm	10
Baruah, Riya: Thermal control of qubits using effective temperatures	11
Björkman, Isak: Two-photon Landau-Zener-Stückelberg-Majorana effect	12
Björn, Vesa: Mercury regolith modeling using MESSENGER spectrophotometry	13
Byggmästar, Jesper: Machine-learned interatomic potentials for complex materials	14
Campbell, Christopher: Nonequilibrium many-body dynamics in supersymmetric quenching	15
Chalangari, Fartash: Electronic Transport in Quantum-Chaotic Nanostructures	16
Chawla, Prateek: Using variational quantum algorithms and tensor network methods to solve the quantum Heisenberg model	17
Chen, Zhehao: Microstructure and phase formation in epitaxial thin Ni-Al films	18
Dahlberg, Aron: Enhancing light outcoupling from TADF thin-films with metallic nanostructures.	19
Danneaux, Gauthier: Nuclear octupole shapes in actinides with Fayans functional	20
De Castro Portugal, Pedro Vinicius: Heat pulses in electron quantum optics	21
Depellette, Joe: Strong actuation and nonlinear response of mass loaded membranes	22
Eklund, Kim: Pyroelectric Effect in Ferroelectric Perovskites Studied with Density Functional Theory .	23
Enkovaara, Jussi: Enabling km-scale coupled climate simulations on GPUs	24
Eyvazi Badelbo, Sioneh: Amorphous silicon metasurface for lasing with tunable directionality	25
Fakhrai Mofrad, Nima: Navigating Fusion Reactor Challenges: Correlations Between Surface Temperature, Plasma Particle Impact Angle and Erosion	26
Fellman, Aslak: Machine-learning interatomic potentials for FCC high-entropy alloys	27
Fernández Bouvier, Tomás: Molecular dynamics insights on the molecular P implantation for scabable spin-qubit arrays	28
Frei Nadarajah, Kristiana: Analysis of Microwave Resonators in High Magnetic Fields	29
Fumega, Adolfo: Moiré-driven multiferroic order in twisted Chromium trihalides	30

Gambino, Davide: Computational investigation of radiation damage in high-temperature superconductors for nuclear fusion applications	31
Geng, Zhuoran: Piezoelectrically Mediated Acoustic Phonon Heat Transfer Across a Vacuum Gap	32
Giombi, Lorenzo: General relativistic bubble growth in cosmological phase transitions	33
Halkoaho, Johannes: Quantifying the calcification of abdominal aorta with deep learning	34
Hamedani, Ali: Developing a machine learning interatomic potential to study radiation-induced damage in 3C-SiC	35
He, Ru: Ultrahigh stability of oxygen FCC stacking sublattice in Ga ₂ O ₃	36
Heikkinen, Matti: Espoo goes quantum, the high school course on quantum computing	37
Herbst, Matthew: Detecting Gravity at the Milligram Scale Using Optomechanics	38
Hippeläinen, Antti: Improved holographic analysis of the proton's structure	39
Holm, Sebastian: Manipulating the charger ion distribution towards fixed properties	40
Hossain, Akbar: Laser assisted sputter ion source-most recent results	41
Huang, Xin: Atomically sharp lateral heterostructures of VSe ₂ —NbSe ₂	42
Häkkinen, Jenni: Exploring the gravitational wave power spectrum from first-order phase transitions ...	43
Ikäheimo, Atso: Density dependence of quantised vortex tension in 4He	44
Immonen, Antti: Wearable temperature distribution sensing platform	45
Jantunen, Ville: Multiscale modeling of irradiation damage evolution for quantum technology	46
Jaries, Arthur: HIBISCUS: A new ion beam cooler-buncher for high-precision experiments with exotic radioactive ions at NUSTAR/FAIR	47
Jaries, Arthur: Recent mass measurements of neutron-rich rare-earth nuclides with JYFLTRAP at IGISOL for the astrophysical r-process	48
Jin, Ruoyan: Developing a general-purpose machine learning interatomic potential for Ge	49
Johansson, Mikael: Non-computing quantum computing	50
Jouttijärvi, Sami: Integrating solar energy to the Finnish power system	51
Juttila, Henri: Improving the detection limit in lung counting with a highly segmented HPGe detector ...	52
Kalikka, Janne: Modelling the structure of amorphous Al ₂ O ₃ under stress	53
Kallio, Antti-Jussi: New method to characterize thin film chemistry	54
Kalliokoski, Matti: Particle Physics with Machine Vision	55
Kamppinen, Aleksii: Computational perovskite solar cell model including optics, electrics and heat	56
Kansanen, Kalle: Photon emission statistics of driven microwave cavities	57
Karttunen, Lauri: Performance evaluation for solar panels in Nordic conditions	58
Karttunen, Sasu: PALM-SLUrb: a single-layer urban surface model for micro to mesoscale atmospheric boundary layer studies	59
Kauppinen, Elina: Calculations about the double-beta decay of ¹⁰⁴ Ru	60
Kauppinen, Jyrki: A New Global Thermometer	61
Ketolainen, Tomi: Electronic structure and electrical conductivity of Ge ₂ Sb ₂ Te ₅ heterostructures with different layer orderings	62

Kivelä, Feliks: Quantum simulation of the pseudo-Hermitian Landau–Zener–Stückelberg–Majorana effect	63
Koikkalainen, Venla: Vortices in the magnetospheric transition region of a global hybrid-Vlasov simulation	64
Kokkonen, Henna: Properties of the new alpha-decaying isotope ^{190}At	65
Korepanova, Nadezda: Comparison of Interatomic Potentials for Silicon Applied to Radiation Damage Studies	66
Korkiamäki, Tatu: Coherent thermal transport control via pillar-based phononic crystals	67
Korkos, Spyridon: Structure formation in miscible and immiscible thin bimetallic films synthesized by temporally modulated vapor fluxes	68
Kornienko, Vladimir: Spurious reflections in target detection with entangled photons	69
Koskinen, Pekka: MOOCs for Versatile Physics Education	70
Kotipalo, Leo: Physics-motivated Cell-octree Adaptive Mesh Refinement in the Vlasiator 5.3 Global Hybrid-Vlasov Code	71
Kporha, Faith: Sputtering of Deuterium Supersaturated tungsten surfaces: A Molecular Dynamics Simulation Approach	72
Krejci, Ondrej: High-throughput catalyst screening for CO ₂ to methanol conversion with machine-learned force-fields	73
Kuldeep, Kuldeep: Proximity induced superconductivity in few-layer WTe ₂ Josephson junction using normal Palladium contacts	74
Kurki, Lauri: Automated Structure Discovery for Scanning Tunnelling Microscopy	75
Kuzmanović, Marko: High-fidelity robust qubit control by phase-modulated pulses	76
Lamponen, Eeli: Superconductivity in flat band systems with resonating valence bond pairing	77
Lauri, Katja Anniina: Attitudes towards Physics among Physics Minor Students	78
Lehto, Emma: Human-in-the-loop applications in Bayesian optimization for materials science	79
Leino, Alekski: Modeling the effects of high energy ion impacts in diamond	80
Leino, Vesa-Matti: Segmentation of trabecular bone in X-ray microtomography using a workflow of elementary image processing methods	81
Leppälä, Ari: Radiative-transfer coherent-backscattering modelling for photometric and polarimetric phase curves of Galilean satellites	82
Lindén, Tomas: I'd like to build and operate a fusion power plant - who will license it?	83
Lindén, Tomas: ALICE- and CMS-experiments disk storage upgrade for LHC Run 3	84
Liski, Anna: Textured grain boundaries in WMoTaNbV high entropy alloy	85
Lopez-Cazalilla, Alvaro: Mechanisms of bubble growth and blistering on metals exposed to hydrogen ..	86
Malykhina, Tetiana: A modified version of the MDRANGE software for calculations in nuclear material physics	87
Mannfors, Emma: Cloud evolution in the high-energy molecular ring Lambda Orionis	88
Mikkonen, Antti: Towards a joint retrieval of aerosols and CO ₂ from space-based hyperspectral imager data	89
Milieva, Anna: Validation of the CMS Precision Proton Spectrometer data using exclusive dilepton events	90

Minkkinen, Tiina: Detecting a gravitational wave background from early universe phase transitions with LISA	91
Molander, Andreas: The new ALICE Fast Interaction Trigger in LHC Run 3	92
Moskalenko, Ilya: Tunable coupler for qutrit-based quantum computing	93
Mukhanova, Ekaterina: Generation and analysis of squeezed states in Josephson Parametric Amplifier ..	94
Myrov, Vladislav: Personalized large-scale modeling of critical synchronization dynamics	95
Nadji Adjim, Franck Louba: Defect generation in single-layer graphene upon sputter deposition of thin metal films	96
Nagy, Rebekka: Micro-Alphatross: Towards High-intensity Negative Helium Beam	97
Niedermeier, Marcel: Computing Chern numbers in two-band models with quantum circuits	98
Nieminen, Jouko: Atomistic modeling of a superconductor-transition metal dichalcogenide-superconductor Josephson junction	99
Nizamov, Rustem: A Novel Method for Quantitative Assessment of Photovoltaic Material Degradation via Analysis of Color Alteration	100
Nuñez, Rafael: Calculating path-dependent electronic stopping in silicon crystals using plane-wave pseudopotentials.	101
Ojala, Aliisa: Computational study of cresol autoxidation: Initial steps in secondary organic aerosol formation	102
Oljemark, Fredrik: Recent Pomeron and Odderon Physics with TOTEM	103
Panero, Marco: Theoretical approach to inclusive semileptonic decays of heavy mesons through lattice QCD	104
Peltokangas, Kenneth: Ilmastomuutoksen luonnontieteellisten perusteiden opettaminen osana Ilmastoasiatuntijan erikoistumiskoulutusta	105
Penttilä, Reko: Mean-field and dynamical mean-field theory studies on flat band superconductivity from two to three dimensions	106
Pereira, Elizabeth: Non-Hermitian topological modes from local loss engineering in photonic arrays ..	107
Poskela, Aapo: Solar Energy and Recycling: A Rapidly Approaching Challenge	108
Prozheev, Igor: Defects in aluminum-rich silicon-doped AlGaN	109
Pyykkönen, Ville: All-optical switching at the two-photon limit with interference-localized states	110
Raasakka, Matti: Comparing resource requirements of noisy quantum simulation algorithms for the Tavis-Cummings model	111
Raju, Ramesh: GLA enhances transmittance and electrical conductivity of ALD Al-doped ZnO for thermoelectric and TCO applications	112
Rantanen, Milla-Maarit: Diamond timing detectors of the CMS Precision Proton Spectrometer	113
Rathnathilaka, Achini: Nanoscale Roughness Characterization of LPCVD-Fabricated SiN Thin Films on SiliconWafers Using AFM	114
Rej, Ewa: Towards gravity detection using optomechanics with mass-loaded resonators	115
Ruohotie, Julia: Intermittency in interplanetary coronal mass ejections observed by Parker Solar Probe and Solar Orbiter	116
Ruotsalainen, Jouni: Double-beta decay Q-value measurements with the JYFLTRAP Penning trap	117
Sihvola, Ari: Peculiarities in scattering and extinction of dielectrically active particles	118

Soljento, Juska: Statistical Study on Turbulent Energy Transfer in Coronal Mass Ejection Sheaths at 1 AU	119
Stråka, Emil: Computational modelling of magnetic colloidal particle self-organization and pattern formation at multiple length scales	120
Swaminathan, Koushik: Coexistence of ergodic and non-ergodic behaviour in one-dimensional toy model of a flat-band superconductor	121
Tevio, Mirja: Evolution of structure functions at NLO without PDFs	122
Tiainen, Ville: Ultra-fast photochemistry in the strong light-matter coupling regime	123
Tinus, Tuomas: Poisoning of a thin-film ALD TiO ₂ photocatalyst by thermal ion diffusion from microscopy glass substrate	124
Toktaganova, Marzhan: Influence of an External Static Magnetic Field on the Dynamics of Vacuum Arc Initiation	125
Turkki, Valtteri: Scanning Droplet Adhesion Microscope for accurate surface characterization	126
Uusikylä, Eetu: Nuclear lifetime analysis using the Advanced Plunger-Particle detector Array device (APPA plunger)	127
Vaaranta, Antti: Heat transport in a superconducting qubit-resonator chain with weak coupling to two thermal baths	128
Valdez Garcia, Joaquin: Challenges and opportunities of using cellulose substrates in photovoltaics ...	129
Vancaeynest, Aurélie: CodeRefinery - supporting your research software development journey	130
Vecsei, PascalMarc: Quantum Phase Transitions in Fermionic Chains with a Lee-Yang Method	131
Veteli, Peitsa: Curiosity over the Lines – Open Data in Interdisciplinary Learning	132
Veteläinen, Onni: Modeling the fragmentation dynamics and valence photoelectron spectra of aminobenzoic acid	133
Vuori, Mikko: Refractive index of Mercury analog particles from light scattering measurements	134
Vuoriheimo, Tomi: Defect stabilization effect in fusion reactor plasma-facing materials	135
Väänänen, Mika: Design and construction of a modular 3D scanner for semiconductor devices	136
Wagner, Andreas: Flux Rope Extraction Scheme for Solar Magnetic Field Simulations	137
Wang, Shubo: Insights into the mechanism of nano Ni ₃ TeO ₆ calcination via in situ synchrotron X-ray diffraction	138
Yildirim, Pelin: Effective Interactions and Density of States in Plasmonic Bose-Einstein Condensation	139
Ylinen, Lauri: Quantum computing algorithm for an inverse travel time problem	140
Yrjänheikki, Sami: Dimuon production in neutrino-nucleus collisions - the SIDIS approach	141
Zevenhoven, Koos: Focused ultrasound in combined magnetic resonance imaging and magnetoencephalography system	142
Zhang, Yuhao: Machine Learning Optimization of Thermally Activated Nylon Actuator Coils	143
Zhelezova, Iuliia: Vacancy defects in Si doped β -(Al,Ga) ₂ O ₃	144
Åhlgren, Harriet: Two-dimensional noble gas clusters in a graphene sandwich	145
Önnerstad, Anna: Latest results on multiplicity-dependent flow, testing the lower limit of flow in small systems with ALICE	146

Two-dimensional metals are nanoscale amoeba

Kameyab Raza Abidi¹, Pekka Koskinen¹

¹NanoScience Center Department of Physics, University of Jyväskylä, 40014 Jyväskylä, Finland

Contact: kameyab.r.abidi@jyu.fi

Due to their delocalized electronic wave functions, metals inherently display isotropic bonding which makes their existence as two-dimensional (2D) nanostructures scarce [1]. Despite this property, there have been successful experimental realizations of atomically thin segments of certain elemental metals within a 2D covalent framework [2]. Yet, this progress has not been systematically reported for all metals, implying that the intrinsic nature of metals concerning the underlying mechanisms that can confer stability in two dimensions remains elusive. The precise mechanisms responsible for stabilizing metals in 2D configurations continue to be a subject of intrigue. A profound understanding at the atomistic level is imperative, and this can be effectively achieved through advanced computational methodologies [3-5].

To complement the *2D metals stability* research, we delve deep into the inherent stability criteria of 45 metals, in six distinct lattices—hexagonal, square, honeycomb, and their buckled analogs. Using density-functional theory, we assessed the dynamical stability of these free-standing metallic monolayers. Our findings indicate that the stability of these structures is more influenced by the available area per atom than merely the minimum energy. Among our observations, 129 stable lattices have been identified, frequently at densities not corresponding to the energy minimum or zero stress. Contrary to conventional energy minimum, we introduce a novel perspective on the stability of 2D metals. We suggest that 2D metals are more akin to nanoscale amoebas—adapting their conformation to the size and shape of the stabilizing pore—rather than being intrinsic structures with fixed lattice constants at zero stress. We anticipate that this approach will pave the way for experimental methodologies aiming to synthesize larger and more robust 2D metal samples, with potential applications in electronics, plasmonics, optics, and catalysis.

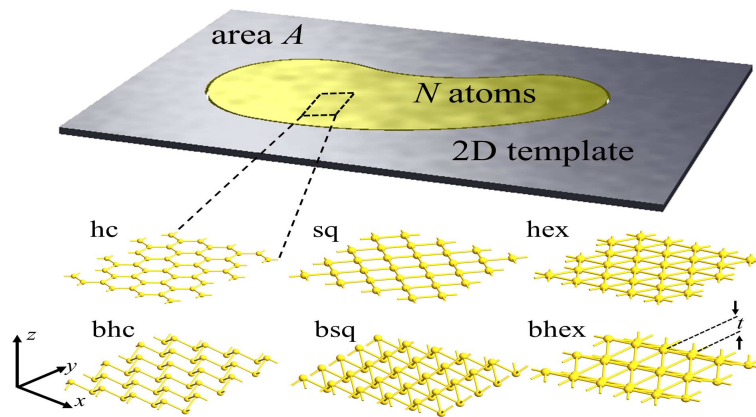


Figure 1: 2D metals' stability framework: A metal patch with N atoms stabilizes on a 2D template pore of area A . Lattice structures like honeycomb (hc), square (sq), and hexagonal (hex), with their buckled variants (bhc, bsq, bhex) are explored. Buckled layer thickness is t

References: [1] T. Wang, *et al.*, *Materials Today Advances* **8**, 100092 (2020); [2] H. Q. Ta, *et al.*, *Advanced Science* **8**, 2100619 (2021); [3] J. Nevalaita and P. Koskinen, *Physical Review B* **97**, 035411 (2018); [4] J. Nevalaita and P. Koskinen, *Nanoscale* **11**, 22019 (2019); [5] S. Ono, *Physical Review B* **102**, 165424 (2020).

Air purifiers as collectors of aerosol particles containing radioactive substances in radiation hazard situations

Philson-Amanda Aden¹

Supervisors: Kari Peräjärvi², and Ville Bogdanoff¹

¹*Department of Physics, University of Jyväskylä, Jyväskylä, Finland,*

²*Radiation and Nuclear Safety Authority (STUK), Vantaa, Finland*

Corresponding author: philson-amanda.pa.aden@jyu.fi

Sheltering indoors is a protective measure performed during radiation hazard situations to decrease the received internal and external dose while a radioactive plume passes through an area [1]. Despite shutting off and sealing all ventilation while sheltering indoors, radioactive substances will still seep into the indoor air [2]. In this master's thesis, portable, commercially available air purifiers were studied as collectors of aerosol particles containing radioactive substances.

In the literature review on the properties of aerosol particles containing radioactive substances produced during radiation hazard situations, the dominant particle size distribution was found to be the accumulation mode, i.e., particles with a diameter of 0.1–1.0 μm [3]. In the measurement campaign, naturally occurring noble gas radon (^{222}Rn) and particulate radon progeny were used to simulate radioactive substances carried into indoor air during a radiation hazard situation. The attached fraction of progeny is associated with an AMAD of 0.25 μm and the unattached fraction with an AMAD of 0.03 μm [4], categorizing them as accumulation mode particles and ultrafine particles, respectively.

In the measurement campaign, the ability to collect radon and radon progeny of two air purifiers, Electrolux EAP300 employing a HEPA filter and Elixair E400 electrostatic purifier, was studied. The activity concentration of the attached radon progeny decreased by an order of magnitude in 100 minutes with the Electrolux EAP300 and in 160 minutes with the Elixair E400, showing that the air purifiers collected these aerosol particles. The air purifiers didn't collect the unattached radon progeny or radon gas. Based on the results, the studied air purifiers would effectively collect accumulation mode aerosol particles containing radioactive substances while sheltering indoors, thus decreasing the effective internal inhaled dose from these particles.

[1] Stuklex, *VAL 1 Suojelutoimet säteilyvaaratilanteessa* (2022).

[2] K. Aakko, S. Salomaa, in *Säteily ympäristössä*, ed. by R. Pöllänen. Säteily- ja ydinturvallisuus, vol 2 (Säteilyturvakeskus, Helsinki, 2003), p. 351.

[3] P. von Schoenberg, P. Tunved, H. Grahn, A. Wiedensohler, R. Krejci, N. Brännström, *Atmos. Chem. Phys.* **21**, 5173 (2021).

[4] F. Paquet, M. R. Bailey, R. W. Leggett, J. L. Lipsztein, J. W. Marsh, T. Fell, S. Tj, D. Noßke, K. F. Eckerman, V. Berkovski, E. Blanchardon, D. Gregoratto, J. Harrison, *Ann. ICRP* **46**, 1 (2017).

Machine learning the Kondo entanglement cloud from local measurements

Faluke Aikebaier^{1,2,3}, Teemu Ojanen^{1,2}, and Jose L. Lado³

¹Computational Physics Laboratory, Physics Unit, Faculty of Engineering and Natural Sciences, Tampere University, FI-33014 Tampere, Finland

²Helsinki Institute of Physics P.O. Box 64, FI-00014, Finland

³ Department of Applied Physics, Aalto University, 00076, Espoo, Finland

faluke.aikebaier@gmail.com

A quantum coherent screening cloud around a magnetic impurity in metallic systems is the hallmark of the antiferromagnetic Kondo effect. Despite the central role of the Kondo effect in quantum materials, the structure of quantum correlations of the screening cloud has defied direct observations. In this work, we introduce a machine-learning algorithm that allows to spatially map the entangled electronic modes in the vicinity of the impurity site from experimentally accessible data. We demonstrate that local correlators allow reconstructing the local many-body correlation entropy in real-space in a double Kondo system with overlapping entanglement clouds. Our machine learning methodology allows bypassing the typical requirement of measuring long-range non-local correlators with conventional methods. We show that our machine learning algorithm is transferable between different Kondo system sizes, and we show its robustness in the presence of noisy correlators. Our work establishes the potential machine learning methods to map many-body entanglement from real-space measurements.

Point Defects in Ga-doped

P. Amoroso¹, W. Särs¹, J. Slotte^{1,2}, F. Tuomisto¹, A. Subramanian³, R.R.Sumathi³ and K. Mizohata¹

¹*Department of Physics, University of Helsinki, Helsinki, Finland*

²*Department of Applied Physics, Aalto University, Espoo, Finland*

³*Leibniz-Institut für Kristallzüchtung (IKZ), Berlin, Germany*

Corresponding author: pejk.amoroso@helsinki.fi

Point defects, such as vacancies, play an important role in determining the optoelectronic properties of semiconductor materials. Positron Annihilation Spectroscopy is a unique method for characterizing and quantifying neutrally and negatively charged vacancy-like defects. However, p-type Ge has been researched very little using Positron Annihilation Spectroscopy due to the low sensitivity of the method to positively charged defects.

Here, we studied highly Ga-doped bulk Ge, with the doping concentration ranging from 10^{18} to 10^{20} cm^{-3} . The bulk crystals were grown by the Czochralski method. The samples were irradiated with 6 MeV protons at room temperature with a fluence of 1×10^{14} cm^{-2} and upwards, thus introducing vacancy defects into the lattice. The vacancy defect distribution was studied using Positron Annihilation Lifetime Spectroscopy. The lifetime setup consisted of two collinear detectors with BaF₂-scintillators and quartz-windowed photomultiplier tubes, with a resolution of 282 ps. A conventional ²²Na positron source was used.

The results were unexpected, initially suggesting outward relaxation at the defect, but switching to inward relaxation for the highest-doped samples. These results will be presented in the poster.

Determining the swimming dynamics of a mesoscale living organism

Lotta Ansas, Rafael Ayala Lara, Sharadhi Nagaraja and Matilda Backholm*

Department of Applied Physics, Aalto University, Espoo, Finland

*Corresponding author: matilda.backholm@aalto.fi

Artemia salina larvae are a millimeter-sized species of brine shrimp, this crustacean has adapted to high salinity waters and therefore lives in aquatic environments like inland brackish lakes or lagoons as well as some coastal areas [1]. As a meso-organism it is swimming in the region of intermediate Reynolds number, denoting that both inertial and viscous forces need to be taken into account while studying its locomotion [2]. Despite the high number of organisms living at the intermediate Reynolds number regime, this regime is not yet comprehensively studied, and better knowledge of it could benefit both understanding of these biological organisms and for example design of artificial mesoscale robotics [3].

Solving the Navier-Stokes equations at intermediate Reynolds numbers for organisms with geometrically complex shapes is not feasible. Instead, our research group performs experiments to decipher the physical laws behind mesoscale swimming dynamics. We use the micropipette force sensor [4] to directly measure the propulsive force of *Artemia* in different stages of its life cycle. After acquiring direct force data with *Artemia*, the videos of experiments are analyzed using the open source animal pose estimation software DeepLabCut, in which deep neural networks are trained to recognize selected key points of the *Artemia* body [5]. By combining the time-resolved force data with the DeepLabCut motion tracking data, we can characterize the swimming dynamics of *Artemia* and inspect the relation between velocity of antennas and resulting swimming force. This is important for understanding physics behind biological swimming at mesoscale.

References:

- [1] G. R. Medina, J. Goenaga, F. Hontoria, G. Cohen, F. Amat, *Hydrobiologia*, 2007, **579**, 41-53.
- [2] T. A. Williams, *Biological Bulletin*, 1994, **187**, 164-173.
- [3] D. Klotsa, *Soft Matter*, 2019, **15**, 8946-8950.
- [4] M. Backholm, O. Bäumchen, *Nature Protocols*, 2019, **14**, 2152-2176.
- [5] T. Nath, A. Mathis, C. A. Chen, A. Patel, M. Bethge, M. W. Mathis, *Nature Protocols*, 2019, **14**, 2152–2176.

Designing frustrated moiré order with twisted van der Waals multiferroics

Tiago V. C. Antão¹, Jose L. Lado¹, and Adolfo O. Fumega¹

¹ Department of Applied Physics, Aalto University, 02150 Espoo, Finland

Corresponding author: tiago.anta@aalto.fi

The design of artificial materials with van der Waals heterostructures has dramatically influenced the landscape of quantum materials. In particular, one possibility that has opened new avenues is the control of the relative twist of stacked monolayer materials. This has led to the field of moiré physics. A paradigmatic example of moiré phenomena is that of twisted bilayer graphene, where a specific twist angle has been shown to result in superconductivity and a variety of correlated states. Engineering twisted structures is not restricted to graphene, as for many materials, the possibility of controlling the twist angle in moiré structures is a valuable degree of freedom, useful for tuning different types of correlated quantum phenomena. For instance, twisted magnetic structures have been shown to host artificial multiferroic order [1]. Another recently isolated novel class of monolayer materials, exemplified by NiI₂ [2], showcases this same kind of multiferroic order, characterized by coexisting electric and magnetic order. The emergence of magnetic frustration, as well as non-collinear textures in the spin ground state of this class of materials, enables the possibility of the coexistence and coupling of the two different orders.

Here we show how the frustrated magnetism inherent in non-collinear spin-spiral ground states via twisting enables the emergence of a moiré multiferroic texture. Specifically we consider a twisted van der Waals multiferroic bilayer and use a combination of ab-initio methods and spin Hamiltonian models to determine how the ground state spin configuration is affected by the twist angle, as well as the strength of the coupling between the two layers. These mechanisms, together with the inherent strong magnetoelectric coupling of multiferroic van der Waals materials provides a strategy to control frustrated magnetic order at the moiré length scale [3]. Ultimately, our strategy establishes a material where moiré multiferroic order can be controlled by electric fields which can couple to the material's electric polarization and spin degrees of freedom.

[1] A. O. Fumega, J. L. Lado 2023 *2D Mater.* **10** 025026 (2023)

[2] Q. Song, C.A. Occhialini, E. Ergeçen et al. *Nature* **602**, 601-605 (2022)

[3] T. V. C. Antão, A. O. Fumega, J. L. Lado to appear in 2024

Multimode Lasing in Supercell Plasmonic Nanoparticle Arrays

Rebecca Heilmann¹, Kristian Arjas¹, Tommi K. Hakala² and Päivi Törmä¹

¹ Department of Applied Physics Aalto University School of Science

²Center for Photonics Sciences University of Eastern Finland

Corresponding author: paivi.torma@aalto.fi

In our recent publication [1] we demonstrated multimode lasing in a plasmonic nanoparticle array. The additional modes are enabled by constructing a supercell structure by removing particles from a square lattice. This makes the lattice sensitive to the new supercell period resulting in a more complex band structure and forming new band edges which support lasing. To understand these modes we employ a structure-factor based calculation that is able to predict the band-structure of a periodic structure with a complex unit cell. With these theoretical tools we identify the lasing modes as the 74th Γ - and 106th X -points of the supercell lattice. This work opens new avenues for nanoparticle array design allowing for greater freedom and control. As demonstrated, these structures can host multimode lasing allowing for the design of structures that provide coherent beams of light with multiple well defined wavelengths and directions.

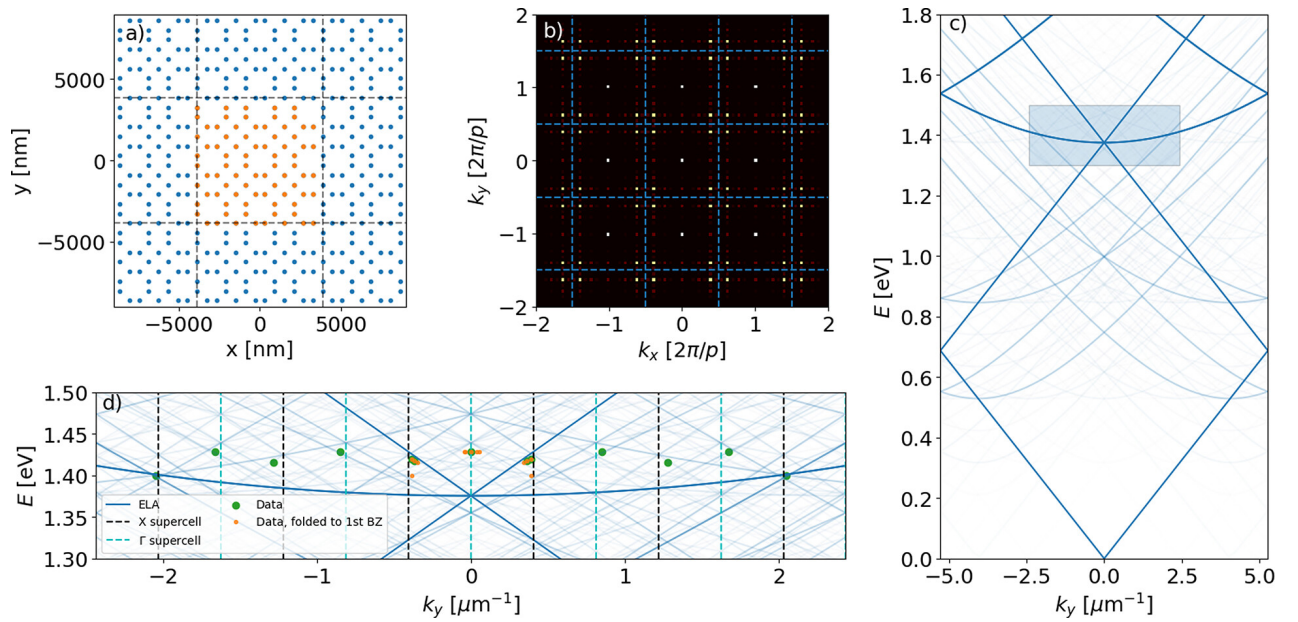


Figure 1: (a) The supercell structure studied. (b) The structure-factor of the system. (c) The calculated band-structure. (d) Close up of the shaded region from (c) with the measured lasing points.

[1] R. Heilmann, ACS Photonics, **10**, 3955-3962 (2023)

Development of Medium Energy Ion Scattering Technique

Aqsa Ashraf¹, Kenichiro Mizohata, Filip Tuomisto, Mikko Ritala

HelsinkiALD, Helsinki Accelerator Laboratory, University of Helsinki, Helsinki, Finland
aqsa.ashraf@helsinki.fi

Materials characterization in fast and reliable way is essential for the development of materials synthesis methods for present day and future applications. Ion beam-based materials characterization methods provide stand-alone solutions based on relatively simple kinematics and cross sections. Medium Energy Ion Scattering Spectroscopy (MEIS) has emerged as a powerful technique for probing surface and near-surface structures with remarkable precision and sensitivity. The evolution of MEIS technique involves innovations in ion beam sources, detectors, and data analysis methods. Medium energy ions offer unique advantages, enabling the investigation of elemental composition, crystallographic orientation, and atomic arrangement of materials. The versatility of MEIS is showcased through its application in diverse research areas, including semiconductor technology, catalysis, and thin film growth.

In this project, a MEIS setup is designed and constructed to the Helsinki Accelerator laboratory, where the 500kV electrostatic accelerator (KIIA) is deployed for the MEIS experiments. Medium energy H and He⁺ ion beams are readily available for the measurements. KIIA equipped with analysis chamber is used to house the detection system for the MEIS. MEIS in energy range 50 – 500 keV has been utilized for deeper materials composition analysis beginning from surface down to a few tens of nm. For practical purposes, when surface contamination is not an issue, a MEIS setup is relatively straightforward to construct into pre-existing medium energy accelerator. A simple electrostatic analyzer provides better than 1 keV energy resolution which combined with a position sensitive 2D-microchannel plate detector (PSD-2D), provides an electrostatic analyzer (ESA) setup with good energy and spatial resolution over wide energy range. [1]

The aim of this research is to gain insights from MEIS studies which will lead us to a deeper understanding of surface interactions, defect structures, and electronic properties, paving the way for tailored material design and optimization.

Keywords: MEIS, Depth Profiling, Elemental Composition, Defect structures

References:

[1] Paolini, F. R., & Theodoridis, G. C. (1967). Charged particle transmission through spherical plate electrostatic analyzers. *Review of Scientific Instruments*, 38(5), 579-588.

Quantifying modelling limitations in reconstructing the magnetic field of the solar corona

E. Asvestari¹, M. Temmer², R. M. Caplan³, J. A. Linker³, S. G. Heinemann¹, R. F. Pinto⁴, C. J. Henney⁵, C. N. Arge⁶, M. J. Owens⁷, M. S. Madjarska^{8,9}, J. Pomoell¹, S. J. Hofmeister^{10,11}, C. Scolini¹², and E. Samara⁶

¹ Department of Physics, University of Helsinki, Finland

² Institute of Physics, University of Graz, Austria

³ Predictive Science Inc., San Diego, USA

⁴ IRAP, Université de Toulouse; UPS-OMP, CNRS; Toulouse, France

⁵ Air Force Research Laboratory, Space Vehicles Directorate, KAFB, NM, USA

⁶ Heliophysics Science Division, NASA Goddard Space Flight Center, USA

⁷ Department of Meteorology, University of Reading, UK

⁸ Max-Planck-Institut für Sonnensystemforschung, Göttingen, Germany

⁹ Space Research and Technology Institute, Bulgarian Academy of Sciences, Sofia, Bulgaria

¹⁰ Columbia Astrophysics Laboratory, Columbia University, New York, USA

¹¹ Leibniz-Institute for Astrophysics Potsdam, Germany

¹² Institute for the Study of Earth, Oceans, and Space, University of New Hampshire, USA

Corresponding author: eleanna.asvestari@helsinki.fi

The solar corona magnetic field consists of two qualitatively distinct types of field lines, closed and open ones. The closed are confined to the corona and can be traced between two opposite polarity foot points in the photosphere. The open ones extend beyond the corona and form the interplanetary magnetic field through which our planet travels. Therefore, knowledge of the coronal magnetic structure is fundamental for space weather research and for understanding our near Earth environment. Due to the physical properties of the solar corona, direct measurements of the strength and structural details of its magnetic field are not possible and can only be determined from model based numerical reconstructions. These employ as inner boundary the photospheric magnetic field strength, inferred from magnetograph measurements. The models used for the coronal magnetic field reconstruction range from empirical to complex state-of-the-art magnetohydrodynamic models. Besides their level of complexity, such models employ different numerical schemes and parametrisations. In this study we explored how the model output is affected by the complexity of the employed model, the selected numerical scheme, the initiation parameters, and the data input. We find that the models considered in this study produce all very comparable open and closed field topologies. Taking the work one step further, we assess how well the modelled areas of open flux on the photosphere agree with coronal holes which are known to be the primary sources of open magnetic field. Due to observational limitations, we selected for this comparison a coronal hole that remained centred within the Earth's field of view for the dates studied and thus most accurately observed. Nevertheless, its area did not compare well with the modelled open magnetic flux area. This work is the result of the collective research by members of the International Space Science Institute (ISSI) team "Magnetic Open Flux And Solar Wind Structuring Of Interplanetary Space".

Probing triaxiality beyond the proton drip line: Spectroscopy of ^{147}Tm

K. Auranen¹, Nuclear Spectroscopy Group¹

¹*Accelerator Laboratory, Department of Physics, University of Jyväskylä, FI-40014 Jyväskylä,*
Corresponding author: kalle.e.k.auranen@jyu.fi

A recoil-decay tagging study of the proton-emitting nucleus ^{147}Tm has been performed in the Accelerator Laboratory of University of Jyväskylä. The ions of interest were selected with the MARA (Mass-Analyzing Recoil Apparatus) vacuum-mode recoil separator, and those were identified based on the observed characteristic proton-emission events taking place at the focal plane spectrometer of MARA. The prompt γ -ray transitions were measured with the JUROGAM3 spectrometer installed at the MARA target position. Two separate proton-emitting states were observed, and the γ -ray transitions feeding these states were studied. The previously proposed level scheme above the $11/2^-$ ($\pi h_{11/2}$) ground state was confirmed, and the level structure was expanded to cover the states above the $5/2^+$ ($\pi d_{5/2}$) isomeric state, which also decays via proton emission. It was found through a comparison to theoretical calculations produced with the nonadiabatic quasiparticle model that the isomeric state is, like the ground state, triaxial in shape, but possibly more deformed than the ground state. Triaxiality here indicates a nuclear shape, which is that of an ellipsoid where all three principal axes are different in length.

[1] K. Auranen *et al.* Phys. Rev. C **108**, L011303 (2023)

Thermal control of qubits using effective temperatures

Riya Baruah,¹ Pedro Portugal,¹ Joachim Wabnig,² and Christian Flindt¹

¹Department of Applied Physics, Aalto University, 00076, Finland

²Nokia Bell labs, Cambridge, CB3 0FA, United Kingdom

Corresponding author: riya.baruah@aalto.fi

Most quantum technologies rely on operating-temperatures in the sub-Kelvin regime, and therefore, control and precise manipulation of the temperature of nano-scale quantum systems are crucial for the advancement of thermal devices. Previously, we have shown that an effective time-dependent temperature can be generated by modulating the frequencies of several quantum harmonic oscillators that mediate the interactions between a thermal reservoir and a quantum system [1]. Here, we adapt this approach to a setup with several qubits that act as the intermediaries between a thermal reservoir and another quantum system, whose temperature we wish to control [2]. The effective time-dependent temperature of the qubits is created by modulating their energy splittings. By exposing the quantum system to the effective temperature of the qubits, the quantum system can be cooled below the temperature of the environment, or its temperature can be modulated periodically.

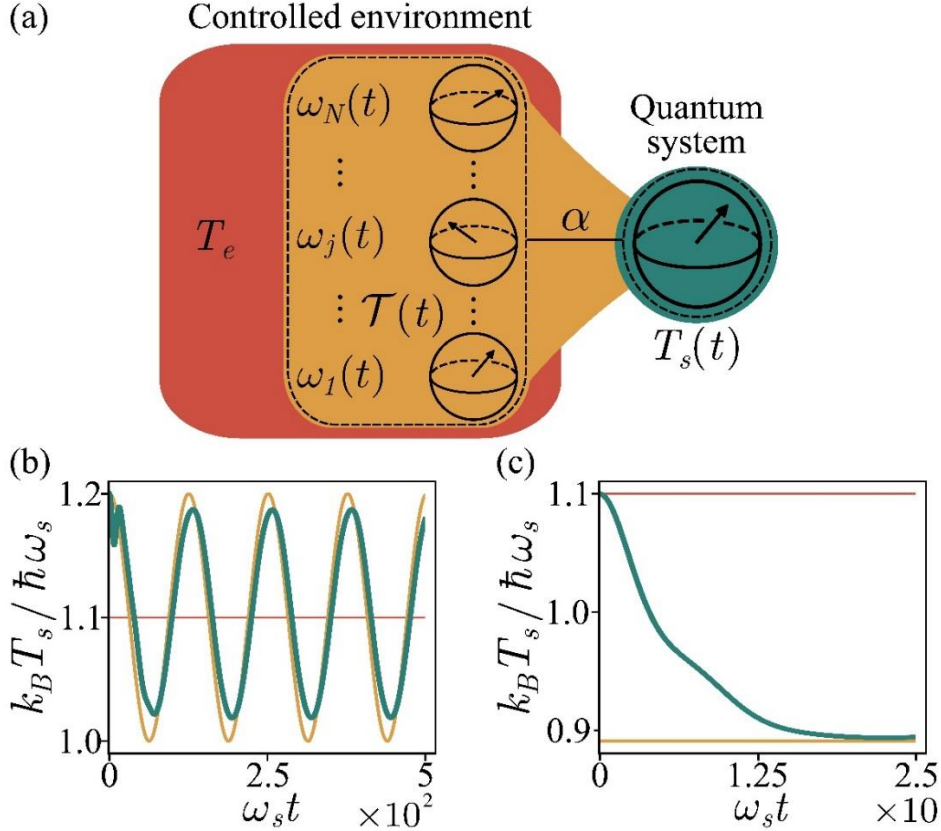


Fig. 1: Effective temperatures. (a) A quantum system (green) is coupled to N qubits (orange) with a coupling strength α , and the qubits are in turn coupled weakly to a thermal reservoir (red) at the constant temperature T_e . We take a qubit with frequency ω_s as the quantum system and show its temperature $T_s(t)$ (green) in response to (b) an effective temperature that varies harmonically in time and (c) an effective temperature below the temperature of the thermal reservoir.

[1] P. Portugal, F. Brange, and C. Flindt, Phys. Rev. Res. **4**, 043112 (2022).

[2] R. Baruah *et al.*, in prep. (2024).

Two-photon Landau-Zener-Stückelberg-Majorana effect

Isak Björkman¹, Marko Kuzmanović², and Gheorghe-Sorin Paraoanu³

¹*Institute Q and QTF Centre of Excellence, Department of Applied Physics, School of Science, Aalto University, FI-00076 Aalto, Finland*

Corresponding author: isak.bjorkman@aalto.fi

In recent decades, a lot of effort has been seen to realize and control a large-scale quantum computer. Among the most promising architectures for such a system is that of superconducting circuits. However, a significant challenge with these qubits is the drifts in system parameters. Therefore, controlling thousands or more qubits - which are needed to perform practical applications - becomes increasingly difficult and various control schemes and workarounds are needed to vanquish such obstacles. One approach to cope with the complexity of the system size is to increase the information held per quantum system by introducing an additional state and thereby reduce the number of qubits. Therefore, in this work, we explore a robust population transfer, from the ground to the second excited state, on the first three levels of a superconducting transmon.

For a transmon, such a transition cannot occur by single photon absorption. However, because of a second-order process, two-photon transitions from the ground state to the second excited state are possible for a drive at the 02-transition frequency. In existing protocols that drive this population transfer, such as the Raman process and (sa)STIRAP, a common problem is the sensitivity to offsets in frequency and amplitude of the drive pulses. Therefore, in search of a method that realizes such a transfer and is robust to some offsets we took inspiration from [1] and approached the problem through a Landau-Zener process.

The Landau-Zener process in this work was a result of modulating the frequency of a one-tone drive around the 02-transition frequency that interchanged the first and third energy levels while avoiding the intermediate level. With this method, the three-level quantum system (approximately) follows the first eigenstate of the Hamiltonian adiabatically to the second excited state. This method showed considerable robustness to both offsets in frequency and amplitude and was eventually tested experimentally on a superconducting transmon. The results showed great agreement with the theory and demonstrates a method that is robust and simple enough to be realized on the majority of control hardware.

[1] Kuzmanović, Marko, et al. "High-fidelity robust qubit control by phase-modulated pulses." arXiv preprint arXiv:2308.13353 (2023).

Mercury regolith modeling using MESSENGER spectrophotometry

V. Björn¹, K. Muinonen¹, A. Penttilä¹, and D. Domingue²

¹ Department of Physics, University of Helsinki, Finland

² Planetary Science Institute, Bel Air, MD, United States

Corresponding author: vesa.bjorn@helsinki.fi

Mercury can be modeled as an atmosphereless Solar System body. Such objects are covered by a regolith which affects how they scatter light. To deduce physical properties of Mercury's regolith, we use spectrophotometry from the MDIS (Mercury Dual Imaging System) instrument of NASA's MESSENGER (MErcury Surface, Space ENvironment, GEochemistry and Ranging) mission. The data comes in eight colors [1] between the wavelengths of 433.2 nm and 996.2 nm, with phase angles from 20 to 130 degrees. There are 37752 data points, of which we use 27618 that are at incidence and emergence angles below 70 degrees.

A theoretical particulate-medium model is used to interpret the observed reflectance. The model includes a shadowing correction that depends on three geometry parameters of the regolith. The first parameter is the packing density, i.e., the ratio of the particles' volume to the total volume. The other two parameters describe the regolith's roughness as a fractional Brownian motion (fBm) surface: the Hurst exponent in the horizontal and the amplitude in the vertical direction.

The numerical implementation of the model includes a set of discrete parameter values [2]. However, using trilinear interpolation, we extend the parameters to have arbitrary values within the range of the discrete values, which are 0.15–0.55 for the packing density, 0.20–0.80 for the Hurst exponent, and 0.00–0.10 for the amplitude (in units of the width of the simulated medium). We optimize the model parameters in least-squares sense using the Nelder–Mead simplex method [3], followed by Markov chain Monte Carlo (MCMC) sampling that uses proposed parameter values drawn from Gaussian distributions. The model parameters are solved for all wavelengths simultaneously, which means that the result is physically consistent. In the present study, the size of the regolith particles follows a uniform distribution between 0.0006 and 0.003, in units of the medium width.

Our preliminary results indicate that Mercury's regolith has a packing density of about 0.51, and an fBm surface with a Hurst exponent of 0.49 and an amplitude of 0.10. Such a regolith is densely packed with moderate horizontal and large height variations. The MCMC solution allows us to predict the spectrophotometry for differing viewing geometries. Future work includes improving the implementation of the model by increasing the range of the parameters and by modifying the size distribution of the regolith particles. The results of our study can be utilized in the BepiColombo mission.

[1] Domingue et al., *Icarus* **257**, 477 (2015)

[2] Wilkman et al., *Planet. Space Sci.* **118**, 250 (2015)

[3] Nelder and Mead, *Comput. J.* **7**(4), 308 (1965)

Machine-learned interatomic potentials for complex materials

J. Byggmästar¹, A. Fellman¹, J. Zhao², K. Nordlund¹, and F. Djurabekova¹

¹ Department of Physics, University of Helsinki, Helsinki, Finland

² Department of Electrical and Electronic Engineering, Southern University of Science and Technology, Shenzhen, China

Corresponding author: jesper.byggmastar@helsinki.fi

Machine-learned (ML) interatomic potentials have become invaluable tools in atomistic materials modelling, enabling nearly quantum-accurate simulations with classical molecular dynamics. However, due to the inherent poor extrapolation of ML for predictions outside the scope of its training data, special care is required when developing ML potentials for complex materials or far-from-equilibrium physics [1]. I will address these aspects and discuss the development of ML potentials for various complex materials, including high-entropy alloys (chemically complex) and gallium oxide (structurally complex), that are general and applicable to simulations of extreme environments such as high-energy irradiation. I will focus on our recent work of simple ML potentials (called tabGAP [2, 3]) that are computationally fast, interpretable, accurate, and especially useful for modelling alloys with many elements. I discuss the development of tabGAPs for iron, tungsten, gallium oxide, and high-entropy alloys as well as simulations revealing novel properties of these materials.

- [1] J. Byggmästar, A. Hamedani, K. Nordlund, F. Djurabekova, *Phys. Rev. B*, 100, 144105 (2019)
- [2] J. Byggmästar, K. Nordlund, F. Djurabekova, *Phys. Rev. B*, 104, 104101 (2021)
- [3] J. Byggmästar, K. Nordlund, F. Djurabekova, *Phys. Rev. Materials* 6, 083801 (2022)

Nonequilibrium many-body dynamics in Supersymmetric Quenching

Christopher Campbell^{1,2}, Thomas Fogarty², and Thomas Busch²

¹ *NANOMO, University of Oulu, Oulu, Finland*

² *Qunatum Systems Unit, Okinawa Institute of Science and Technology, Onna-son, Okinawa Japan*

Corresponding author: christopher.campbell@oulu.fi

Nonequilibrium dynamics deepens our understanding in the control of quantum system, such as an ultracold atomic gas, in response to some change to its environment. The simplest way to do induce excitations in a system is through a quench, where a perturbation to parameters of a Hamiltonian is suddenly introduced, allowing a system to evolve in an environment that differs from its initial preparation. In some instances this perturbation originates from the trapping potential, where the eigenspectrum of the original Hamiltonian shifts, inducing excitations in the a quantum system. As the system evolves, calculations such as the survival probability are used to follow the dynamics, which requires information of the initial and final Hamiltonian and its respective eigenspectra.

The eigenspectra between Hamiltonians that are derived from supersymmetry do not experience such a perturbation on the other hand. From their algebraic construction using supersymmetric operators A and A^\dagger , the eigenspectra between two partner potentials are near degenerate, and only differ by the removal of ground state energy of the original Hamiltonian. Because of this degeneracy, calculations such as the survival probability can be written purely in terms of the initial Hamiltonian by utilizing supersymmetric intertwining properties. This consequently preserves different properties of a quantum system that are dependent on the eigenspectrum, such as the revival time of the system.

In this work we use the algebra of supersymmetry to construct an analytical framework used to study quenches between supersymmetric Hamiltonians. This is accomplished by preparing a spin polarized Fermi gas in one Hamiltonians potential and allowing it to evolve in a supersymmetric partner potential. Notably, by using an infinite square well (ISW), a supersymmetric quench reveals signatures of perfect fidelity at the revival time of the ISW, which are retained at finite temperatures. This non-thermalizing effect is then advanced upon in the ISW hierarchy of potentials and later generalized for potentials that contain an n^2 dependency on their eigenspectra.

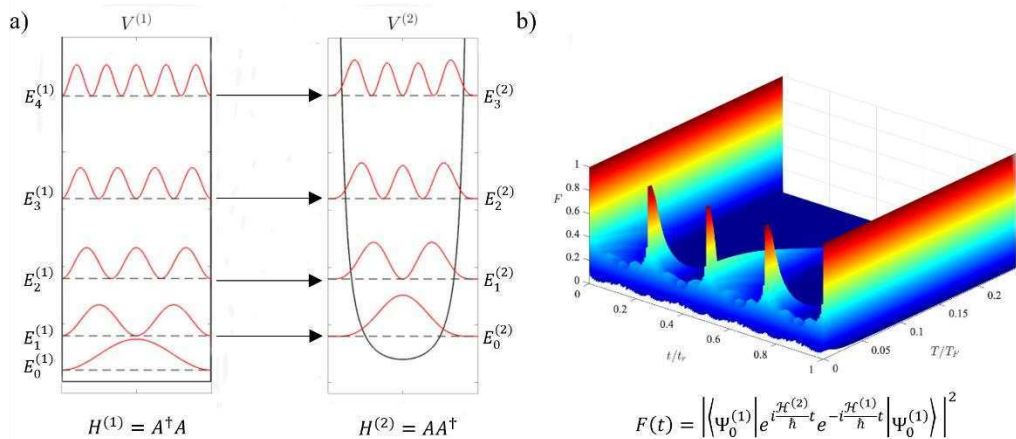


Fig. 1: a) Schematic of supersymmetric potentials used in quenching models. Here, a Hamiltonian is factorized into supersymmetric operators A and A^\dagger , and by reversing the order of operation a new Hamiltonian is constructed with an eigenspectrum nearly identical to the first. b) The many-body survival probability of a spin polarized Fermi gas of 30 particles quenched from the ISW ($V^{(1)}$) to its first partner potential ($V^{(2)}$) plotted against the revival time and temperature of the gas.

[1] [C.Campbell et.al., Phys. Rev. Research 4, 033014 \(2022\).](#)

Electronic Transport in Quantum-Chaotic Nanostructures

F. Chalangari¹, S. Selinummi¹, J. Keski-Rahkonen², and E. Räsänen^{1,2}

¹ Computational Physics Laboratory, Tampere University, Tampere 33720, Finland

² Department of Physics, Harvard University, Cambridge, Massachusetts 02138, USA

Corresponding author: fartash.chalangari@tuni.fi

In the exploration of mesoscopic two-dimensional (2D) nanostructures, we employ the Landauer-Büttiker approach to gain insights into and control over the electrical properties of chaotic quantum transport systems [1, 2]. On the classical side, it is widely acknowledged that dynamics is difficult to predict due to chaos, for instance stemming from impurities in a nanostructure. However, in mesoscopic systems, we can push the limit further by employing quantum coherence for our benefit. A striking visual manifestation of quantum mechanical suppression of classical chaos is a *quantum scar* [3], where the probability density of an eigenstate condensates in the vicinity of an unstable classical periodic orbit.

Our transport setup consists of a 2D quantum dot of an arbitrary shape [4], strongly coupled to finite-width leads [2]. The system is also exposed to an external uniform magnetic field. The computational framework enables calculations of transmission, conductivity, and currents in multi-terminal 2D transport devices. Additional tools facilitate the computation of the local density of states, showcasing possibilities to exploit quantum scars, for example, the so-called bouncing-ball states [5], in the *control* of quantum transport. This approach enables a multitude of applications in quantum electronics.

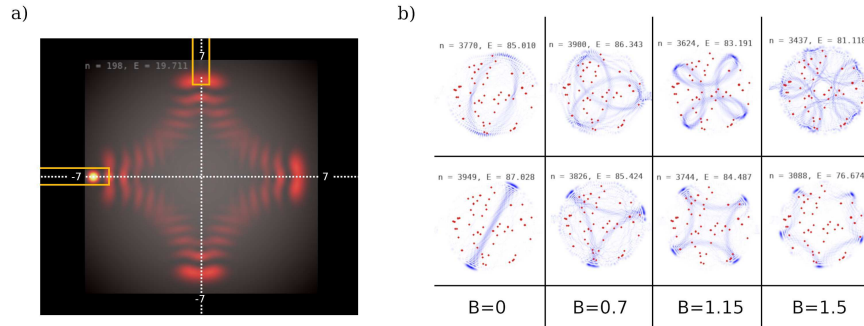


Figure 1: **a)** Eigenstate of a harmonically confined 2D quantum dot strongly coupled to two perpendicular leads in the presence of external magnetic field $B = 1.15$ a.u. [5] **b)** Perturbation-induced quantum scars in the presence of Gaussian impurities and different external magnetic fields [3].

[1] See, e.g., M. Ventra, *Electrical Transport in Nanoscale Systems*, Cambridge University Press, Cambridge (2008). G. Stefanucci, *Nonequilibrium Many-Body Theory of Quantum Systems: a Modern Introduction*, Cambridge University Press (2013).

[2] R. Duda, J. Keski-Rahkonen, J. Solanpää, and E. Räsänen, *Comp. Phys. Commun.* 270, 108141 (2022).

[3] E. J. Heller, *Phys. Rev. Lett.* 53, 1515 (1984); P. J. J. Luukko, B. Drury, A. Klales, L. Kaplan, E. J. Heller, and E. Räsänen, *Sci. Rep.* 6, 37656 (2016). J. Keski-Rahkonen, A. Ruhanen, E. J. Heller, and E. Räsänen, *Phys. Rev. Lett.* 123, 214101 (2019).

[4] P. J. J. Luukko and E. Räsänen, *Comp. Phys. Commun.* 184, 769 (2013).

[5] S. Selinummi, F. Chalangari, J. Keski-Rahkonen, and E. Räsänen, submitted (2024).

Using variational quantum algorithms and tensor network methods to solve the quantum Heisenberg model

Prateek Chawla¹, Jose Lado¹, and Christian Flindt¹

¹*Department of Applied Physics, Aalto University, Finland*
prateek.chawla@aalto.fi

Variational Quantum Algorithms (VQAs) are a promising strategy to leverage the potential of quantum computers towards solving problems in quantum many-body physics. These methods utilize the toolbox of classical optimization and parameterized quantum circuits to achieve shallow circuit depths, which is important to get useful output from noisy quantum devices [1].

Tensor networks are a computational technique that allows us to efficiently store large quantum states by providing an efficient parameterization of the wavefunction, helping ease the memory requirements. Specifically, the finite precision of tensor networks allows one to emulate quantum circuits with varying degrees of entanglement. This makes it possible to emulate circuits with a tunable degree of entanglement, helping us analyze VQA performance in realistic quantum circuits.

In this work, we showcase a VQA built and tested on a tensor network quantum circuit simulator capable of solving the benchmark problem of one-dimensional transverse-field Ising model using a physically inspired ansatz, and show how this can be extended to simulate the one-dimensional Heisenberg anti-ferromagnet with isotropic coupling. We will analyze the role of maximal entanglement in the circuit, shedding light on the most promising regimes to employ VQAs in near-term quantum computers.

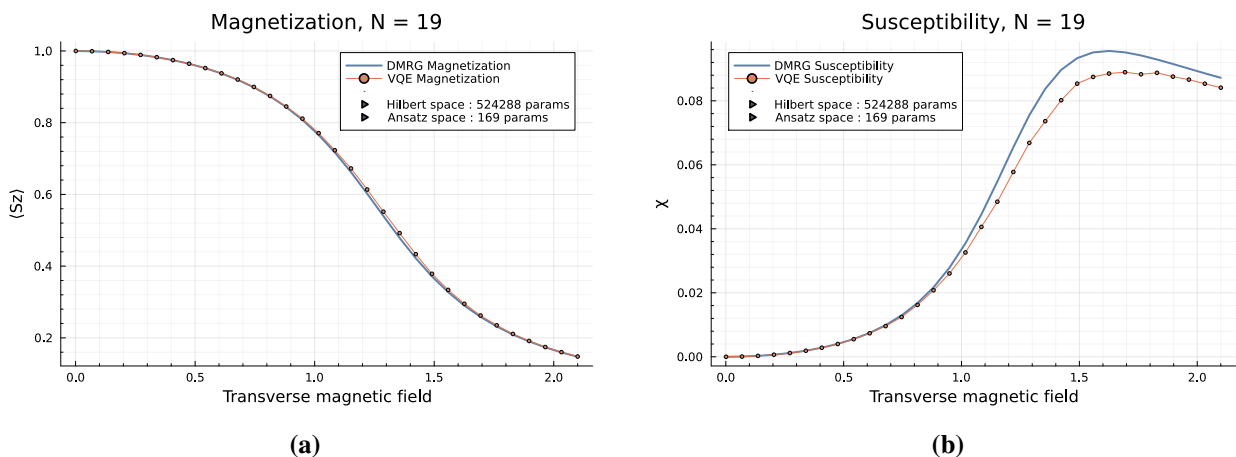


Figure 1. Figure showing the simulator performance on a finite Ising spin chain of length 19.

- [1] M. Cerezo, A. Arrasmith, R. Babbush, S. C. Benjamin, S. Endo, K. Fujii, J. R. McClean, K. Mitarai, X. Yuan, L. Cincio, and P. J. Coles, “Variational quantum algorithms”, [Nature Reviews Physics](#) **3**, 625 (2021).

Microstructure and phase formation in epitaxial thin Ni-Al films

Zhehao Chen¹, Kostas Sarakinos^{1,2} and Filip Tuomisto¹

¹Department of Physics, University of Helsinki, Helsinki, Finland

²Department of Physics, KTH Royal Institute of Technology, Sweden

Corresponding author: Zhehao.Chen@helsinki.fi

The Ni-Al binary system is of great technological relevance due to the formation of the intermetallic Ni₃Al L12 phase (Pm-3m) which exhibits a relatively high melting point, a high strength and also a relatively low ductility. Ni-Al compounds in the bulk form are routinely synthesized by air melting and casting process. Atom-by-atom growth of thin films from the vapor phase offer an alternative route for alloy synthesis, whereby high supersaturation at the vapor-solid interface imposes limited atomic assembly kinetics and often enables formation of metastable phases against the predictions of thermodynamics. In the present work, we study growth, microstructure, and phase formation in epitaxial thin Ni-Al films synthesized by magnetron sputtering. Films are deposited on MgO (001) substrates and the Al content is varied between 0 and 25 at%, as determined by elastic recoil detection analysis. X-ray diffractometry (XRD) analyses (Bragg-Brentano, rocking curve, and pole figure measurements) show that all samples grow epitaxially along the <100> crystallographic direction. Moreover, XRD data reveal that films with Al content up to 11 at.% are Ni-Al solid solutions, whereas films with Al content above 11 at.% exhibit diffraction peaks that correspond to both the fcc Ni and the L12 Ni₃Al phases. These results are corroborated by electron diffraction in the framework of transmission electron microscopy (TEM) measurements. Concurrently, high-resolution TEM analyses show that Ni film is epitaxially grown on the MgO (100) substrate surface with not distinct grain/domain boundaries. We also find that at the epilayer-substrate interface the in-plane interplanar spacing of the Ni lattice expands, accompanied by incommensurate registry between Ni and MgO lattice planes, to accommodate the 17% lattice misfit between Ni and MgO.

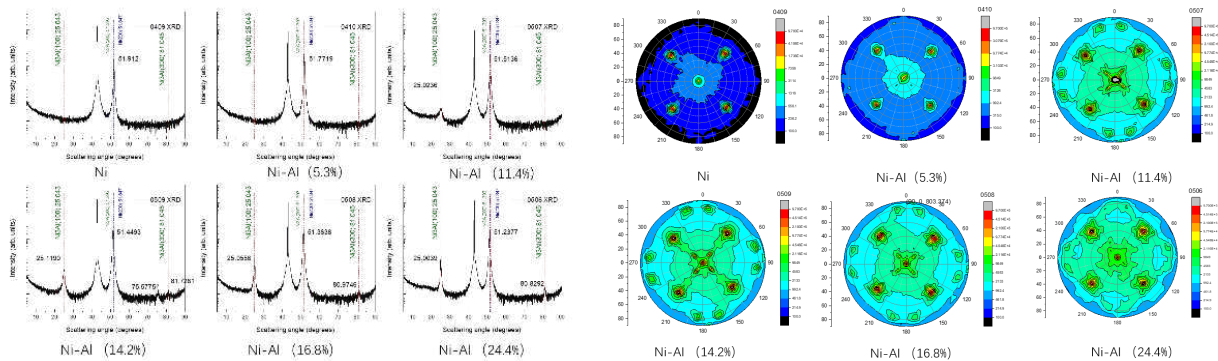


Fig.1.XRD and Pole figure characterization for Ni and Ni-Al(X) thin films. Pole figures were measured at (111) orientation.

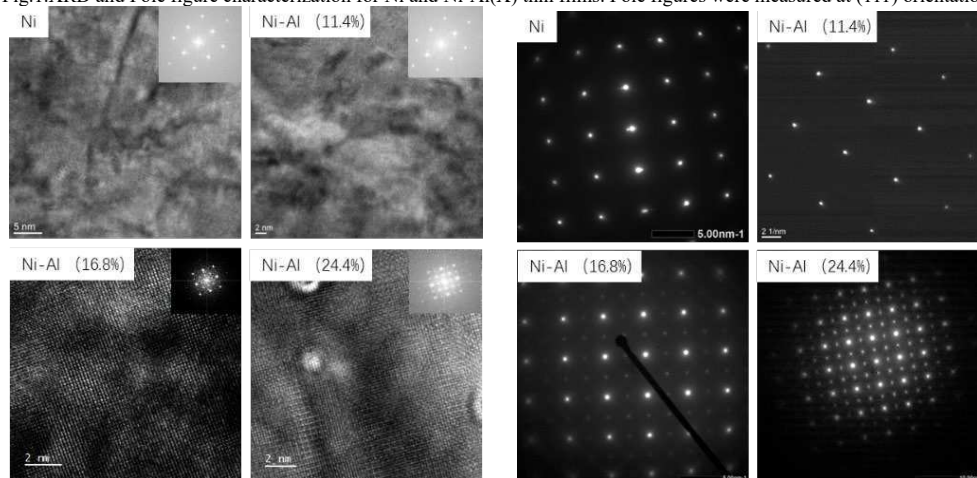


Fig.2 Bright field HR TEM and electron diffraction of Ni and Ni-Al(X) thin films from (100) zone axis.

Enhancing light outcoupling from TADF thin-films with metallic nanostructures.

Aron Dahlberg¹, Joel Lehinkoinen², and Päivi Törmä³

¹*Quantum Dynamics, Department of Applied Physics, Aalto University, Finland*
aron.dahlberg@aalto.fi

Organic light emitting diodes (OLEDs) find widespread use in displays; however, their low external quantum efficiency (typically approximately 20 %) and efficiency roll-off at higher current densities hinder their use in other applications, such as lighting. While thermally-activated delayed fluorescent (TADF) emitters can exhibit near unity internal quantum efficiencies, light outcoupling efficiency is limited due to total internal reflection at dielectric interfaces, waveguide modes and surface plasmon polaritons.

Nanostructures inside and outside the OLED structure have been previously used to enhance light outcoupling. Here, we propose a solution to enhance outcoupling efficiency by coupling the photons emitted from the emissive layer of the OLED to the surface lattice resonance modes via scattering from metallic nanoparticle arrays embedded in the OLED structure.

We observe a significant increase in the light outcoupling efficiency and a change in the shape of the intensity spectrum from an optically pumped device with an embedded nanoparticle array compared to a pure thin-film reference device. We use finite-difference time-domain simulations to study the origin of the enhancement, and ascribe it to collimation of light within the escape cone of the device–air interface.

Nuclear octupole shapes in actinides with Fayans functionals

G. Danneaux¹, M. Kortelainen¹

¹ Department of Physics, University of Jyväskylä, Jyväskylä, Finland

Corresponding author: gauthier.j.danneaux@jyu.fi

Static octupole deformation, also called reflection asymmetric by contrast with the more usual and more easily perceptible quadrupole deformation, manifests a profound signature on the observables of nuclei and so on the systematics of the nuclear ground state properties and excitation spectra [1]. Furthermore, these shapes are expected to appear in the actinide and superheavy region of the nuclear chart, having important connection to e.g. nuclear Schiff moment [2]. These factors present a non-negligible impact on the systematic behaviour of nuclear properties, thus posing an important test for theoretical nuclear structure models.

The modern tool of the choice to address the complex inner structure of nuclei is the nuclear density functional theory (DFT). The key element of DFT is the energy density functional (EDF), which incorporates complex nuclear interactions, of which results can then be compared to experimental data [3]. Encompassing many nuclear properties and forces, the typical Skyrme functional thus present many constants. This gives rise to a wide variety of Skyrme-based EDFs, each adjusted via vast amounts of experimental nuclear data.

In order to improve accuracy, new Fayans EDFs have been recently developed, enriching the traditionally used Skyrme EDFs with the Fayans pairing term [4]. Fayans EDFs have been successfully tested on isotopic chains via the comparison with brand new charge radii measurements [5][6][7]. Based on an earlier theoretical survey in which some actinides clusters have been expected to present strong octupole deformation [8], our work aims to both verify the expected precision of the newly adjusted Fayans EDFs compared to Skyrme EDF based models, and confirm the stronger octupole preponderance in Fayans EDFs.

As such, this is a first-of-its-kind systematic survey of octupole deformation and associated nuclear properties computed with the Fayans EDFs. We then compared our results to recent studies on pear-shaped nuclei regions [9]. Moreover, we have also found that these new Fayans functionals also present rather promising results regarding odd-even effects, namely on radii, in isotopic chains.

[1] P. A. Butler, Proc. R. Soc. A, **476** (2020)

[2] J. Dobaczewski, J. Engel, M. Kortelainen et al., Phys. Rev. Lett., **121**, 23 (2018)

[3] J. Bonnard, J. Dobaczewski, G. Danneaux et al., Phys. Lett. B, **843**, (2023)

[4] P.G. Reinhard, W. Nazarewicz, Phys. Rev. C, **95**, 6 (2017)

[5] A.J. Miller, K. Minamisono, A. Klose et al., Nature Physics, **15** (2019)

[6] Á. Koszorús, X. Yang, W. Jiang, Nature Physics, **17** (2021)

[7] M. Reponen et al., Nature Commun., **12**, 1 (2021)

[8] S. Ebata and T. Nakatsukasa, Physica Scripta, **92**, 6 (2017)

[9] Y. Cao, S.E. Agbemava, A.V. Afanasjev et al., Phys. Rev. C, **102**, 12 (2020)

Heat Pulses in electron quantum optics

Pedro Portugal¹, Fredrik Brange¹, and Christian Flindt¹

¹*Department of Applied Physics, Aalto University, 00076, Finland*

Corresponding author: pedro.decastroportugal@aalto.fi

Electron quantum optics aims to realize ideas from the quantum theory of light with the role of photons being played by charge pulses in electronic conductors. Experimentally, the charge pulses are excited by time-dependent voltages, however, one could also generate heat pulses by heating and cooling an electrode [1,2]. Here, we explore this intriguing idea by formulating a Floquet scattering theory of heat pulses in mesoscopic conductors [3]. The adiabatic emission of heat pulses leads to a heat current that in linear response is given by the thermal conductance quantum. However, we also find a high-frequency component, which ensures that the fluctuation-dissipation theorem for heat currents, whose validity has been debated, is fulfilled. The heat pulses are uncharged, and we probe their electron-hole content by evaluating the partition noise in the outputs of a quantum point contact. We also employ a Hong–Ou–Mandel setup to examine if the pulses bunch or antibunch. Finally, to generate an electric current, we use a Mach–Zehnder interferometer that breaks the electron-hole symmetry and thereby enables a thermoelectric effect.

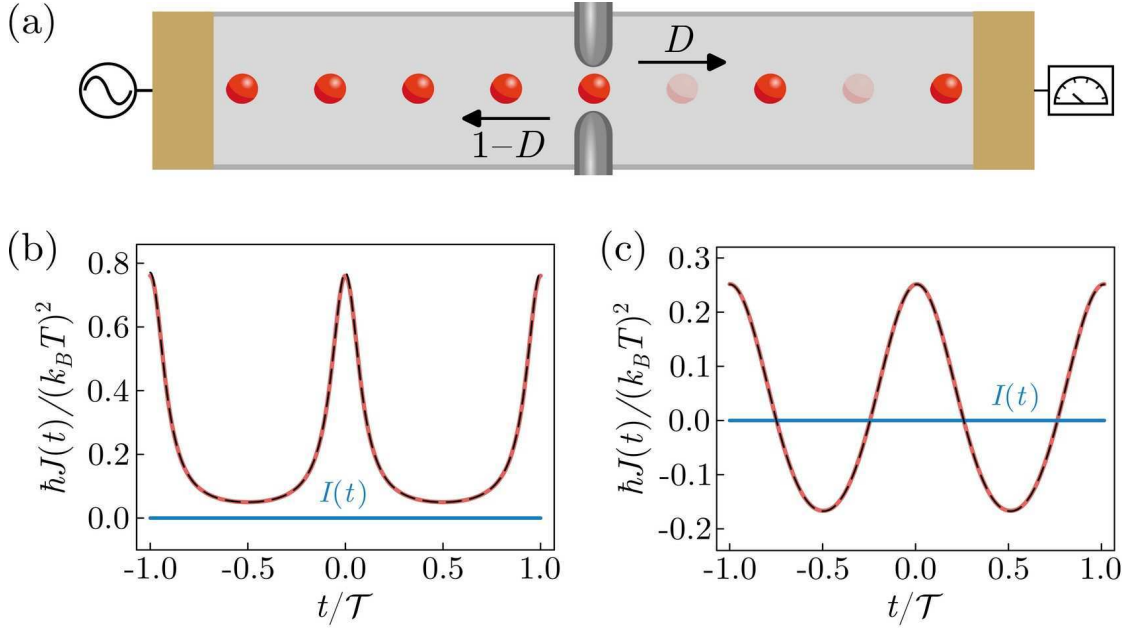


Fig. 1: Periodic heat pulses in a mesoscopic conductor. (a) Two-terminal setup with a source and a drain electrode connected by a quantum point contact with transmission D . Heat pulses are emitted from the source electrode (left), and the electric current and the heat current are measured in the drain electrode (right). (b) Heat current for Lorentzian pulses. The dashed line indicates the static result with the time-dependent temperature of the source electrode inserted. The electric current vanishes. (c) Similar results for a cosine drive.

[1] P. Portugal, C. Flindt, and N. Lo Gullo, Phys. Rev. B **104**, 205420 (2021)

[2] P. Portugal, F. Brange, and C. Flindt, Phys. Rev. Res. **4**, 043112 (2022)

[3] P. Portugal, F. Brange, and C. Flindt, arXiv:2311.16748 (2023)

Strong actuation and nonlinear response of mass loaded membranes

Joe Depellette¹, Ewa Rej¹, Richa E Cutting¹ and Mika A Sillanpää¹

¹ QTF Centre of Excellence, Department of Applied Physics, Aalto University, FI-00076 Aalto, Finland

Corresponding author: joe.depellette@aalto.fi

Micro-mechanical resonators with high force sensitivities are utilised as sensors in many experiments. When paired with microwave optomechanics a range of useful techniques are introduced, such as the ability to measure the oscillation amplitude of a resonator. Influencing the properties of micro-mechanical resonators allows a single device design to be modified for a wide range of experimental applications. One particular modification is mass loading, where the effective mass of a resonator is significantly increased during the fabrication process. Strong actuation of massive resonators can be used to create a time dependent gravitational source, forming part of a setup with the goal to measure gravitational forces between two devices [1]. The onset of nonlinearity conflicts with this goal, limiting the oscillation amplitude one can induce. In this work, a 2 mm square Si₃N₄ membrane is mass loaded with a 1 mg gold sphere and a microwave cavity readout is implemented. The membrane is electrostatically driven and the oscillation amplitude is measured; a nonlinear response with geometric and electrostatic contributions is observed.

[1] Liu Y, Mummery J, Zhou J, Sillanpää M A. Gravitational forces between nonclassical mechanical oscillators. *Physical Review Applied*. 2021 Mar 1;15(3):034004.

Pyroelectric Effect in Ferroelectric Perovskites Studied with Density Functional Theory

Kim Eklund¹ and Antti J. Karttunen¹

¹*Department of Chemistry and Materials Science, Aalto University, Espoo, Finland*

Corresponding author: kim.eklund@aalto.fi

Ferroelectric perovskites such as BaTiO₃, KNbO₃, and PbTiO₃ and various solid solutions based on them, such as Pb(Ti_xZr_{1-x})O₃ (PZT), are important functional materials in electrical engineering and related applications. In the pyroelectric effect, exhibited by all ferroelectrics, the spontaneous polarization of the polar material changes upon temperature fluctuation. This electric polarization is extractable as a current. Pyroelectrics are used in various sensor applications and other electronics, but the promise of turning heat fluctuation to electrical energy also shows potential for waste heat harvesting applications. Measurement of the pyroelectric effect is rather complicated experimentally, and computational tools could aid in the design of novel pyroelectrics by providing an accurate route to modelling and screening of the pyroelectric properties.

Study of the finite-temperature phonon properties and finite-temperature displacements is enabled by the self-consistent phonon calculation (SCPH) formalism implemented in the ALAMODE package developed by Tadano *et. al.* [1,2]. We have developed a computational methodology, based on density functional theory (DFT), SCPH, and Berry phase theory of polarization, to evaluate the primary pyroelectric coefficient of tetragonal-structured perovskite ferroelectrics at finite temperatures [3]. The total pyroelectric coefficient consists of two parts, primary and secondary, where the secondary effect is a piezoelectric contribution. The secondary part can be evaluated with quasi-harmonic approximation (QHA) combined with the calculation of elastic and piezoelectric constants. Results obtained for BaTiO₃ show reasonable agreement with experimentally measured values, indicating that the supercell-based methodology can further be used for known and predicted perovskite solid solutions.

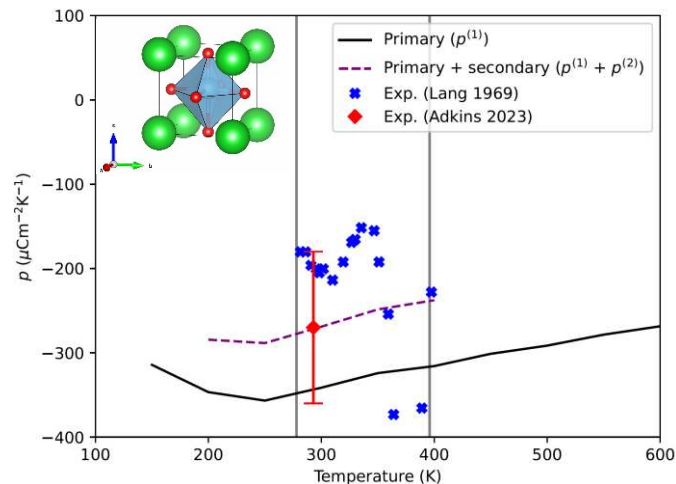


Fig. 1: Pyroelectric coefficient of BaTiO₃ at finite temperatures calculated with DFT [3].

[1] T. Tadano, Y. Gohda, and S. Tsuneyuki, *J. Phys.: Condens. Matter* **26**, 225402 (2014).

[2] T. Tadano and S. Tsuneyuki, *Phys. Rev. B* **92**, 054301 (2015).

[3] K. Eklund and A.J. Karttunen, *J. Phys. Chem. C* **127**, 21806 (2023).

Enabling km-scale coupled climate simulations on GPUs

J. Enkovaara¹, Claudia Frauen², Daniel Klocke³, Lukas Klufft³, Luis Kornblueh³, Sergey Kosukhin³, Tuomas Lunttila¹, Rene Redler³, and Reiner Schnur³

¹ CSC - IT Center for Science, Espoo, Finland

²Deutsches Klimarechenzentrum, Hamburg, Germany

³Max-Planck-Institut für Meteorologie, Hamburg, Germany

Corresponding author: jussi.enkovaara@csc.fi

The Icosahedral Nonhydrostatic (ICON) weather and climate model is a modelling framework for numerical weather prediction and climate simulations. ICON is implemented mostly in Fortran 2008 with the GPU version based mainly on OpenACC. ICON is used on a large variety of hardware, ranging from classical CPU cluster to vector architecture and different GPU systems.

An ICON model configuration developed for km-scale climate simulations is used as a scientific prototype for the digital twin of the Earth for climate adaptation within the Destination Earth program of the European Commission. Here we focus on our effort to run these coupled ICON configurations at km-scale on LUMI, a HPE Cray EX system with a GPU partition based on AMD MI250x's.

We present the model configuration, performance results and scalability of the simulation system on Lumi and compare it with results on other GPU and CPU based systems.

Amorphous silicon metasurface for lasing with tunable directionality

Sioneh Eyvazi¹, Evgeny Mamonov¹, and Päivi Törma¹

¹*Department of Applied Physics, School of Science, Aalto University, Espoo, Finland*
Sioneh.eyvazibadelbo@aalto.fi

All-dielectric subwavelength gratings are highly efficient optical meta-devices that can manipulate light at the nanoscale with low dissipative losses [1]. This study explores resonant modes of partially etched amorphous silicon nanocylinders. Our preliminary results show the formation of several modes, which make such a system interesting for lasing applications.

Due to the periodic nature of the grating, the interaction between waveguiding modes and localized Mie resonances results in highly effective light-matter interactions [2]. An advantageous feature of these systems is the formation of quasi-flatbands [3]. This distinctive characteristic holds promise for applications in nonlinear image processing and topological photonics [4].

Here, we use partially etched amorphous silicon nanocylinders with subwavelength periodicity (Fig. 1(a)). Typical transmission spectra (Fig. 1(b)) of the structure show the presence of Mie resonances hybridized with waveguiding modes, photonic flatbands, and higher-order diffraction coupled to waveguiding modes within the infrared spectral region. The complicated modal structure of the studied samples allows us to use different modes for lasing: bright and dark modes, as well as modes propagating in different directions with respect to the nanocylinder array axes.

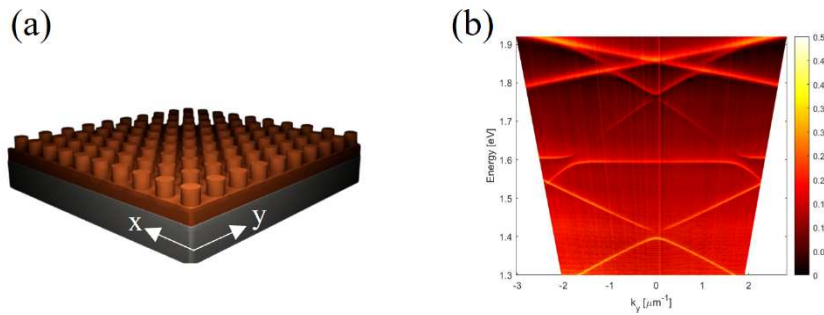


Fig. 1: (a) Schematic of the sample consists of a nanoarray placed on top of a waveguiding layer. The waveguiding layer is 40nm thick, and the periodicity of the grating is 530 and 340 nm in the x and y direction, respectively. (b) Extinction spectrum of a-Si metasurface.

One key aspect of the systems under study is the presence of photonic flatbands, which are observed in different structures, including waveguide arrays and coupled cavity arrays [5]. Despite this, lasing in this mode has not been reported. As part of our future work, we intend to address this gap and achieve lasing in photonic flatbands.

- [1] Luque-González, José Manuel, et al. "A review of silicon subwavelength gratings: building break-through devices with anisotropic metamaterials." *Nanophotonics* 10.11 (2021): 2765-2797.
- [2] Zhang, Zhenghe, et al. "High-Q collective Mie resonances in monocrystalline silicon nanoantenna arrays for the visible light." *Fundamental Research* 3.5 (2023): 822-830.
- [3] Amedalor, Reuben, et al. "High-Q guided-mode resonance of a crossed grating with near-flat dispersion." *Applied Physics Letters* 122.16 (2023).
- [4] Munley, Christopher, et al. "Visible Wavelength Flatband in a Gallium Phosphide Metasurface." *ACS Photonics* (2023).
- [5] Choi, Minh, et al. "Nonlocal, Flat Band Meta-optics for Monolithic, High Efficiency, Compact Photodetectors." *arXiv preprint arXiv:2312.05395* (2023).

Navigating Fusion Reactor Challenges: Correlations Between Surface Temperature, Plasma Particle Impact Angle and Erosion

N. Fakhrayi Mofrad¹, A. Sand¹

¹ Nuclear Materials and Engineering (NuME), Aalto University, Espoo, Finland

Corresponding author: nima.fakhrayimofrad@aalto.fi

There are challenges to overcome to have a fully operating fusion power plant. One is to understand and control the Plasma-Wall Interactions (PWIs) to increase the availability and lifetime of the device [1, 2]. These interactions could cause erosion and limit the lifetime and performance of the wall. Furthermore, the eroded impurities could enter the plasma core, dilute the fuel, and cause energy loss. Moreover, the redeposition of these impurities is also one of the main contributors to tritium retention, which is one of the major concerns in the development of fusion reactors [3, 4].

This study focuses on assessing the behaviour of Beryllium (Be) as wall material. Be has been under investigation for its potential application in fusion reactors over the years. However, its behavior under diverse reactor environment remains not fully understood. To Address this gap, we simulated the erosion of Be due to Hydrogen (H), Deuterium (D), and Tritium (T) plasma irradiations.

Initially, Be structures were loaded with H (D or T) to set up a pre-existing concentration of the incident ion, based on the work of Safi et al. [5]. After preparing the structures, non-cumulative molecular dynamics (MD) simulations were carried out for each isotope, varying the impact energy (10 - 200 eV), incident angle (0° - 75°), and surface temperature (300 - 800K).

Results indicate a strong dependence of the sputtering yield on the type, energy and impact angle of the incoming plasma particle. The probability of the plasma particle being reflected from surface or for it to cause outgassing also exhibits a clear correlation with the plasma particle properties. Furthermore, the balance between physical sputtering and swift chemical sputtering [6] (with the latter depicted in Figure 1, where a BeD molecule is sputtered), also depends on the characteristics of the plasma particle. While the effect of impact energy and angle has been quite extensively studied, the inclusion of isotope type in the analysis adds a unique dimension, providing a thorough comparison of their effects. For instance, increasing the mass of the plasma particle results in a more efficient momentum transfer to the substrate atoms, which increases the physical sputtering yield, while decreasing the probability of molecular sputtering and reflection.

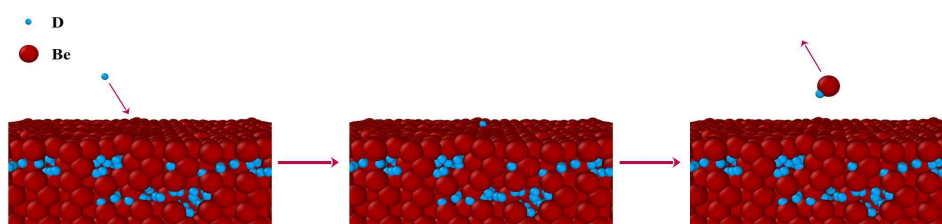


Figure 1: Schematic of a molecular sputtering event.

- [1] J.W. Coenen et al, Nuclear Materials and Energy, **12** (2017)
- [2] K. Nordlund et al, J. Phys. D: Appl. Phys., **47**, 224018 (2014)
- [3] G. Alberti et al, Nucl. Fusion, **63**, 026020 (2023)
- [4] S. I. Krasheninnikov, Plasma Phys. Control. Fusion, **64**, 124005 (2022)
- [5] E. Safi et al, J. Phys. D: Appl. Phys., **50**, 204003 (2017)
- [6] C. Bjorkas et al, New Journal of Physics, **11**, 123017 (2009)

Machine-learning interatomic potentials for FCC high-entropy alloys

A. Fellman¹, J.Byggmästar¹, F. Djurabekova¹, and K. Nordlund¹

¹ Department of Physics, University of Helsinki, Helsinki, Finland

Corresponding author: aslak.fellman@helsinki.fi

Accurate interatomic potentials are essential for reliable molecular dynamics simulations. Machine learning (ML) interatomic potentials have increasingly become commonplace in molecular dynamics simulations, as they can provide near quantum level accuracy while allowing for simulations of large systems well above the ones achievable in methods such as density functional theory (DFT). In this work, we have developed Gaussian approximation potentials (GAP [1]) for FCC high-entropy alloys (HEA). HEAs are alloys consisting of 5 or more constituent elements randomly arranged in near equal proportions. Specifically, we created a performant low-dimensional tabulated version of the model (tabGAP [2]) for AlCrCuFeNi HEAs as well as constituent alloys thereof. The model was trained on an extensive database of energies and forces created using DFT calculations. The tabGAP incorporates a fixed short-range repulsive potential with the intention of better describing short-range interactions relevant for radiation damage simulations. Using the developed ML potential we have simulated overlapping collision cascades in various compositions. We have investigated fundamental defect properties and damage production of the overlapping cascades and compared them between different compositions.

[1] A. P. Bartók, M. C. Payne, R. Kondor, and G. Csányi, *Physical Review Letters* 104,10.1103/PhysRevLett.104.136403 (2010).

[2] J. Byggmästar, K. Nordlund, and F. Djurabekova, *Phys.Rev. B*104, 104101 (2021).

Molecular dynamics insights on the molecular P implantation for scabable spin-qubit arrays

Tomás Fernández Bouvier¹, Ville Jantunen ¹, Álvaro López Cazalilla ¹ and Flyura Djurabekova¹

¹ Accelerator Laboratory, University of Helsinki

Corresponding author: tomas.fernandezbouvier@helsinki.fi

Future quantum computing technologies require an implantation precision which is higher than any focused ion beam technology existing currently. Towards improving the placement precision of P donors in a Si diamond lattice, the use of a PF₂ molecular ion instead of a single atom P ion has significantly improved the detection confidence of the implant while preserving a low straggling in its placement. [1]

Although the overall results seem promising, the deviations from the intended placement of a P donor in Si are expected due to the highly stochastic nature of ion implantation. Computer simulations using the molecular dynamics method can provide more additional details on the process. In my presentation, I will discuss the physics of the energy deposited by the ions moving in the material via electronic stopping power which translates into an electric signal used in experiment for detection of the ion's placement position. Said signal is different in channeling and off-channeling directions.

In this work, we are investigating the synergies in energy deposition due to simultaneous impact of three ions during a molecular ion implantation. To mitigate this, we will explore the effect of a 5 nm amorphous SiO₂ layer which grows naturally on the pure Si wafer's surface. I will also describe in detail the damage caused by the highly energetic particles in the lattice and I will delve into the long-term damage evolution processes and how the annealing conditions can be improved in such a way that their post-implantation diffusion of the P atom is minimum while guaranteeing a total recovery of the substrate.

[1] Danielle Holmes, Benjamin Wilhelm, Alexander M. Jakob, Xi Yu, Fay E. Hudson, Kohei M. Itoh, Andrew S. Dzurak, David N. Jamieson, and Andrea Morello. Improved placement precision of donor spin qubits in silicon using molecule ion implantation. *Advanced Quantum Technologies*, n/a(n/a):2300316.

Analysis of Microwave Resonators in High Magnetic Fields

K. Frei Nadarajah, P. Hakonen, and M. Kumar

Low Temperature Laboratory, Department of Applied Physics, Aalto University, Espoo, Finland

Corresponding author: kristiana.nadarajah@aalto.fi

In this work, we analyze the behavior of superconducting microwave resonators in high magnetic fields. Abrikosov vortices penetrate the superconductor in magnetic fields above the critical value, leading to a breakdown of the Cooper pairs. The resulting dissipation limits the quality factor (Q) of the resonators and thus inhibits their practical application. To improve the Q of the resonators we develop a method to increase their resilience to the aforementioned dissipation processes. The proposed resonators will give rise to the development of a chiral cavity quantum electrodynamics (CQED) platform to study quantum Hall states that form in high fields. This will allow us to investigate topological many-body physics using microwave photons in the gigahertz regime.

Moiré-driven multiferroic order in twisted Chromium trihalides

Adolfo O. Fumega¹, Jose L. Lado¹

¹*Department of Applied Physics, Aalto University, FI-00076 Aalto, Finland*

Corresponding author: adolfo.oterofumega@aalto.fi, jose.lado@aalto.fi

Layered van der Waals compounds have revolutionized the artificial design of materials. The unique degrees of freedom offered by this class of materials allow new strategies to engineer states of matter. In particular, the weak van der Waals interlayer bonding enables the introduction of a specific twist angle between the layers.

In this presentation we will show how to artificially engineer a multiferroic order using twisted chromium trihalide CrX_3 ($X=\text{Cl}$, Br , and I) bilayers [1]. The theoretical analysis introduced here is performed using a combination of spin models and ab initio calculations. Firstly, we show the emergence of a spin texture as a result of the site-dependent interlayer magnetic exchange created by the moiré. The presence of spin-orbit coupling combined with that emergent non-collinear magnetic order induces an electric polarization and a strong magnetoelectric coupling in the system. Among the three chromium trihalides, we found that CrBr_3 displays the strongest multiferroic order. We show that its magnetoelectric coupling allows us to electrically tune the magnetic texture of the moiré system. Specifically, we show that it is possible to generate and control magnetic skyrmions in twisted CrBr_3 with an external electric field.

[1] Adolfo O Fumega and Jose L Lado, *2D Mater.* 10 025026 (2023).

Computational investigation of radiation damage in high-temperature superconductors for nuclear fusion applications

D. Gambino^{1,2}, F. Ledda^{3,4}, A. Leino², J. Byggmästar², K. Nordlund², F. Djurabekova², D. Torsello^{3,4}, F. Laviano^{3,4}

¹ Department of Physics, Chemistry and Biology (IFM), Linköping University, Linköping, Sweden

² Department of Physics, University of Helsinki, Helsinki, Finland

³ Department of Applied Science and Technology, Politecnico di Torino, Torino, Italy

⁴ Istituto Nazionale di Fisica Nucleare, Sezione di Torino, Torino, Italy

Corresponding author: davide.gambino@liu.se

Compact fusion reactors have been recently proposed for achieving sooner and cheaper fusion energy, which could provide enormous amounts of energy at a low carbon footprint and therefore help in the transition away from fossil fuels. The development of such designs is enabled by high-temperature superconducting tapes based on rare-earth barium cuprates (REBCOs), which can generate the needed strong magnetic fields thanks to the high critical currents typical of these materials. Nonetheless, the compact design introduces challenges on the radiation hardness of the employed materials, since neutrons escaping from the vacuum vessel will reach all parts of the reactor [1]. The superconducting properties of REBCOs are strongly dependent on the defect landscape of the sample, calling for a detailed investigation of radiation damage in these systems.

For these reasons, we have investigated [1] the expected radiation environment in the ARC reactor [2] and we have carried out molecular dynamics simulations of radiation damage in $\text{YBa}_2\text{Cu}_3\text{O}_7$ (YBCO) at relevant conditions. We employ an interatomic potential recently developed [3] for the simulation of radiation damage in this system. We find that generated defects have sizes comparable to the coherence length of YBCO, and we observe temperature transients of several kelvins above the initial temperatures, all important effects for the superconducting properties under operational conditions. Differences between radiation damage at operating conditions and in available experimental settings are stressed. Recent developments in the analysis of radiation damage from atomistic simulations and comparison with experiments will be shown, as well as improvement of the computational model.

[1] D. Torsello, D. Gambino *et al.*, *Supercond. Sci. Technol.* **36**, 014003 (2023)

[2] B. Sorbom *et al.*, *Fusion Eng. Des.* **100**, 378-405 (2015)

[3] R. Gray *et al.*, *Supercond. Sci. Technol.* **35**, 035010 (2022)

Piezoelectrically Mediated Acoustic Phonon Heat Transfer Across a Vacuum Gap

Zhuoran Geng¹ and Ilari J. Maasilta¹

¹ Nanoscience Center, Department of Physics, University of Jyväskylä, Jyväskylä, Finland

Corresponding author: zhgeng@jyu.fi

Heat transfer across a vacuum gap is commonly understood to occur solely through far/near-field radiation. However, recent studies suggest that acoustic phonons can 'jump' or 'tunnel' through such gaps, facilitated by mechanisms like the van der Waals force and electrostatic force [1,2]. This phenomenon enables the transfer of heat between two solids, although it is notably significant only when gap widths are less than 1 nm at room temperature.

Our research focused on piezoelectricity as another potential mechanism that could enable the tunneling of acoustic phonons across vacuum gaps, extending beyond the typical charge-charge interaction distance [3,4]. Our findings reveal that resonant tunneling can be achieved for specific phonon modes, resulting in a unity power transmission between two solids [5]. Our numerical analysis indicates that while the heat flux attributable to acoustic phonon tunneling remains lesser than that from near-field radiative heat transfer at room temperature (Figure 1a), it becomes the dominant mechanism at lower temperatures (Figure 1b), surpassing other mechanisms over vacuum distances up to hundreds of nanometers wide [6].

To demonstrate this phenomenon experimentally, we designed a measurement at sub-Kelvin temperatures using microscopic devices comprised of two closely spaced suspended AlN beams (Figure 1c). The results clearly show that heat transfer between the beams occurs, affirming our theoretical findings.

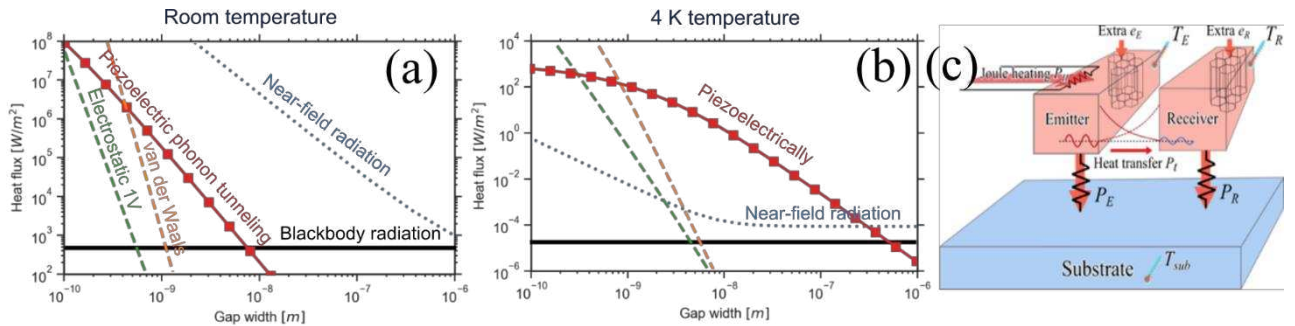


Fig. 1: Numerical results of emitted heat fluxes driven by different close-range mechanisms at (a) 300 K and (b) 4 K. (c) The schematic of the thermal model of the device used in our experiment.

- [1] J. B. Pendry, K. Sasiithlu, and R. V. Craster, Phys. Rev. B 94. 075414 (2016).
- [2] A. I. Volokitin, J. Phys. Condens. Matter **32**, 215001 (2020).
- [3] M. Prunnila and J. Meltaus, Phys. Rev. Lett. **105**, 125501 (2010).
- [4] Z. Geng and I. J. Maasilta, Phys. Rev. Res. **4**, 033073 (2022).
- [5] Z. Geng and I. J. Maasilta, Commun. Phys. **6**, 178 (2023).
- [6] Z. Geng and I. J. Maasilta, arXiv:2209.08287.

General relativistic bubble growth in cosmological phase transitions

L. Giombi¹ and Mark Hindmarsh^{1,2}

¹ Department of Physics and Helsinki Institute of Physics, University of Helsinki, Finland

² Department of Physics and Astronomy, University of Sussex, Brighton, United Kingdom

Corresponding author: lorenzo.giombi@helsinki.fi

We use a full general relativistic framework to study the self-similar expansion of bubbles of the stable phase into a flat Friedmann-Lemaître-Robertson-Walker Universe in a first order phase transition in the early Universe. With a simple linear barotropic equation of state in both phases, and in the limit of a phase boundary of negligible width, we find that self-similar solutions exist, which are qualitatively similar to the analogous solutions in Minkowski space, but with distinguishing features. Rarefaction waves extend to the centre of the bubble, while spatial sections near the centre of the bubble have negative curvature. Gravitational effects redistribute the kinetic energy of the fluid around the bubble, and can change the kinetic energy fraction significantly. The kinetic energy fraction of the gravitating solution can be enhanced over the analogous Minkowski solution by as much as $O(1)$, and suppressed by a factor as large as $O(10)$ in case of fast detonations. The amount of negative spatial curvature at the centre of the bubble is of the same order of magnitude of the naive expectation based on considerations of the energy density perturbation in Minkowski solutions, with gravitating deflagrations less negatively curved, and detonations more. We infer that general relativistic effects might have a significant impact on accurate calculations of the gravitational wave power spectrum when the bubble size becomes comparable to the cosmological Hubble radius, affecting the primary generation from the fluid shear stress, and inducing secondary generation by scalar perturbations.

Quantifying the calcification of abdominal aorta with deep learning

Johannes Halkoaho^{1,3}, Oskari Niiranen^{2,4}, Eero Salli¹, Tuomas Kaseva¹, Sauli Savolainen^{1,3}, Marko Kangasniemi¹, Harri Hakovirta^{2,5,6}

¹ Department of Radiology, HUS Diagnostic Center, HUS, Helsinki

² University of Turku, Department of Surgery, Turku

³ Department of Physics, University of Helsinki

⁴ Department of Surgery, Seinäjoki Central Hospital, Seinäjoki

⁵ Division of Gastroenterology and Urology, Turku University Hospital, Turku

⁶ Department of Surgery, Satasairaala, Pori

Corresponding author: johannes.halkoaho@helsinki.fi

The calcification of the abdominal aorta has been shown to correlate with cardiovascular risk [1]. Traditional methods for quantifying calcifications of the abdominal aorta often depend on manual interpretation of imaging. This study [2] introduces a machine learning based approach. Utilizing a dataset of 58 CT-angiography volumes representing various sclerosis stages, we developed two V-Net [3] ensemble neural network models. The first model segments the abdominal aorta and its branches, while the second segments the calcifications. The blood vessels were shortened to a fixed length using a separate algorithm after the model had made the prediction. The models performed well as evident in the achieved Dice scores (0.69 for calcifications, 0.96 for the aorta, 0.74 for its branches and 0.72 for the common iliac arteries) and volumetric similarities (0.80 for calcifications, 0.98 for the aorta, 0.87 for its branches and 0.91 for the common iliac arteries). This research presents a neural network model based method capable of simultaneously segmenting the aorta, its branches, and calcifications in contrast-enhanced CT angiography scans, offering potential for enhancing the efficiency and accuracy of cardiovascular risk assessments.

- [1] Jonas W Bartstra, Willem P Th M Mali, et al. “Abdominal aortic calcification: from ancient friend to modern foe”. In: *European Journal of Preventive Cardiology* 28.12 (Apr. 2020), pp. 1386–1391. ISSN: 2047-4873. DOI: 10.1177/2047487320919895.
- [2] Johannes Halkoaho, Oskari Niiranen, et al. “Quantifying the calcification of abdominal aorta and major side branches with deep learning”. In: *Clinical Radiology (Accepted)* ().
- [3] Fausto Milletari, Nassir Navab, et al. “V-Net: Fully Convolutional Neural Networks for Volumetric Medical Image Segmentation”. In: *CoRR* abs/1606.04797 (2016). arXiv: 1606.04797. URL: <http://arxiv.org/abs/1606.04797>.

Developing a machine learning interatomic potential to study radiation-induced damage in 3C-SiC

Ali Hamedani¹, and Andrea E. Sand¹

¹*Department of Applied Physics, Aalto University, 00076 Aalto, Espoo, Finland*

Corresponding author: ali.ahamedani@aalto.fi

Silicon carbide (SiC) has been a long-standing subject of study for its application in harsh environments. Theoretically, the nano-structural state of irradiation-induced defects in cubic SiC (3C-SiC) has been extensively studied with molecular dynamics using various empirical interatomic potentials. However, these potentials show significant discrepancy in predicting some of the properties, e.g. threshold displacement energies and defect formation and migration energies that are crucial in describing the evolution of defects generated in collision cascades. We present a Gaussian approximation machine learning potential (GAP) [1], trained over the data collected from density functional theory (DFT) calculations. The dataset comes with representative perfect and defective crystalline structures, with which we train our potential using the turbo-SOAP [3] many-body descriptor. The high repulsion of the energetic atoms encountered in collision cascades is captured by appending the ZBL [2] repulsive potential and inclusion of respective configurations in the dataset. The potential shows excellent agreement with DFT in predicting bulk, thermal, vibrational, and defect properties.

Acknowledgment: This work was funded by the European Union (ERC-2022-STG, project MUST, No. 101077454). Views and opinions expressed herein are those of the authors only and do not necessarily reflect those of the European Union or the European Research Council Executive Agency. Neither the European Union nor the granting authority can be held responsible for them.

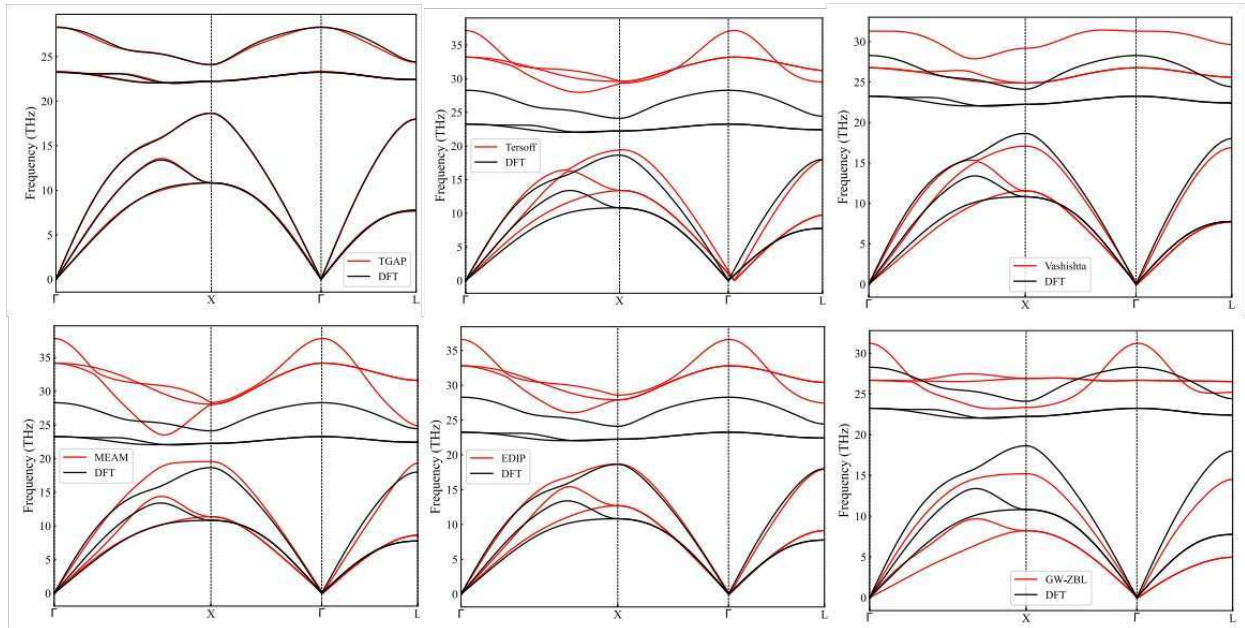


Fig. 1: Phonon bands in 3C-SiC simulated with empirical and presented potential (TGAP)

[1] Bartók, Albert P., et al. "Gaussian approximation potentials: The accuracy of quantum mechanics, without the electrons." *Physical review letters* 104.13 (2010): 136403.

[2] Ziegler J.F., Biersack J.P. and Littmark U., *The Stopping and Range of Ions in Matter* (Pergamon, New York) 1985.

[3] Caro, Miguel A. "Optimizing many-body atomic descriptors for enhanced computational performance of machine learning based interatomic potentials." *Physical Review B* 100.2 (2019): 024112.

Ultrahigh stability of oxygen FCC stacking sublattice in Ga₂O₃

R. He¹, J. Zhao³, J. Byggmästar¹, H. He^{1,4} and F. Djurabekova^{1,2}

¹ Department of Physics, University of Helsinki, P.O. Box 43, FI-00014, Finland

²Helsinki Institute of Physics, University of Helsinki, P.O. Box 43, FI-00014, Finland

³Department of Electrical and Electronic Engineering, Southern University of Science and Technology, Shenzhen 518055, China

⁴School of Nuclear Science and Technology, Xi'an Jiaotong University, Xi'an, Shaanxi 710049, China

Corresponding author: ru.he@helsinki.fi

Ga₂O₃ has been found to exhibit excellent radiation hardness properties, making it an ideal candidate for use in a variety of applications that involve exposure to ionizing radiation, such as space exploration, nuclear power generation, and medical imaging[1]. Understanding the behavior of Ga₂O₃ under irradiation is therefore crucial for optimizing its performance in these applications and ensuring their safe and efficient operation.

We used molecular dynamics simulations with the newly developed machine-learned Gaussian approximation potentials to investigate the radiation damage in β -Ga₂O₃. We inspected the gradual structural change in the β -Ga₂O₃ lattice with increasing doses of Frenkel pair implantations. The results revealed that O-Frenkel pairs have a strong tendency to recombine and return to their original sublattice sites. The accumulation of pure Ga-Frenkel pairs in the simulation cells might induce a transition of β to γ -Ga, while the O sublattice remains in the FCC crystal structure, which theoretically demonstrated the recent experimental finding that β -Ga₂O₃ transfers to the γ phase following ion implantation[2]. To gain a better understanding of the natural behavior of β -Ga₂O₃ under irradiation, we utilized collision cascade simulations. The results revealed that the O sublattice in the β -Ga₂O₃ lattice is robust and less susceptible to damage, despite O atoms having higher mobility.

Our theoretical models on the radiation damage of β -Ga₂O₃ provide insight into the mechanisms underlying defect generation and recovery during experimental ion implantation, which has significant implications for improving the radiation tolerance of Ga₂O₃, as well as optimizing its electronic and optical properties.

[1] Pearson, S. J., et al. "A review of Ga₂O₃ materials, processing, and devices." Applied Physics Reviews 5.1 (2018).

[2] A. Azarov, J. Fernández, J. Zhao, et al., Universal radiation tolerant semiconductor, Nature Communications 14, 4855 (2023).

Espoo goes quantum, the high school course on quantum computing

Matti Heikkinen¹, Ilkka Tittonen² and Niklas Halonen¹

¹*Otaniemi Upper Secondary School*

²*Department of Electronics and Nanoengineering, Aalto University*

Corresponding author: matti.heikkinen@eduespoo.fi

The quantum computing hands-on course was and is realized as a collaboration between Aalto University and the Espoo high school network introducing students to the reality of quantum computers and their applications. The course explores how information is expressed in the memory of conventional computers using bits and in the memory of quantum computers using qubits. Students learn the quantum mechanical rules and principles that the qubits follow, and the potential situations where the computational power of quantum computers could surpass that of conventional computers. The course involves generating code in the Python programming language, which can be sent to a real quantum computer in the cloud. It also provides a general picture of what quantum computing means in practice and examines several potential application areas.

The course content includes an introduction to the principles and applications of quantum computing in science. Students will learn to program even on a real quantum computer. The course begins by reviewing the necessary prerequisites from complex numbers, vector mathematics, matrix calculations, binary numbers, and the operation of basic logical circuits used by traditional computers. In addition to the classical background, the course teaches the principles of physics closely related to the operation of a quantum computer and the calculations of logical gates used in quantum computing to determine the states of qubits. The goal of the course is to produce code understood by a real quantum computer in the Python programming language.

Furthermore, the course discusses the billions of euros invested in quantum computing worldwide, presents reported business cases, and expected impacts on society. The course is completed by participating in workshops, following lectures published online, submitting tasks published online via the Google Classroom environment, participating in visits or course meetings, and there is also the possibility to complete it as distance online learning making it possible for students to take part everywhere in Finland.

Detecting Gravity at the Milligram Scale Using Optomechanics

Ewa Rej¹, Joe Depellette¹, Richa E. Cutting¹, Matthew Herbst¹, Yulong Liu², Mika. A. Sillanpää¹

¹Department of Applied Physics, Aalto University, FI-00076 Aalto, Finland

²Beijing Academy of Quantum Information Sciences, Beijing, China

Corresponding author: matthew.herbst@aalto.fi

Combining quantum mechanics and gravity into one unified theory remains the holy grail of physics. One experimental approach towards reaching this goal is to measure gravity at increasingly small scales, with set-ups based on torsion balances reaching masses of ~ 100 mg. However, the next step of measuring gravitational attraction between objects in quantum states does not seem feasible in such systems. Here we present progress towards a different approach, which implements micro-mechanical oscillators at cryogenic temperatures, optomechanically coupled to microwave cavities. These types of devices are well suited, since they can be prepared in their quantum ground state and quantum-mechanically entangled. In our experiment, we load a 1.3 mg gold sphere onto a silicon nitride membrane, forming a massive oscillator with a drum mode at 2 kHz. Using feedback cooling, as well as ~ 160 dB of vibrational isolation with respect to the pulse tube in the dilution refrigerator, we are able to reduce the oscillator's effective temperature by three orders of magnitude down to ~ 1 mK. In close proximity, a piezo-actuated 80 mg gold sphere acts as a time-dependent gravitational source, which can be detected by the oscillator if electromagnetic and vibrational cross-talk is sufficiently suppressed. We discuss the current status of the experiment, as well as the next steps towards measuring gravity between two quantum-mechanically entangled objects.

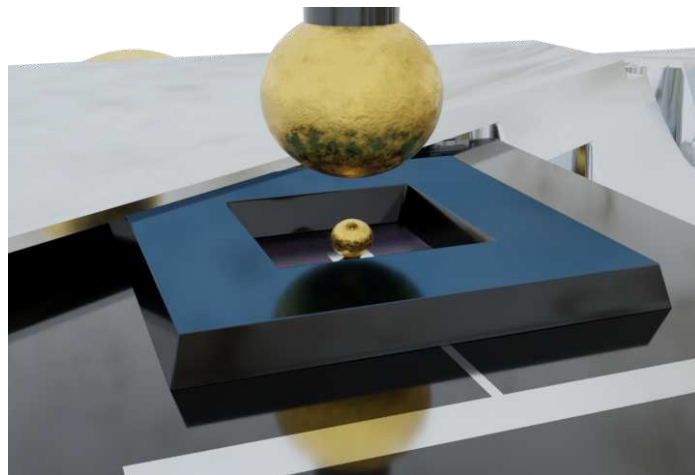


Figure 1: Digital render of the experiment. The large, gold sphere is piezo-actuated, causing a periodic gravitational force which we measure with the small, gold test mass.

[1] Yulong Liu, Jay Mummery, Jingwei Zhou, and Mika A. Sillanpää, *Gravitational Forces Between Nonclassical Mechanical Oscillators*, Phys. Rev. Appl. **15**, 034004 (2021).

Improved holographic analysis of the proton's structure

A. Hippeläinen¹, N. Jokela¹, M. Järvinen^{2,3} and R. Paatelainen¹

¹ Department of Physics and Helsinki Institute of Physics, P.O. Box 64, FI-00014, University of Helsinki, Finland

² Asia Pacific Center for Theoretical Physics, Department of Physics Pohang 37673, Republic of Korea

³ Pohang University of Science and Technology, Pohang 37673, Republic of Korea

Corresponding author: antti.hippelainen@helsinki.fi

We study the proton's structure with holographic methods. The primary results are correct predictions for gravitational form factors, which are then used to compute mechanical properties of the proton.

This study follows the path set forward by the construction of the upcoming Electron-Ion-Collider in Brookhaven, New York [1]. The extended capability of probing the structure of the proton up to the inclusion of spin effects motivates one to study and develop also holographic methods. These allow the study of strongly coupled theories at non-asymptotically high energy scales, making this analysis possible.

The holographic model used is Improved Holographic QCD (IHQCD) [2, 3], which is optimized especially to reproduce the gluonic mass spectra. This makes it ideal for computing gluonic gravitational form factors. These are a major component in describing the structure of the proton, especially the so-called D -term, which has also been hailed the “last global unknown”.

We compute these form factors of the proton with IHQCD as the gravitational background and the proton as a Dirac fermion [4]. Gravitational form factors between models are identified based on index structure. They are fit to most recent lattice data, and we obtain a good fit for both the global D -term and an energy scale agreeing with QCD.

After this, mechanical properties of the proton are studied thoroughly with form factors [5], including for example pressure and shear forces inside the proton. These agree with both experimental and lattice data especially qualitatively, fulfilling physical requirements, and thus describing realistically the inner workings of the proton.

[1] Electron-Ion Collider, <https://www.bnl.gov/eic/>

[2] Kiritsis et al., JHEP **02**, 2008 (2008)

[3] Kiritsis et al., JHEP **02**, 2008 (2008)

[4] Mamo et al., PRD **8**, 101 (2020)

[5] Polyakov et al., IJMPA **26**, 33 (2018)

Manipulating the charger ion distribution towards fixed properties

Sebastian Holm¹, Tiia Laurila¹, Lauri Ahonen¹, Jesse Haataja¹, Juha Kangasluoma¹ and Dominik Stolzenburg^{1,2}

¹INAR / University of Helsinki, Helsinki, Finland

²Institute for Materials Chemistry, TU Wien, Vienna 1060, Austria

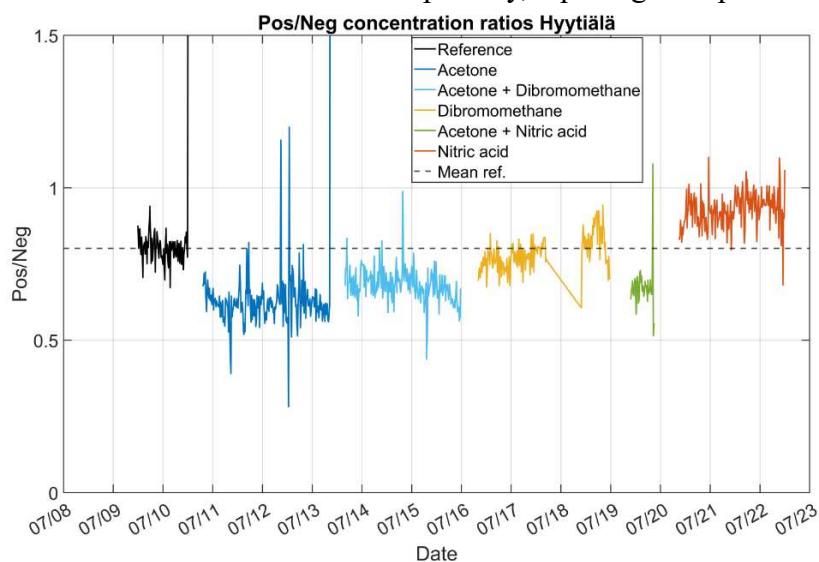
Corresponding author: sebastian.holm@helsinki.fi

The charged fractions of aerosols are conventionally determined by using charging theories. Fuchs' theory [1] is applied to predict the charged fractions for bipolar aerosol chargers in the transition regime. Wiedensohler [2] fitted above mentioned theory with fixed ion properties, which became the standard for the calculation of charged fractions for data inversion of aerosol size distributions. However, in ambient "real-world" measurements the properties of charger ions can vary significantly, thus leading to substantial differences from the predictions by Wiedensohler's approximation. Changes in the carrier gas through the charger and trace impurities in the gas itself are affecting the ion properties [3], leading to significant uncertainties in aerosol size-distribution measurements [4].

Here we show that the charger ion properties can be efficiently manipulated by the introduction of known trace compounds to the sample flow through a bipolar aerosol charger. Our work covers measurements conducted in laboratory environment in Helsinki and in the boreal forest of Hyytiälä, Finland. A Ni-63 radioactive bipolar ion source was used in combination with a half mini type and a Hauke type DMA to determine the electrical mobility size distributions of the charger ions and the aerosol size distribution simultaneously. The doping chemicals were introduced to the charger in the vapour phase by bubbling compressed air through the liquids. Acetone, dibromomethane, and nitric acid were used as dopants. During the field measurements, the timespan of each chemical combination was between one to three days to yield some variations in ambient conditions.

Fig. 1 shows the concentration ratios of positively and negatively charged particles measured by the Hauke type DMPS from the field measurements in Hyytiälä 2020. The black line furthest to the left is the reference where a "clean" charger was used. The addition of doping chemicals to the charger shifts this ratio, indicating that the charged fractions were significantly altered. Acetone, acetone-dibromomethane and nitric acid-dibromomethane combinations affected the ratio towards the negatively charged ions. Nitric acid by itself shifted the ratio towards the positively charged ions, while the addition of dibromomethane had seemingly marginal effect on the ratio. We connect the shift in charged fractions to the different charger ion mobility distributions measured by the high-resolution half mini DMA and verify this by charging efficiency measurements performed in the laboratory.

Our results show that manipulating the charger ion distribution via chemical doping can significantly manipulate the charged fractions under varying ambient conditions and shift charging efficiencies towards a desired polarity, opening the possibility to enhance signal and decrease



systematic uncertainties in aerosol size distribution measurements.

Fig. 1: Concentration ratios of positively and negatively charged ions in Hyytiälä.

[1] Fuchs, N. A., *Geofis. Pura. Appl.*, 56(1), 185-193 (1963).

[2] Wiedensohler, A. J. *Aerosol Sci.*, 19(3), 387-389 (1988).

[3] Steiner, G., & Reischl, G. P., *J. Aerosol Sci.*, 54, 21-31 (2012).

[4] Kangasluoma, J., & Kontkanen, J., *J. Aerosol Sci.*, 112, 34-51 (2017).

Laser assisted sputter ion source—most recent results

A. Hossain,^{1, a)} O. Tarvainen,² M. Reponen,¹ R. Kronholm,¹ J. Julin,¹ T. Kalvas,¹ V. Toivanen,¹ M. Kivekäs,¹ and M. Laitinen¹

¹⁾*Accelerator Laboratory, Department of Physics, University of Jyväskylä, FI-40014 Jyväskylä, Finland*

²⁾*STFC ISIS Pulsed Spallation Neutron and Muon Facility, Rutherford Appleton Laboratory, Harwell, OX11 0QX, UK*

(Dated: 29 January 2024)

Caesium sputter ion sources are used for the production of negative ion beams for Ion Beam Analysis (IBA) and Accelerator Mass Spectrometry (AMS) applications. The negative ion production in the Source of Negative Ions by Caesium Sputtering (SNICS) occurs on the surface of a cathode, which contains the ionized materials and is exposed to caesium ion bombardment¹. Vogel introduced a hypothesis based on resonant ion pair production where the negative ion yield could be enhanced by exposing the cathode to a laser beam resonantly exciting neutral caesium atoms to 7p electronic states². JYFL-ACCLAB have demonstrated that the photo-assisted production of negative ions can be provoked by a non-resonant lasers with the photon energy exceeding a certain threshold, and a significant beam current enhancement factor was observed^{3–5}. Furthermore, we have also reported that the extracted beam currents of negative ions of halide elements can be increased by a factor of up to 9⁶. Recently, we have observed a priming effect, i.e. applying a number of laser pulses at certain ion source settings causes the beam current measured without the laser to increase significantly and remain high after ceasing the laser pulsing (Unpublished, Accepted by Conference Editor).

In this presentation, we present the overview of our existing results and the corresponding qualitative model for the laser-assisted beam current enhancement mechanism. Finally, we present the results of our first attempts to sustain a stable beam current at the elevated level over several hours, achieved through active control of the laser power.

REFERENCES

¹P. Williams, “The sputtering process and sputtered ion emission,” *Surface Science* **90**, 588–634 (1979).

²J. S. Vogel, “Lasis: The laser assisted sputter ion source,” *Nuclear Instruments and Methods in Physics Research Section B: Beam Interactions with Materials and Atoms* **438**, 89–95 (2019).

³O. Tarvainen, R. Kronholm, M. Laitinen, M. Reponen, J. Julin, V. Toivanen, M. Napari, M. Marttinen, D. Faircloth, H. Koivisto, and T. Sajavaara, “Experimental evidence on photo-assisted O[−] ion production from Al₂O₃ cathode in cesium sputter negative ion source,” *Journal of Applied Physics* **128**, 094903 (2020).

⁴O. Tarvainen, R. Kronholm, M. Laitinen, M. Reponen, J. Julin, V. Toivanen, M. Napari, M. Marttinen, T. Kalvas, D. Faircloth, H. Koivisto, and T. Sajavaara, “Photo-assisted O[−] and Al[−] production with a cesium sputter ion source,” *AIP Conference Proceedings* **2373**, 020001 (2021).

⁵A. Hossain, O. Tarvainen, M. Reponen, R. Kronholm, J. Julin, T. Kalvas, V. Toivanen, M. Kivekäs, and M. Laitinen, “Photo-enhanced o-, h- and br- ion production in caesium sputter negative ion source—no evidence for resonant ion pair production,” *Journal of Physics D: Applied Physics* **55**, 445202 (2022).

⁶A. Hossain, O. Tarvainen, M. Reponen, R. Kronholm, J. Julin, T. Kalvas, V. Toivanen, M. Kivekäs, and M. Laitinen, “Photo-assisted cl-, br- and i- production in caesium sputter ion source,” *Journal of Instrumentation* **18**, C07002 (2023).

^{a)}Electronic mail: akbar.a.hossain@jyu.fi

Atomically sharp lateral heterostructures of VSe₂—NbSe₂

Xin Huang¹, Héctor González-Herrero², Orlando J. Silveira¹, Peter Liljeroth¹,
Adam S. Foster¹, Jani Sainio¹

¹*Department of Applied Physics, Aalto University, FI-00076 Aalto, Finland*

²*Departamento Física de la Materia Condensada, Universidad Autónoma de Madrid, Madrid E-28049, Spain*

We explore the potential of lateral heterostructures of transition metal dichalcogenides for creating artificial designer quantum materials. While vertical heterostructures, by stacking van der Waals materials, have been extensively produced, realizing high-quality lateral heterostructures with atomically sharp interfaces remains a major experimental challenge. Here, we develop one-pot two-step molecular beam lateral epitaxy, and fabricate atomically precise and well-defined lateral heterostructures of 1T-VSe₂ and 1H-NbSe₂. Scanning tunneling microscopy and spectroscopy reveal several distinct types of interfaces, with corroboration by density functional theory calculations. And interfaces exhibit a 1D array of electronic states and zero-bias anomalies. Our results demonstrate a general approach for constructing high-quality lateral heterostructures and building 1D arrays of interface states and paving the way for further studies of quantum materials.

Exploring the gravitational wave power spectrum from first-order phase transitions

Jenni Häkkinen^{*1}, Deanna C. Hooper¹, David J. Weir¹

¹*Department of Physics and Helsinki Institute of Physics, PL 64, FI-00014 University of Helsinki, Finland*

*Corresponding author: jenni.hakkinen@helsinki.fi

As the very young and hot universe cooled down, it may have undergone a phase transition (PT) due to the spontaneous breaking of the electroweak symmetry. In many extensions of the Standard Model of particle physics this electroweak PT is of first order, which would allow the production of early-universe gravitational waves (GWs). The PT proceeds via bubble nucleation, and these expanding and colliding bubbles produce a stochastic background of GWs in the frequency range of the future space-based GW detector LISA. This gives us a direct window to the earliest moments of the universe when it was less than a second old. The potential GW signal depends on the underlying particle physics model as it determines the properties of the PT. We present two alternative ways to compute the GW power spectrum from the PT parameters with the PTPlot[†] tool: one using a broken power law ansatz of the shape of the power spectrum and another using numerical hydrodynamical calculations of the bubble fluid profile and the Sound Shell Model. Additionally, we estimate the likelihood of detecting a signal with LISA by looking at the signal-to-noise ratio of these scenarios.

[†]ptplot.org

Density dependence of quantised vortex tension in ^4He

A. E. Ikaheimo, T. Kamppinen, and V. B. Eltsov

Department of Applied Physics, Aalto University, Espoo, Finland

Corresponding author: atso.ikaheimo@aalto.fi

At temperatures below 2.1 K, liquid helium enters a superfluid state in which a fraction of the fluid loses all viscosity. Flow in the superfluid is irrotational except in the presence of quantized vortices. Singly quantized vortices are energetically favored in ^4He , so all vortices present in a superfluid are identical [1].

We have designed and manufactured nanoelectromechanical resonators which are sensitive to force from a quantised vortex attached to the device [2]. A pinned vortex both increases the resonant frequency and decreases the quality factor of the resonator. Different pinning configurations, distinguished by discrete shifts in frequency and damping, are observed when vortices are produced by a quartz tuning fork near the device. Converting these shifts to the magnitude of vortex tension requires precise knowledge of the geometry of the attached vortex, which is still unclear.

We have confirmed that the observed changes in the resonant frequency of the device are caused by the tension of the attached vortex, as the tension is proportional to the density of the fluid. The density of the fluid increases with pressure.

The resonant properties of the device have been measured at pressures between 1 and 12 bar and at temperature 20 mK both with and without an attached vortex. The frequency shift of the most probable vortex configuration (type 1 in Fig. 2) has been found to increase with the helium density at a rate comparable to the expected effect of the tension increase.

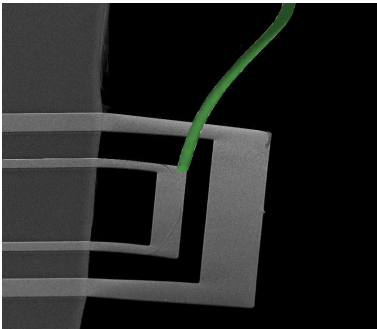


Figure 1: SEM image of a resonator with a possible vortex configuration.

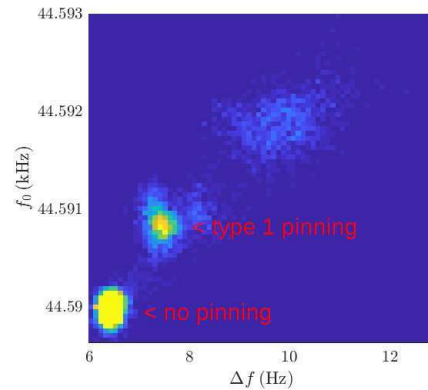


Figure 2: 2D histogram of measured resonant frequency as a function of measured resonance width at 3.2 bar.

- [1] R. J. Donnelly, *Quantized Vortices and Turbulence in Helium II*, Cambridge U. Press. (1991)
- [2] T. Kamppinen, Superfluid ^4He as a rigorous test bench for different damping models in nanoelectromechanical resonators, *Phys. Rev. B* **107**, 014502 (2023)

Wearable temperature distribution sensing platform

Immonen A.¹, Goel P.², Koskinen T.², Pekkanen M.¹, Kärkkäinen T.J.¹, Peltonen H.^{3,4},
Kuisma M.¹, Silventoinen P.¹, and Tittonen I.²

¹ Laboratory of Applied Electronics, LUT University, Lappeenranta, Finland

² Department of Electronics and Nanoengineering, Aalto University, Finland,

³ Sport Business Management, University of Applied Science, Jyväskylä

⁴ Faculty of Sport and Health Sciences, University of Jyväskylä

Corresponding author: antti.immonen@lut.fi

A vital role of the human circulatory system is to distribute the metabolic heat between the body core and the peripheral parts. These thermal flow patterns can reveal important information about the bodily processes behind the observed skin surface heat flow signature. This can then be interpreted and inferred into insights about metabolism, vascular health or processes of thermoregulation.

Our solution builds upon using a wearable temperature distribution sensor. The actual measurement is based on an ALD thermoelectric thin film in which the selected materials are safe for the human body contact and conform with the curvatures of the human body, enabling a proper contact. In contrast with conventional single-point measurements of wearables, the thin film enables mapping of the temperature distribution. Further, the thin film can be tailored quite freely in size.

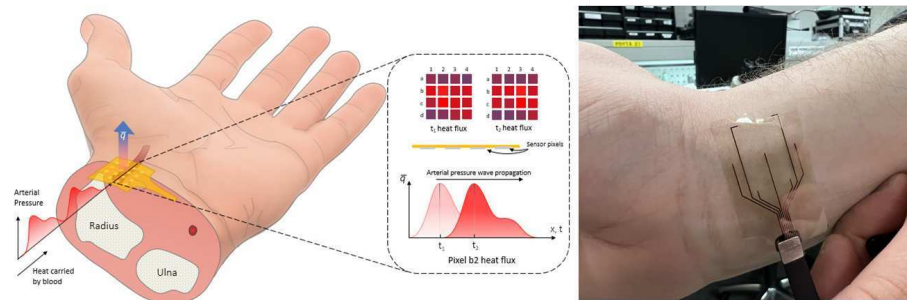


Figure 1: Temperature and heat measurement modalities of the sensor film. A multi-thermoleg thermocouple was deposited on a flexible substrate by means of atomic layer deposition and interfaced with a flexible printed circuit.

Interestingly, thermoelectricity enables transduction of electric signal directly from the temperature difference without necessarily having to be externally powered. The technological challenges to be discussed are related to measurement of thermal gradients in the film to form a two-dimensional thermal map, formation of electric contacts with the thin film and an improvement of the overall signal-to-noise ratio.

Thermal information can be recorded with a high spatiotemporal resolution to gain heightened context-awareness and of the measurement conditions and heat transfer. Based on the skin surface measurements, subcutaneous temperatures can be estimated more reliably than conventional wearables. The proposed measurement platform enables differentiation of physiological processes such as endothelial function and improved signal robustness against the unpredictable dynamics of environmental coupling which have traditionally made continuous wrist-based temperature measurement practically infeasible or unreliable.

Multiscale modeling of irradiation damage evolution for quantum technology

Ville Jantunen¹, Tomás Fernández Bouvier¹, Aleksi Leino¹, and Flyura Djurabekova¹
¹ *Division of Materials Physics, Faculty of Science, University of Helsinki, Helsinki, Finland*

Corresponding author: ville.jantunen@helsinki.fi

Solid state quantum technology is based on manufacturing specific point defects in a suitable host matrix. Two examples of such point defects are substitutional P in Si, and the NV-center in diamond. P and N can be introduced in their corresponding host materials using existing ion beam technology, or as often is the case with N, they may already be present in the material.

As a byproduct, irradiation creates defects, such as interstitials and vacancies in the material. Vacancies are required to form the NV centers in diamond, but may be detrimental for the P cubits in Si as they can convert them into E-centers (PV).

We model the irradiation process in these two materials with a multiscale approach consisting of Molecular Dynamics and Kinetic Monte Carlo in order to capture the primary damage formation during the irradiation, and during longer time scales after it. We focus on the modeling workflow, using P in Si and NV-center as examples.

**Development and commissioning of HIBISCUS:
A new ion beam Radio Frequency Quadrupole Cooler Buncher for
high-precision experiments with exotic radioactive ions at
NUSTAR/FAIR**

A. Jaries^{1,2} for the MATS-LaSpec Experiment Collaboration
¹*University of Jyväskylä, Department of Physics, Accelerator Laboratory,
PO Box 35, FI-40014 University of Jyväskylä, Finland and*
²*Helsinki Institute of Physics, FI-00014, Helsinki, Finland*

NUSTAR (Nuclear Structure, Astrophysics and Reactions) experiment at FAIR will explore exotic nuclei far from stability. The mass measurements and laser spectroscopy will be performed with the MATS and LaSpec experiments. In order to fully utilise the unique production capabilities at FAIR, the radioactive beams have to be slowed down and bunched for the experiments. For this purpose, a new ion beam cooler-buncher has been built in the JYFL accelerator laboratory of University of Jyväskylä, Finland, where the device is being commissioned and characterized before transportation to its final location in the low-energy branch of FAIR [1]. The cooler-buncher — a Finnish in-kind contribution named HIBISCUS — is a central device as it will transform the beam of ions from the upstream cryogenic stopping cell behind the Super FRS [2] to be suitable for downstream experiments at MATS and LaSpec experimental halls [3]. The device features an enclosed quadrupolar electrode configuration for application of a radio frequency electric field for ion confinement and is filled with helium gas for ion cooling. The axial field is realized with progressively shorter wedge-shaped electrodes placed in-between the radiofrequency electrodes. Ions can be extracted as a continuous beam or collected into a pair of potential wells in subsequent enclosures on the exit side of HIBISCUS, for beam bunching. In this mode, HIBISCUS can be set to deliver bunches either with low energy spread or low temporal spread. Upon extraction, the ions are accelerated back to 6 keV of energy to be then sent to downstream setups and experiments.

- [1] P. Spiller et al., NIM A 561 (2) (2006) 305–309
- [2] M. Winkler et al., NIM B 266 (19-20) (2008) 4183–4187
- [3] D. Rodríguez et al., EPJ ST 183 (2010) 1–123

Recent mass measurements of neutron-rich rare-earth nuclides with the JYFLTRAP double Penning Trap at IGISOL for the astrophysical r-process.

A. Jaries¹ on behalf of the I283 Experiment Collaboration
¹*University of Jyväskylä, Department of Physics, Accelerator Laboratory,
PO Box 35, FI-40014 University of Jyväskylä, Finland*

High precision atomic mass spectrometry of neutron-rich rare-earth nuclides near $A \sim 165$ was performed recently with the JYFLTRAP double Penning trap [1] using the phase-imaging ion cyclotron resonance technique [2] at the IGISOL facility in the JYFL Accelerator Laboratory. Altogether eleven masses were measured, with a typical relative accuracy in the 10^{-8} range. The mass measurements continued the previous successful measurement campaigns at JYFLTRAP in this region [3,4] and now reached up to the $N=104$ neutron midshell, important for studying how the nuclear structure evolves further from stability. The properties of these nuclides also impact the models describing the formation of the rare-earth abundance peak around $A \sim 165$ in the astrophysical rapid neutron capture (r) process [5], which has produced around half of the heavy-element abundances in the Solar System and takes place at least in neutron-star mergers. As variations in nuclear masses affect all the relevant nuclear properties of neighboring nuclei that depend on the mass, reducing their related uncertainties give better constraints on the calculated astrophysical reaction rates. The latter are thus critical inputs for modelling the stellar nucleosynthesis and for understanding origins of different chemical elements found on Earth and their abundances in the Solar System.

- [1] T. Eronen et al., *The European Physical Journal A* 48 (2012) 46
- [2] D. A. Nesterenko et al., *The European Physical Journal A* 54 (2018) 154
- [3] M. Vilen et al., *Physical Review Letters* 120, 262701 (2018)
- [4] M. Vilen et al., *Physical Review C* 101, 034312 (2020)
- [5] M. Mumpower et al. *Physical Review C* 85, 045801 (2012)

Developing a general-purpose machine learning interatomic potential for Ge

Ruoyan Jin¹, Ali Hamedani¹, and Andrea Sand¹

¹*Department of Applied Physics, Aalto University, 00076 Aalto, Espoo, Finland*

Corresponding author: andrea.sand@aalto.fi

We present a general-purpose Gaussian approximation machine learning interatomic potential (GAP [1]) for Ge. Our dataset includes data from density functional theory (DFT) calculations where we cover different crystalline phases, defects, liquid and amorphous phases, and surfaces. We use a two-body and a turboSOAP [2, 3] many-body descriptor to train our potential. Along with the general properties, we consider the capability of the potential in simulating radiation-induced damage. For that purpose we append the potential with the ZBL repulsive potential [4] and include the relevant structures in the dataset. The potential already shows excellent agreement with DFT in predicting bulk properties, where it outperforms existing common classical potentials [5, 6].

This work was funded by the European Union (ERC-2022-STG, project MUST, No. 101077454). Views and opinions expressed herein are those of the authors only and do not necessarily reflect those of the European Union or the European Research Council Executive Agency. Neither the European Union nor the granting authority can be held responsible for them.

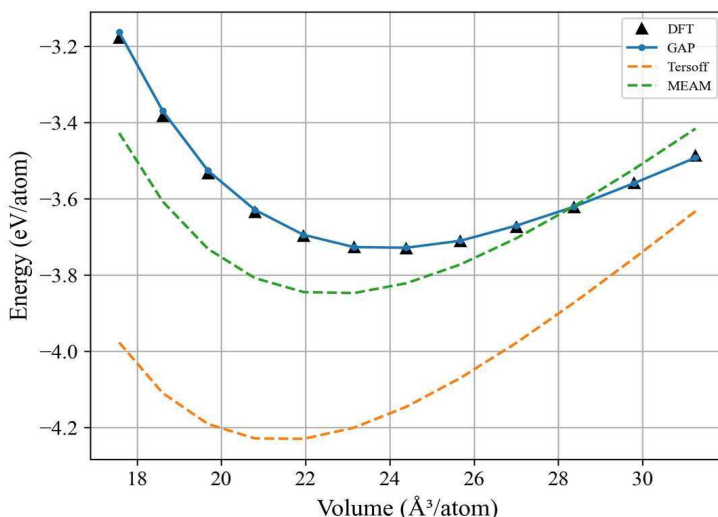


Fig. 1: Energy-volume curve for Ge diamond structure predicted by GAP model as compared with the DFT, MEAM and Tersoff models.

- [1] Bartók, A.P. et al. Gaussian Approximation Potentials: The Accuracy of Quantum Mechanics, without the Electrons, *Phys. Rev. Lett.* **104**, 136403 (2010).
- [2] Bartók, A.P. et al. On representing chemical environments, *Phys. Rev. B* **87**, 184115 (2013).
- [3] Caro, M.A. Optimizing many-body atomic descriptors for enhanced computational performance of machine learning based interatomic potentials, *Phys. Rev. B* **100**, 024112 (2019).
- [4] Ziegler, J.F. et al. The Stopping and Range of Ions in Matter, in *Treatise on Heavy-Ion Science: Volume 6: Astrophysics, Chemistry, and Condensed Matter*, edited by D. Allan Bormley (Springer, Boston, 1985), pp. 93-129.
- [5] Kim, E.H. et al. A modified embedded-atom method interatomic potential for Germanium, *Calphad*, **32(1)**, 34 (2008).
- [6] Mahdizadeh, S.J. et al. Optimized Tersoff empirical potential for germanene, *J. Mol. Graph. Model*, **72**, 1 (2017).

Non-computing quantum computing

Mikael Johansson
CSC – IT Center for Science, Espoo, Finland
mikael.johansson@csc.fi

From the point-of-view of classical computing, quantum computers are strange. By construction, they possess the ability to explicitly use quantum physical phenomena to their advantage, in itself a feat sure to attract envy in the most powerful of classical supercomputers. An even more curious feature is found in how quantum computers can blur the border between simulation and experiment. As a by-product of taming the quantum world to run mathematical algorithms, quantum computers are in themselves high-precision quantum laboratories.

While the eager computational scientists still have to contain themselves for a bit before quantum computers will solve the computational bottlenecks in their modelling workflows, quantum advantage can already now be found elsewhere. Quantum computers have for example been transformed into new states of matter in the form of time crystals [1,2], behaved in wormhole-like manners [3], and coerced into becoming something like black holes [4]. In these *non-computing* applications, the quantum processing units, QPUs, in a sense become what they simulate.

This is not a scientific presentation, it is a presentation for scientists. With quantum computers now available both in the cloud and as part of supercomputing infrastructure [5], the doors have been opened for a rather new type of science and physics research. There's a new tool in town, let's put it to good use!



Fig. 1: Artificial artist's rendition of non-computing quantum computing applications.

- [1] X. Mi *et al.*, “Time-crystalline eigenstate order on a quantum processor”, *Nature* **601**, 531 (2022). <https://doi.org/10.1038/s41586-021-04257-w>
- [2] P. Fray and S. Rachel, “Realization of a discrete time crystal on 57 qubits of a quantum computer”, *Sci. Adv.* **8**, eabm7652 (2022). <https://doi.org/10.1126/sciadv.abm7652>
- [3] D. Jafferis *et al.*, “Traversable wormhole dynamics on a quantum processor”, *Nature* **612**, 51 (2022). <https://doi.org/10.1038/s41586-022-05424-3>
- [4] Y.-H. Shi *et al.*, “Quantum simulation of Hawking radiation and curved spacetime with a superconducting on-chip black hole”, *Nat. Commun.* **14**, 3263 (2023). <https://doi.org/10.1038/s41467-023-39064-6>
- [5] The Finnish Quantum-Computing Infrastructure FiQCI. <https://fiqci.fi/>

Integrating solar energy to the Finnish power system

Sami Jouttijärvi¹, Lauri Karttunen¹, Samuli Ranta², and Kati Miettunen¹

¹*Solar Energy Materials and Systems, Department of Mechanical and Materials Engineering, University of Turku, Turku, Finland*

²*New Energy Research, Turku University of Applied Sciences, Turku, Finland*

Corresponding author: sami.jouttijarvi@utu.fi

Solar photovoltaic (PV) electricity production is growing rapidly in Finland. In a power system with a high share of PV, the intermittent and weather-dependent nature of the PV production causes challenges, such as oversupply of PV electricity around noon and rapid decrease of PV production during afternoon, inducing high electricity price variation and need for balancing power generation. These challenges will be relevant in Finland in the future, as the PV production increases.

To mitigate the side effects of increasing PV production, smart integration of PV to the power system, considering the temporal compatibility of PV production and electricity load, is crucial. Vertical bifacial PV (VBPV, **Figure 1**) is an attractive option, especially in the Nordics, where VBPV provides better temporal match with electricity load and higher annual production compared with conventional monofacial PV [1]. Thus, VBPV enables high self-consumption in residential houses and high production during morning and evening, when the electricity price peaks, increasing the economic value [1] and grid compatibility [2] of PV electricity.

The Nordic solar irradiation conditions, especially low solar elevation, are suitable for VBPV, but they create challenges for solar irradiance modelling. Most of the state-of-the-art irradiance modelling tools work insufficiently with low solar elevation, highlighting the need for tools that work well in Nordic conditions [3]. Moreover, finding suitable installation sites for VBPV is a major challenge due to shading vulnerability [4]. Our work aims to increase the share of PV in the Finnish power system by identifying the optimal PV solutions and by removing the barriers halting their implementation.

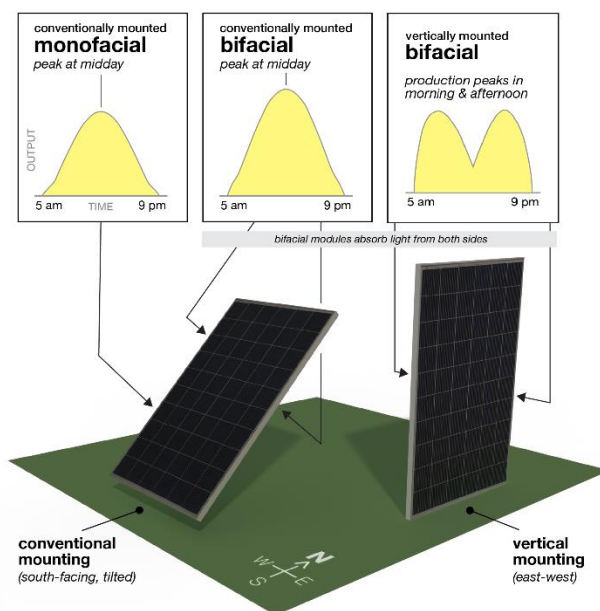


Figure 1: A schematic illustration of a conventionally mounted mono- or bifacial panel and a vertically mounted bifacial solar panel. Vertical bifacial panel has high production during the morning and evening. Modified based on figures created by Glen Forde / University of Turku.

[1] S. Jouttijärvi et al. *Appl Energy*, under review, 2023.

[2] S. Jouttijärvi et al. *Sol Energy* 262, 111819, 2023, doi: 10.1016/j.solener.2023.111819

[3] M. Manni et al. *Renew Energy* 220, 119722, 2024, doi: 10.1016/J.RENENE.2023.119722

[4] B. Viriyaraj et al. *Front Built Environ* 10, 2024, doi: 10.3389/fbuil.2024.1343036

Improving the detection limit in lung counting with a highly segmented HPGe detector

H. Jutila^{1,2}, P. T. Greenlees^{1,2}, T. Torvela³ and M. Muikku³

¹Accelerator Laboratory, Department of Physics, University of Jyväskylä, Finland

²Helsinki Institute of Physics, University of Helsinki, Finland

³STUK – Radiation and Nuclear Safety Authority, Vantaa, Finland

Corresponding author: henri.m.jutila@jyu.fi

There exist many problems associated with whole-body counting and lung counting which aim to determine the level of contamination in a human body. Even small amounts of radioactive material containing, e.g., americium, plutonium, or both are extremely dangerous when inhaled or digested due to the long biological half-life. However, observing these radioisotopes directly via low energy gamma-ray detection is difficult. Problems arise in the form of Compton scattering background events which make it hard to identify the low-energy gamma rays. Typically measurements are long and require a low background room or sufficiently shielded mobile measurement laboratory for field measurements. In principle, if the interaction point can be localized it is possible to distinguish the low-energy events from high-energy events. Due to the nature of gamma-ray interactions with matter, the low-energy gamma rays are absorbed in the “front” of a germanium detector while the background events will be distributed more uniformly inside the detector. The identification of the events can be achieved using an electrically segmented germanium detector with optimized geometry. Signals from different segments can be isolated from each other and used to discriminate between different interaction types. Furthermore, such a detector could be combined with additional detectors such as a scintillator-based shield to further suppress background.

A highly segmented High Purity Germanium (HPGe) detector was used to measure radiation from ²⁴¹Am activity located inside the lungs of an anthropomorphic phantom with various active and passive shield configurations. It was found that the background suppression shield does not play a significant role in reducing the Minimum Detectable Activity (MDA) compared to a veto based on the segmentation in the depth direction of the HPGe when measuring low-energy gamma rays. A reduction of up to 57 % in the MDA was obtained. The MDA could be further improved by a thinner lateral segmentation and an optimal anti-Compton shield coupled with an active or passive backplate. The new detector application would be particularly useful in mobile whole-body counting units where the natural background radiation poses a challenge when measuring low-energy gamma rays.

This research is part of the RAD3S project in the HIP technology programme and is carried out in collaboration between the University of Jyväskylä and the Finnish Radiation and Nuclear Safety Authority (STUK).

Modelling the structure of amorphous Al₂O₃ under stress

J. Kalikka¹

¹ Computational Physics Laboratory, Tampere University, Finland

Corresponding author: janne.kalikka@tuni.fi

Oxide glasses are a family of hard but brittle materials at room temperature. Many applications could use a hard and light material but the tendency to fracture severely limits the use of oxide glasses in critical or load-bearing components. Al₂O₃ is a binary ceramic material, which has multiple crystalline phases, and can also exist in amorphous glassy form.

The unusual nanoscale ductility of pulsed laser deposited (PLD) Al₂O₃ at room temperature was shown experimentally[1], and the atomistic mechanisms were studied using a classical molecular dynamics simulations in order to gain insight into what makes this possible. It was found that the PLD grown structure of amorphous Al₂O₃ is dense, uniform and "flaw free" enough to allow plastic deformation to happen via interatomic bond switching during loading.

In general, any defects in the material act as pinning points, facilitating stress build-up and eventual fracture. However, if the activation energy for bond switching between the atoms is low enough with respect to the initial flaw size, the structure will deform via bond switching before the stress build-up in the flaws is high enough to cause fracture. Another requirement for plasticity is that the volume fraction of nanoscale cavities or voids in the structure is small enough and that the cavities do not span spatially large areas so that they don't restrict the bond switching by limiting the number of non-nearest neighbour atoms near a given atom.

Later it was shown that the plasticity can also be seen in the microscale, in a study about micropillar compression[2], and a finite element method model was developed to model a full micropillar deformation in addition to atomistic simulations of the bulk and nanoscale pillars or wires.

[1] Frankberg *et al.*, *Science* **366**, 864-869 (2019)

[2] Frankberg *et al.*, *Adv. Mater.*, **35**, 2303142 (2023)

New method to characterize thin film chemistry

Antti-Jussi Kallio¹, Alexander Weiß², Mikko Heikkilä², Rene Bes¹, Marianna Kemell², Mikko Ritala², Simo Huotari¹,

¹Department of Physics, P.O.Box 64, FI-00014 University of Helsinki, Finland

²Department of Chemistry, P.O.Box 55, FI-00014 University of Helsinki, Finland

Corresponding author: antti-jussi.kallio@helsinki.fi

In order to achieve highly precise control over matter at the atomic level using atomic layer deposition, the challenge is to understand the evolution of the local chemical environment and the oxidation state of the element of interest during the different stages of film growth. X-ray absorption spectroscopy allows to determine the local chemical environment and oxidation states of a given element. This technique has been very rarely available outside of large scale facilities such as synchrotrons and is thus not used for routine characterization as X-ray diffraction is nowadays. Thanks to the recent development in X-ray optics we have been able to construct a laboratory-scale X-ray spectrometer, enabling thin film characterization at Helsinki Center for X-ray spectroscopy [1].

Here we present laboratory-scale X-ray absorption spectroscopy applied to the research of nanometer-scale thin films. We demonstrate the Cu K edge X-ray absorption near edge structure (XANES) and extended X-ray absorption fine structure (EXAFS) of CuI and CuO thin films [2,3] grown with atomic layer deposition. Film thicknesses in the investigated samples ranged from 12 to 248 nm. Even from the thinnest films, XANES spectra can be obtained in 5–20 minutes and EXAFS in 1–4 days. In order to prove the capability of laboratory-based XAS for *in situ* measurements on thin films, we demonstrate an experiment on *in situ* oxidation of a 248 nm thick CuI film at a temperature of 240 °C. The study has enabled new research on inorganic chemistry and materials and created tools for novel *in situ* studies on thin films

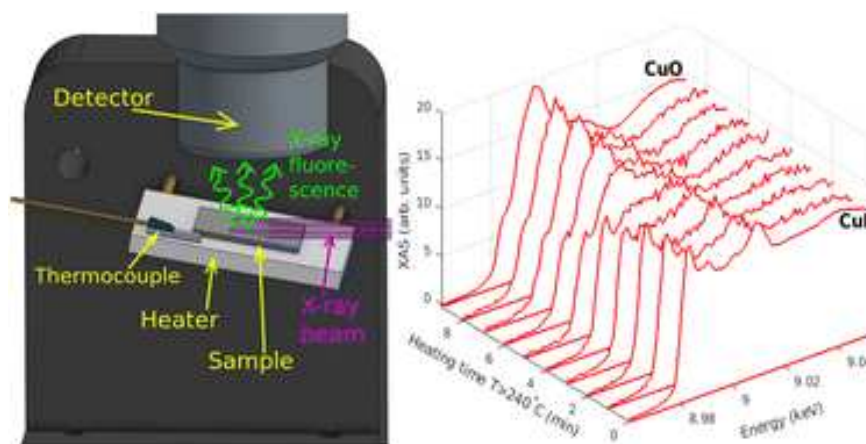


Fig. 1: Optimized setup for fluorescence mode detection along with obtained spectra during *in situ* annealing.

- [1] <https://www.helsinki.fi/en/infrastructures/center-for-x-ray-spectroscopy>
- [2] A.-J. Kallio, A. Weiß, R. Bes, M.J. Heikkilä, M. Ritala, M. Kemell, S. Huotari, Laboratory-scale X-ray absorption spectroscopy of 3d transition metals in inorganic thin films, Dalton Trans., 2022,51, 18593-18602
- [3] A. Weiß, J. Goldmann, S. Kettunen, G. Popov, T. Iivonen, M. Mattinen, P. Jalkanen, T. Hatanpää, M. Leskelä, M. Ritala, M. Kemell, Conversion of ALD CuO Thin Films into transparent conductive p-type CuI thin films, Adv Mater. Interfaces, 2023, 10, 2201860

Particle Physics with Machine Vision

M. Kalliokoski¹

¹ Detector Laboratory, Helsinki Institute of Physics, University of Helsinki, Helsinki, Finland

Corresponding author: matti.kalliokoski@helsinki.fi

Solid State Nuclear Track (SSNTD) detectors are samples of solid material, such as emulsion films, crystals, plastic or glass. When exposed to nuclear radiation the traversing particles will produce submicroscopic trails of continuous damage in the materials. The trails can be made visible with chemical etching.

The number of tracks is dependent on the intensity and composition of radiation. At MoEDAL-MAPP experiment [1] the NTD foils (CR39, Makrofol and PET) are exposed to the radiation environment of the Large Hadron Collider (LHC). In this environment the dominant radiation damage to the foils will be produced by neutrons. In comparison to tracks of heavier charged particles such as magnetic monopoles, the tracks are shallow and form a diffusive surface to the foils.

We use large area optical scanning system [2] to study the MoEDAL-MAPP foils. The system allows to scan an area of about one square meter at 330 nm pixel resolution. It has a rolling shutter CMOS camera with various illumination options.

To reduce the effects of diffusion, we developed a method using thin liquid layers which will improve the optical transparency for the tracks that are of interest. The etch pits will be identified and categorized by various machine learning methods. These results are then used in reverse Monte Carlo simulations to detect and identify the original interactions.

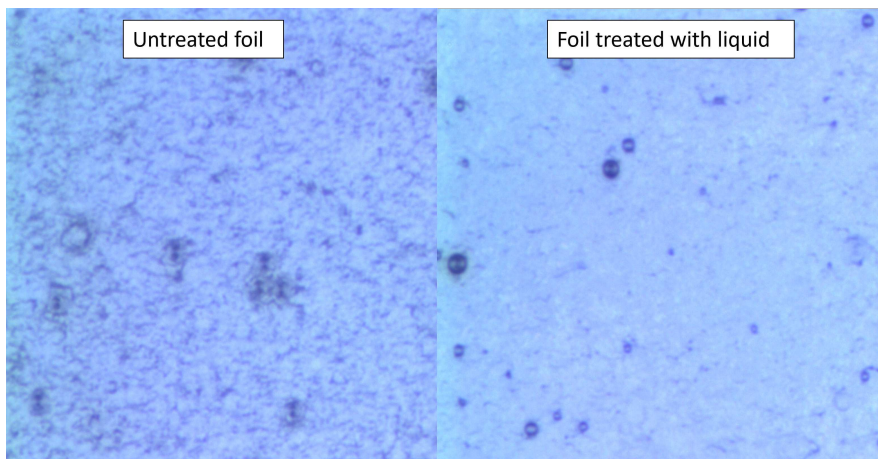


Figure 1: Comparison of untreated and treated CR39 foils that have exposed to LHC radiation environment. With liquid foil method the tracks become more pronounced and detectable.

In this presentation I will discuss the optical analysis methods, show the machine learning techniques and present the inverse Monte Carlo tools that are required for the analysis.

[1] B. Acharya et al., EPJ C **82**, 694 (2022)

[2] T. Hildén et al., Nucl. Instr. Meth. A **770** p. 113-122 (2015)

Computational perovskite solar cell model including optics, electrics and heat

A. Kamppinen, H. Palonen, and K. Miettunen

Department of Mechanical and Materials Engineering, University of Turku, Turku, Finland

Corresponding author: aleksi.kamppinen@utu.fi

Perovskites are a fascinating group of materials with many applications thanks to their versatile and modifiable properties. One of the timely applications is in photovoltaics. Perovskite solar cells (PSCs) hold a promise for efficient and affordable renewable energy. To study PSCs, we apply computational modelling covering the optical, electrical, and thermal aspects of device physics, see Figure 1 for a model illustration.

Optical and electrical simulations are commonly applied to understand and optimise solar cell operation, especially in laboratory setting. We utilize well established methods, namely transfer matrix and drift-diffusion, to study these perspectives. However, in real world application photovoltaics are subject to different environmental conditions, such as variations in temperature. Cell temperature is a diverse research question because the temperature affects the device operation and it is also affected by the device operation and its properties, in addition to the ambient conditions. Thus, coupling models accounting for different phenomena occurring in the cell is required. In our recent study [1], we showed how perovskite properties affect heat generation in planar PSCs and how the changes in self-heating translate to different device temperature and power production.

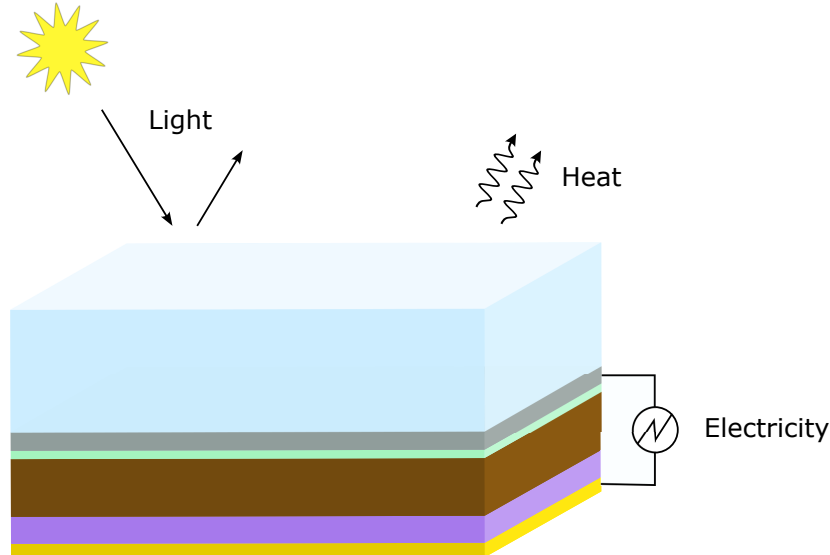


Figure 1: Illustration of the energy flows in the model. Multilayer structure of a typical planar PSC (from top down): substrate, (transparent) contact, electron transport layer, perovskite, hole transport layer and contact.

[1] A. Kamppinen, H. Palonen, K. Miettunen, "Self-heating of planar perovskite solar cells depending on active material properties" (2024) *Under review*

Photon emission statistics of driven microwave cavities

K. S. U. Kansanen^{1,2}, P. Portugal², F. Brange², C. Flindt², and P. Samuelsson¹

¹ *Department of Physics and NanoLund, Lund University, Lund, Sweden*

² *Department of Applied Physics, Aalto University, Espoo, Finland*

Corresponding author: kalle.kansanen@teorfys.lu.se

Recent experimental advances have made it possible to detect individual quantum jumps in open quantum systems. We discuss our recent theoretical work describing the statistics of photons emitted from a microwave cavity that is driven resonantly by an external field [1], and our efforts to extend the approach to multiple cavities [2]. We employ a Lindblad master equation dressed with counting fields to obtain the generating function of the photon emission statistics using a theoretical framework based on Gaussian states. It allows us to determine the distribution of photon emissions depending on the measurement time, as well as the photon waiting time distributions and the second-order coherence functions $g^{(2)}$ of the outgoing light. For a single cavity, our focus is on the differences between a parametric and a coherent drive, which either squeezes or displaces the cavity field as in Fig. 1. We also highlight results for two cavities which connect photon emission cross-correlations to entanglement between the cavities. These predictions may be tested in future microwave quantum optics experiments.

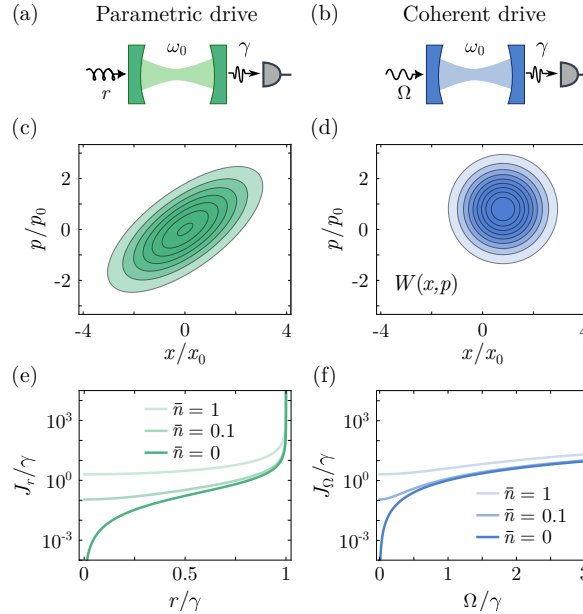


Figure 1: (a)-(b) Driven microwave cavities. (c)-(d) Corresponding squeezed and displaced Wigner functions. (e)-(f) Average emission currents as a function of the drive strength. Different curves correspond to different temperatures through the number \bar{n} of thermal photons in the cavity. [1]

[1] P. Portugal, F. Brange, K. S. U. Kansanen, P. Samuelsson, and C. Flindt, *Phys. Rev. Res.* **5**, 033091 (2023)

[2] K. S. U. Kansanen, P. Portugal, C. Flindt, and P. Samuelsson, in preparation

Performance evaluation for solar panels in Nordic conditions

Lauri Karttunen¹, Sami Jouttijärvi¹, Aapo Poskela¹, Heikki Palonen¹, Hugo Huerta², Milica Todorović¹, Samuli Ranta², Kati Miettunen¹

¹Department of Mechanical and Materials Engineering, Faculty of Technology, University of Turku, Vesilinnantie 5, 20500, Turku, Finland

² Department of Chemical Industry, Faculty of Engineering and Business, Turku University of Applied Sciences, Joukahaisenkatu 7, 20520, Turku, Finland

Corresponding author: lauri.p.karttunen@utu.fi

In this work, we compare five various state-of-the-art performance metrics for vertical bifacial photovoltaics (VBPV) in Nordic conditions [1]. Performance metrics indicate how well PV system is producing power compared what it is expected to produce, and thus they are important for tracking the operation and estimating the health of a PV system. Especially, the long-term performance losses of PV are estimated by tracking the time-series of performance metrics. However, there has been a lack of understanding which performance metrics are suitable for solar panels in Nordics. We use minute-resolution datasets from vertical bifacial PV panel and a weather station in Turku, Finland (60°N), covering four years. Our results show that all performance metrics introduced anomalies during winters, as visible in Fig. 1. These anomalies suggest that the current performance metrics are insufficient for modelling power under field conditions far from standard test conditions, which causes difficulties in a long-term performance assessment of solar panels. As two possible reasons, we have demonstrated that (1) the temperature coefficient of power varies under different irradiance conditions, and (2) that the efficiency of the module decreases in low irradiance conditions. In the performance metrics, both the temperature coefficient and efficiency are assumed to be constants. Among the metrics, the 6k regression method produces the least seasonal variability, indicating its best suitability for Nordic conditions. This is because the complex regression model can learn to model the power output in a wide range of outdoor conditions. This work highlights that the common performance evaluation methods for solar panels are insufficient in Nordic conditions.

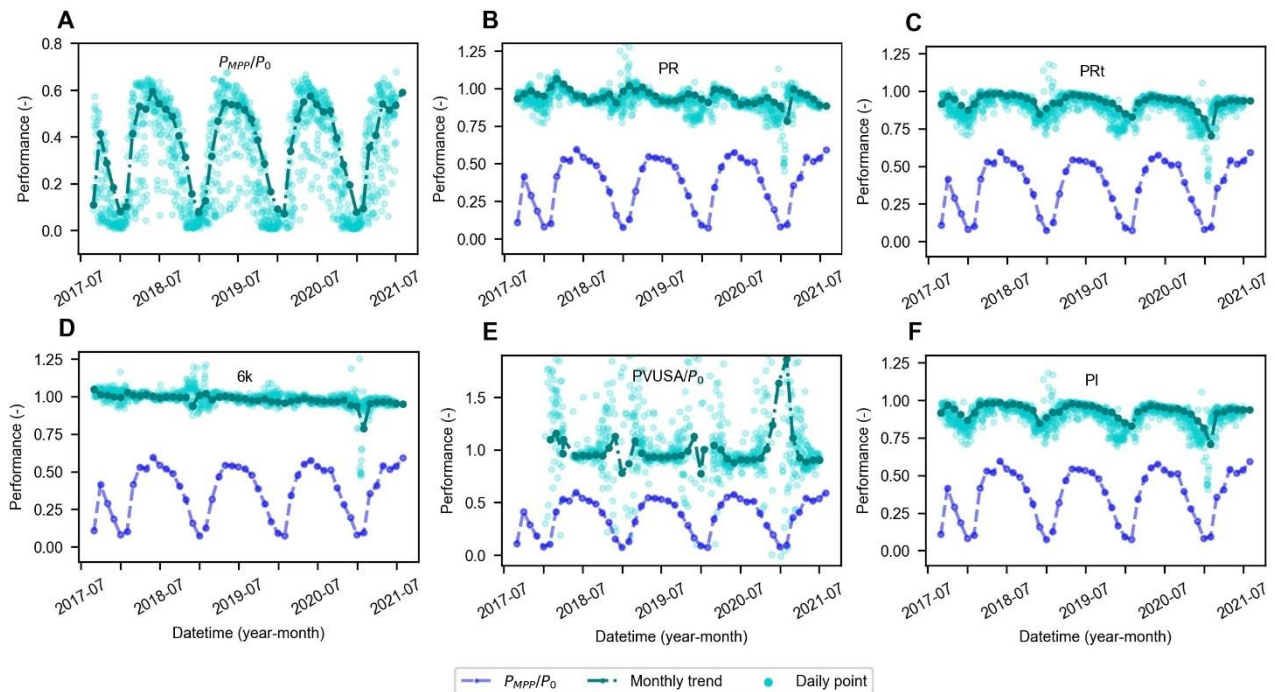


Fig. 1: Monthly and daily datapoints of different performance metrics: A: power, B: performance ratio, C: temperature-corrected performance ratio, D: 6k regression methods, E: PVUSA regression methods, F: performance index. To have the same scale, power and PVUSA were normalized by front side power rating P_0 . The figure and caption are from [1].

[1] L. Karttunen *et al.*, Renewable Energy **219**, 119473 (2023).

PALM-SLUrb: a single-layer urban surface model for micro to mesoscale atmospheric boundary layer studies

S.Karttunen¹, M. Sühring², E. O'Connor³ and L. Järvi^{1,4}

¹ Institute for Atmospheric and Earth System Research / Physics, Faculty of Science,
University of Helsinki, Finland

²Institute of Meteorology and Climatology, Leibniz University of Hannover, Hannover, Germany

³Finnish Meteorological Institute, Helsinki, Finland

⁴Helsinki Institute of Sustainability Science, Faculty of Science, University of Helsinki, Finland

Corresponding author: sasu.karttunen@helsinki.fi

The PALM model system [1] is a state-of-the-art modelling framework for studying oceanic and atmospheric boundary layers. It is most well-known for its use in high-resolution microscale (i.e. grid resolution in the order of metres) large-eddy simulations of boundary layers, and for excellent scaling on modern high-performance computing (HPC) environments.

The implementation of a land surface model [2] and a building surface model [3] in PALM has made it possible to model coupled surface fluxes of radiation, momentum and heat online during the simulations. However, modelling urban fluxes with the respective models requires usage of grid resolutions capable of resolving the individual buildings and street canyons within the urban canopy. On the other hand, atmospheric boundary layers including urban boundary layers are heavily influenced by mesoscale phenomena, with horizontal dimensions up to tens of kilometres. In order to simulate these mesoscale phenomena together with the metre-scale resolved urban canopy, computationally unfeasible problem sizes would have to be utilized.

In order to bridge the gap between meso and microscales in urban studies, the self-nesting system of PALM [4] can be applied. However, even with the self-nesting system, the computational costs to represent large urban areas at the building resolving scale remain high. Hence, as an alternative strategy, we present a newly developed single-layer urban surface model PALM-SLUrb to represent urban canopies on lower non-building-resolving grids. PALM-SLUrb models the radiative fluxes, including reflections and trapping of radiation within the urban canopy, as well as the turbulent transport of momentum and heat. As the whole urban canopy is represented as a single urban layer, the model poses no restrictions for the horizontal resolution. The model is online coupled to the atmospheric simulation, allowing for a timely response on changing atmospheric conditions.

[1] B. Maronga et al.: Overview of the PALM model system 6.0, *Geosci. Model Dev.* **13**, 1335–1372 (2020)

[2] K. F. Gehrke et al.: Modeling of land–surface interactions in the PALM model system 6.0: land surface model description, first evaluation, and sensitivity to model parameters. *Geosci. Model Dev.* **14**, 5307–5329 (2021)

[3] J. Resler et al.: PALM-USM v1.0: A new urban surface model integrated into the PALM large-eddy simulation model. *Geosci. Model Dev.* **10**, 3635–3659 (2017)

[4] A. Hellsten et al.: A nested multi-scale system implemented in the large-eddy simulation model PALM model system 6.0. *Geosci. Model Dev.* **14**, 3185–3214 (2021)

Calculations about the double-beta decay of ^{104}Ru

Elina Kauppinen¹, Jenni Kotila^{2,3}

¹Department of Physics, University of Jyväskylä, P.O. Box 35, FI-40014, Jyväskylä, Finland

²Finnish Institute for Educational Research, University of Jyväskylä, P.O. Box 35, FI-40014, Jyväskylä, Finland

³International Centre for Advanced Training and Research in Physics (CIFRA), P.O. Box MG12, 077125 Bucharest-Magurele, Romania

Corresponding author: elina.k.kauppinen@jyu.fi

The double-beta decay of nuclei is an interesting phenomenon when diving beyond the border of nuclear and particle physics. This phenomenon is still, in many ways, a mystery, and many research groups try to tackle the problems arising from it. One of the most known peculiarities in this topic is the neutrinoless double-beta decay ($0\nu\beta\beta$). In $0\nu\beta\beta$, no neutrinos are emitted in the decay process, and therefore, the decay violates the lepton number conservation law. This kind of process is still yet to be observed, and if it would be seen in an experiment, it would mean new physics beyond the standard model.

While the neutrinoless mode of the double-beta decay draws most of the attention, the two-neutrino double-beta decay also has aspects that need to be studied more. The calculation of the half-lives includes the nuclear matrix elements (NMEs) and the phase-space factors. While the phase-space factors can be calculated very precisely if the Q-value of the decay is known precisely, the NMEs still have much variation in results. These differences arise from different nuclear models and the still unknown quenching of the axial vector coupling constant, g_A . The search for the appropriate value of g_A for the description of neutrinoless double-beta decay is ongoing. New measurements of double beta decays may therefore provide new information on the axial vector coupling constant when combined with theoretical predictions.

In this presentation, I will review some preliminary results from the calculations about one of the double-beta decay candidates, ^{104}Ru . For this work, I have done phase-space factor calculations and also calculated NMEs for this decay using the microscopic interacting boson model (IBM-2) [1]. A comprehensive publication about the phase-space factor calculations can be read from [2] and about the NME [3, 4]. The estimates for the half-lives of two-neutrino and neutrinoless double-beta decay of ^{104}Ru can be obtained from these calculations.

The results suggest that the half-life of the two-neutrino double-beta decay should be short enough to be even experimentally observable, although there would be some restrictions concerning the Q-value of the decay. Also, the half-life estimates for the neutrinoless double-beta decay are calculated.

[1] F. Iachello and A. Arima, *The Interacting Boson Model* (1987) Cambridge: Cambridge University Press

[2] J. Kotila and F. Iachello, *Phys. Rev. C* **85**, 034316 (2012)

[3] J. Barea and F. Iachello, *Phys. Rev. C* **79**, 044301 (2009)

[4] J. Barea, J. Kotila and F. Iachello, *Phys. Rev. C* **91**, 034304 (2015)

A New Global Thermometer

Jyrki Kauppinen¹ and Pekka Malmi

¹Gasera Ltd, Lemminkäisenkatu 59, 20520 Turku

Corresponding author: jyrki.kauppinen@gasera.fi

The accuracy of the measured global temperature anomalies is low. The satellite measurements and ground stations observations are even conflicting with each others. Thus better global temperature anomalies are required for example to use in studies of climate change. Our research of climate change [1 - 5] gave us a hint about a new method to measure the global temperature. In this method [5] we measure the concentration p_e of carbon dioxide emitted by the oceans. The emitted component depends on the surface temperature T . According to Henry's Law the equilibrium concentration of CO_2 is a function of the temperature. This temperature dependence is simply given by a global emission strength α so that the increase of p_e is $\alpha\Delta T$, where the differences are measured from the previous equilibrium 1700 century. In order to apply Henry's Law as a function of time t we have to know that the measured concentration are convolved by the impulse response $I(t) = \exp(-t/\tau)/\tau$, where τ is the response time. This response time describes how fast the concentration goes to the equilibrium. So the measured concentration of the emitted CO_2 is the convolution of $\alpha I(t)$ and $\Delta T(t)$ i.e. $p_e(t) = \alpha I(t) * \Delta T(t)$. The global temperature difference ΔT starting from the previous equilibrium 1700 century is given by

$$\Delta T(t) = [\text{deconvolution of } p_e(t) \text{ by } I(t)]/\alpha = [p_e(t) + \tau dp_e(t)/dt]/\alpha,$$

and

$$p_e(t) = p_m(t) - 280 \text{ ppm} - p_h(t),$$

where $p_m(t)$ is the measured total concentration of CO_2 in the atmosphere, 280 ppm is the concentration in 1700 century and $p_h(t)$ is the contribution from a human release $p_r(t)$ of CO_2 to the atmosphere. This very small portion $p_h(t)$ of the human release $p_r(t)$ stays in the atmosphere. According to Henry's Law $p_h(t) = p_r(t) - I(t) * p_r(t)$, where the convolution is a portion dissolved in the oceans. Roughly $p_h(t) = \tau dp_r(t)/dt$. We have derived the values 83 ppm/°C and 7.4 yr of α and τ , respectively [5].

There are many advantages of the method. It is very easy to use, because we need only the CO_2 data from Mauna Loa in Hawaii once a month in order to calculate a new temperature value. Note that Henry's Law is valid for every gas in the atmosphere. Thus it turns out that probably N_2O is suitable for the use as the global thermometer. Demonstrations of the global thermometer will be presented.

- [1] J. Kauppinen, J. Heinonen, and P. Malmi. Major portions in climate change; physical approach. *International Review of Physics*, 5(5):260-270, (2011).
- [2] J. Kauppinen, J. Heinonen, and P. Malmi. Influence of relative humidity and clouds on the global mean surface temperature. *Energy & Environment*, 25(2):389-399, (2014).
- [3] J. Kauppinen and P. Malmi. Major feedback factors and effects of the cloud cover and the relative humidity on the climate. *arXiv e-prints*, page arXiv:1812.11547, (2018).
- [4] J. Kauppinen and P. Malmi. No experimental evidence for significant anthropogenic climate change. *arXiv e-prints*, page arXiv: 1907.00165, (2019).
- [5] J. Kauppinen and P. Malmi. No reliable studies of climate change without Henry's Law and a new thermometer for the global temperature. *page arXiv: 2304.01245*, (2023).

Electronic structure and electrical conductivity of $\text{Ge}_2\text{Sb}_2\text{Te}_5$ heterostructures with different layer orderings

Tomi Ketolainen and Janne Kalikka

Computational Physics Laboratory, Tampere University, P.O. Box 692, FI-33014 Tampere, Finland

Corresponding author: tomi.ketolainen@tuni.fi

Chalcogenide phase change materials (PCMs) have been studied extensively in the past decades because these materials have shown promise in several applications comprising e.g. memory devices and optical systems. In chalcogenide PCMs, an external electric voltage can be used to make a transition from an amorphous phase to a crystalline one, leading to a significant change in the electrical resistivity and optical reflectivity. One scientifically interesting and technologically relevant chalcogenide PCM is $\text{Ge}_2\text{Sb}_2\text{Te}_5$.

Previous experimental studies suggest that a large contrast in the electrical conductivity of $\text{Ge}_2\text{Sb}_2\text{Te}_5$ can be achieved also in heterostructures comprising specific sequences of single-atom layers without the amorphous-to-crystalline phase transition [1]. In this work, we explore the effect of different layer orderings (see Fig. 1) on the electrical conductivity and basic electronic properties of $\text{Ge}_2\text{Sb}_2\text{Te}_5$ heterostructures. We use the VASP code package based on density functional theory (DFT) together with the DFT-D3 van der Waals correction and BolzTraP2 code to compute electrical conductivity and electronic band structures for six previously investigated stacking configurations.

Our calculations show that the in-plane (along the atomic layers) electrical conductivity is clearly larger than the out-of-plane (perpendicular to the atomic layers) electrical conductivity. Some layer orderings result in larger out-of-plane electrical conductivities than the other structures. The PBE and HSE06 band structure calculations show that some structures are metallic whereas others are semiconducting. According to the PBE calculations, the semiconducting structures have band gaps between 0.3 and 0.4 eV. In the HSE06 calculations, band gaps of 0.4–0.7 eV are obtained for semiconducting structures. Our studies indicate that the layer ordering in $\text{Ge}_2\text{Sb}_2\text{Te}_5$ heterostructures affects the electrical conductivity remarkably although the differences between the selected six structures are not as large as those observed experimentally in $\text{Ge}_2\text{Sb}_2\text{Te}_5$ heterostructures.

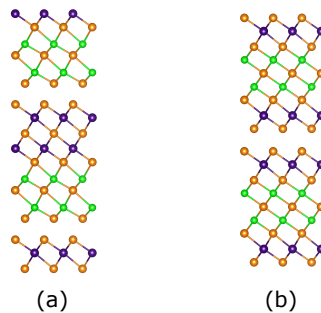


Figure 1: (a) Ferro and (b) Kooi structures of $\text{Ge}_2\text{Sb}_2\text{Te}_5$.

[1] R. E. Simpson *et al.*, Nat. Nanotechnol. **6**, 501 (2011)

Quantum simulation of the pseudo-Hermitian Landau–Zener–Stückelberg–Majorana effect

F. Kivelä¹, S. Dogra¹, and G. S. Paraoanu¹

¹ Department of Applied Physics, Aalto University, Espoo, Finland

Corresponding author: feliks.kivela@aalto.fi

The Hamiltonians used in standard quantum mechanics are Hermitian, which guarantees the realness of energies as well as unitary time evolution, which results in a conservation of probability. However, it is possible to extend the theory to non-Hermitian Hamiltonians, particularly interesting of which are those satisfying parity–time (PT) symmetry, or more generally pseudo-Hermiticity, as they can still exhibit real eigenvalues despite their non-Hermiticity.

A simulation of a time-independent PT-symmetric non-Hermitian Hamiltonian on a quantum processor has previously been demonstrated [1], and this work expands the methodology to the simulation of the time-dependent non-Hermitian non-PT-symmetric Hamiltonian used in a pseudo-Hermitian extension of the Landau–Zener–Stückelberg–Majorana (LZSM) model. This Hamiltonian is of the form

$$\hat{H}(t) = \frac{1}{2} \begin{bmatrix} -vt & \Omega_0 \\ k\Omega_0 & vt \end{bmatrix}, \quad (1)$$

where Ω_0 , v and k are real parameters. The parameter k controls the degree of non-Hermiticity; $k = 1$ reduces to the standard, Hermitian LZSM model [2].

The simulation is implemented by using Naimark dilation to transform a non-Hermitian Hamiltonian for one qubit into a Hermitian Hamiltonian for a qubit and an ancilla, so that the ancilla = 0 subspace of the measured results undergoes nonunitary time-evolution corresponding to the original non-Hermitian Hamiltonian. We have performed simulations on a quantum computer accessed via the IBM Quantum Platform, and observe results in line with predictions based on a theoretical treatment [3] of the pseudo-Hermitian LZSM system. These include properties such as the dependence of transition rates on time and parameters and the replacement of the conservation of total probability present in Hermitian systems by the formulas

$$kP_{0 \rightarrow 0} + P_{0 \rightarrow 1} = k \quad (2)$$

$$kP_{1 \rightarrow 0} + P_{1 \rightarrow 1} = 1, \quad (3)$$

where $P_{i \rightarrow j}$ is the transition rate from state $|i\rangle$ to state $|j\rangle$, as the dynamical invariants of a pseudo-Hermitian system.

[1] S. Dogra, A. A. Melnikov, and G. S. Paraoanu, *Commun. Phys.* **4**, 26 (2021).

[2] O. V. Ivakhnenko, S. N. Shevchenko, and F. Nori, Nonadiabatic Landau–Zener–Stückelberg–Majorana transitions, dynamics, and interference, *Physics Reports* **995**, 1 (2023).

[3] T. Torosov and N. V. Vitanov, Pseudo-Hermitian Landau–Zener–Stückelberg–Majorana model, *Phys. Rev. A* **96**, 013845 (2017).

Vortices in the magnetospheric transition region of a global hybrid-Vlasov simulation

V. Koikkalainen¹, M. Palmroth^{1,2}, M. Grandin¹, E. Kilpua¹, I. Zaitsev¹, A. Workayehu¹, G. Cozzani¹, L. Turc¹, F. Tesema¹, J. Suni¹, Y. Pfau-Kempf¹, U. Ganse¹

¹ Department of Physics, University of Helsinki, Finland

²Space and Earth Observation Centre, Finnish Meteorological Institute, Finland

Corresponding author: venla.koikkalainen@helsinki.fi

In this study we aim to understand the formation of large-scale vortices in the magnetospheric transition region and study their effect on the ionosphere. The hybrid-Vlasov global magnetospheric model Vlasiator [1] has recently been complemented with a more robust ionosphere solver, allowing for the study of magnetosphere-ionosphere coupling. With the inclusion of the ionospheric boundary model, interesting new phenomena emerge in the transition region, between Earth's dipolar magnetic field and the magnetotail.

Large-scale vortices with wavelengths of about $4 R_E$ (Earth radii) form and dissipate in the transition region over a time scale of 300 seconds. These vortices can be seen when plotting e.g. density, velocity, magnetic field, and electric field. They appear to have counterparts in the ionospheric part of the model. In the ionosphere, field-aligned currents can be seen to match the structure of the magnetospheric waveform.

The features of the event in the magnetosphere, such as changes in flux tube entropy and the presence of magnetic field B_z minima may be an indication of the vortices being the result of the ballooning/interchange instability, which has previously been studied in MHD (e.g. [2]) and PIC simulations (e.g. [3]).

- [1] M. Palmroth, U. Ganse, Y. Pfau-Kempf, M. Battarbee, L. Turc, T. Brito, M. Grandin, S. Hoilijoki, A. Sandroos, and S. Alfthan, "Vlasov methods in space physics and astrophysics," *Living Reviews In Computational Astrophysics*, vol. 4, p. 1, Aug. 2018, <https://doi.org/10.1007/s41115-018-0003-2>.
- [2] K. Sorathia, V. Merkin, E. Panov, B. Zhang, J. Lyon, J. Garretson, A. Ukhorskiy, S. Ohtani, M. Sitnov, and M. Wiltberger, "Ballooning-Interchange Instability in the Near-Earth Plasma Sheet and Auroral Beads: Global Magnetospheric Modeling at the Limit of the MHD Approximation," *Geophysical Research Letters*, vol. 47, article e2020GL088227, 2020, <https://onlinelibrary.wiley.com/doi/abs/10.1029/2020GL088227>.
- [3] P. Pritchett and F. Coroniti, "Plasma sheet disruption by interchange-generated flow intrusions," *Geophysical Research Letters*, vol. 38, 2011, <https://onlinelibrary.wiley.com/doi/abs/10.1029/2011GL047527>.

Properties of the new α -decaying isotope ^{190}At

H. Kokkonen¹, K. Auranen¹, J. Uusitalo¹, S. Eeckhaudt¹, T. Grahn¹, P.T. Greenlees¹, P. Jones¹, R. Julin¹, S. Juutinen¹, M. Leino¹, A.-P. Leppänen¹, M. Nyman¹, J. Pakarinen¹, P. Rahkila¹, J. Sarén¹, J. Sorri¹, and M. Venhart^{1,2}

¹*Accelerator Laboratory, Department of Physics, University of Jyväskylä, FI-40014 Jyväskylä, Finland*

²*Institute of Physics, Slovak Academy of Sciences, SK-84511 Bratislava, Slovakia*
Corresponding author: henna.e.kokkonen@jyu.fi

An α -decay of yet the most neutron-deficient astatine isotope, ^{190}At , was identified. The nucleus was produced via fusion-evaporation reaction $^{109}\text{Ag}(^{84}\text{Sr},3n)^{190}\text{At}$ and the RITU (Recoil Ion Transfer Unit) gas-filled recoil separator was used to separate the beam from the reaction products. Measured properties of the α -decay are a half-life of $1.0^{+1.4}_{-0.4}$ ms and an α -particle energy of 7750(20) keV. Assuming a ground state to ground state decay these decay properties correlate to an unhindered decay and consequently spin and parity of (10^-) is suggested. The identified properties were compared with the predictions of the systematics and selected mass models of the nearby nuclei. In addition, the possibility of proton emission was considered due to the nucleus locating beyond the drip line. In the presentation, the experimental details and the already published [1] results will be discussed.

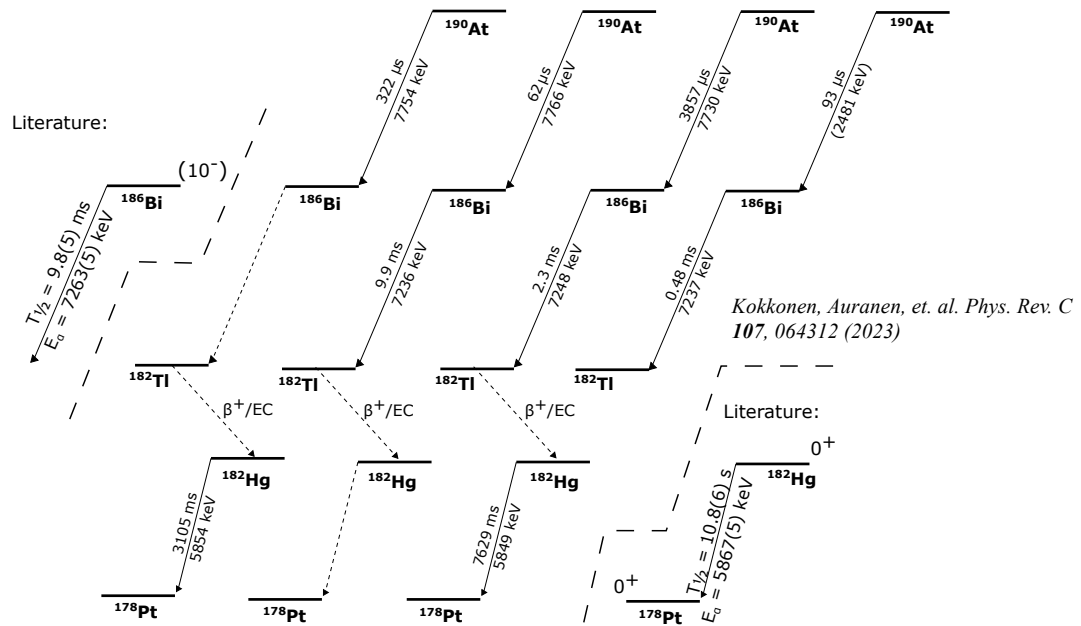


Fig. 1: Figure taken from Ref. [1]. The four observed decay chains of the ^{190}At and the recorded data. The thin dashed lines refer to unobserved decays. The data given in literature [2,3] for formerly known nuclei are shown above and below the thicker dashed lines.

- [1] H. Kokkonen, K. Auranen, J. Uusitalo, S. Eeckhaudt, T. Grahn, P. T. Greenlees, P. Jones, R. Julin, S. Juutinen, M. Leino, A.-P. Leppänen, M. Nyman, J. Pakarinen, P. Rahkila, J. Sarén, C. Scholey, J. Sorri, and M. Venhart, *Phys. Rev. C* **107**, 064312 (2023).
- [2] B. Singh and J. C. Roediger, *Nucl. Data Sheets* **111**, 2081 (2010).
- [3] E. Achterberg, O. Capurro, and G. Marti, *Nucl. Data Sheets* **110**, 1473 (2009).

Comparison of Interatomic Potentials for Silicon Applied to Radiation Damage Studies

N. Korepanova¹, A. Hamedani¹, and A.E. Sand¹

¹ Department of Applied Physics, Aalto University, Espoo, Finland

Corresponding author: nadezda.korepanova@aalto.fi

Many silicon-based devices are exploited in highly radioactive environments such as space, nuclear power plants, and high-energy physics experiments. Constant radiation exposure progressively degrades material properties and leads to the ultimate failure of the devices. In principle, with a reliable method to model and simulate the radiation effects in the semiconductor, it would be possible to predict the probability of a failure happening for a given, well-known, and characterized electronic component.

Here, we focus on molecular dynamics (MD) simulations of radiation damage as an initial step in the multiscale approach. In MD, interactions between atoms are defined by interatomic potentials, which have an essential influence on results. Semi-empirical interatomic potentials are computationally efficient, yet are unable to accurately describe various material parameters and give widely differing predictions of radiation damage. Machine learning interatomic potentials (MLIP) can overcome this obstacle and bring all of the underlying physical and chemical aspects of the system to MD simulations.

In this work, we compare the performance of popular semi-empirical potentials for silicon: Stillinger-Weber (SW) [1] and Tersoff (T3) [2], to the C-TGAP MLIP [3, 4] that was modified to be applicable for cascade simulations. For the subsequent comparative study, we evaluate the number of generated point defects, their clustering behavior, and cluster morphology.

This work was partly supported by the Research Council of Finland through Project No. 349622, and by the Emil Aaltonen foundation.

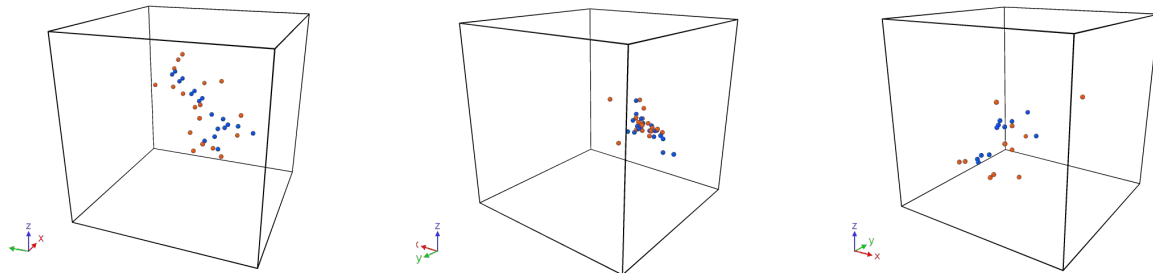


Figure 1: Damage created by 1 keV PKA. From left to right - **T3**, **SW**, and **C-TGAP**. Blue dots denote vacancies and red are interstitials.

[1] F.H. Stillinger and T.A. Weber. *Phys. Rev. B*, 31, Apr 1985. DOI: 10.1103/PhysRevB.31.5262

[2] R. Devanathan, et al. *J. Nucl. Mater.*, 253, 1998. DOI: 10.1016/S0022-3115(97)00304-8

[3] M. Caro. *Phys. Rev. B* 100, 2019. DOI: 10.1103/PhysRevB.100.024112

[4] GAP interatomic potential for silicon, M. Caro DOI: 10.5281/zenodo.5734462

Coherent thermal transport control via pillar-based phononic crystals

T. A. S. Korkiamäki¹, T. A. Puurtinen¹, T. Loippo¹, B. Graczykowski², and I. J. Maasilta¹

¹ Nanoscience Center, Department of Physics, University of Jyväskylä, Finland

² Faculty of Physics, Adam Mickiewicz University, Poland

Corresponding author: tatu.a.s.korkiamaki@jyu.fi

For some time now, phononic crystals (PnCs) have been used to control thermal conductance in insulating and semiconducting materials [1]. At cryogenic temperatures, PnCs have been proposed to be used to improve sensitive infrared detectors and quantum bits. The mechanisms by which PnCs work can be generally divided into two categories: (i) one where incoherent, diffusive, particle-like scattering dominates, and (ii) another where the coherent, wave-like scattering is operational. A large majority of earlier thermal conduction studies have concentrated on geometries where a membrane is perforated by a periodic array of holes. Much less studied are 2D pillar-based PnCs, where the lattice is formed by a periodic array of pillars. For such PnCs, the phonon spectrum can also include localised resonances which cannot carry heat.

In this work, we have fabricated and measured the sub-Kelvin thermal conductance of four pillar-based PnCs with different lattice constants (a) ranging from 300 nm to 5 μm (Fig. 1). We observed a significant reduction in thermal conductance compared to an unaltered membrane, close to an order of magnitude for the $a = 1 \mu\text{m}$ PnC. To our knowledge, this is the largest experimentally observed reduction achieved with a pillar-based PnC.

Coherent theory finite element method (FEM), and incoherent theory Monte Carlo simulations were used to compute the thermal conductance of the PnCs. We have also directly measured the phonon dispersion with Brillouin light scattering, the results corresponding to our FEM calculations. For small lattice constants, the experimental thermal conductance qualitatively matches the coherent theory, whereas the larger lattice constants agree with incoherent theory. This is interpreted as a breakdown of coherence, induced by the surface roughness of the pillars.

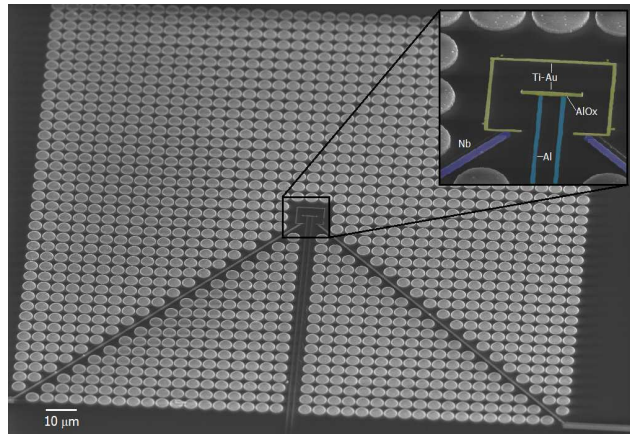


Figure 1: A 5 μm lattice constant Al pillar PnC, with a heater-thermometer structure highlighted in the zoom-in.

[1] M. Nomura et al., Mater. Today Phys. ., **22**, 100613 (2022).

Structure formation in miscible and immiscible thin bimetallic films synthesized by temporally modulated vapor fluxes

Spyridon Korkos^{1,2}, Antti-Jussi Kallio¹, Ryan Trevorah¹, Rene Bes¹, Kenichiro Mizohata¹, Simo Huotari¹, and Kostas Sarakinos^{1,2}

¹*Department of Physics, University of Helsinki, 00014 Helsinki, Finland*

²*KTH Royal Institute of Technology, Department of Physics, Roslagstullsbacken 21, 114 21 Stockholm, Sweden*

Corresponding author: spyridon.korkos@helsinki.fi

The physical attributes of multicomponent thin films are defined by the chemical composition and atomic arrangement across different length scales. The atomic arrangement is predominantly influenced by the complex interplay among thermodynamics which either allow or impede miscibility and compound formation, kinetic conditions that affect the rates of atomic-scale structure-forming processes, and the arrival pattern of vapor species at the film growth front. In this study, AgAu and AgCu thin films are deposited using vapor fluxes modulated with sub-monolayer (ML) and microsecond resolution [1]. This is achieved by applying electrical power to spatially separated magnetron sources in the form of unipolar pulse trains. This approach allows flux temporal profiles from co-deposition to fluxes where 4 ML of Ag and Au or Cu vapors are deposited in an alternating fashion. Power is adjusted to deposit equimolar samples, as determined by ion beam analysis (time-of-flight elastic recoil detection analysis, Rutherford backscattering spectrometry) techniques. X-ray diffractometry measurements show a Face-Centered cubic (FCC) structure for both systems at different synthesis conditions, while the deposition of 4 ML per pulse train shows the formation of superlattice structure. Local atomic structure is revealed by extended x-ray absorption fine structure measurements at European synchrotron radiation facility shedding light onto the atomic arrangement of neighboring atoms for different synthesis conditions.

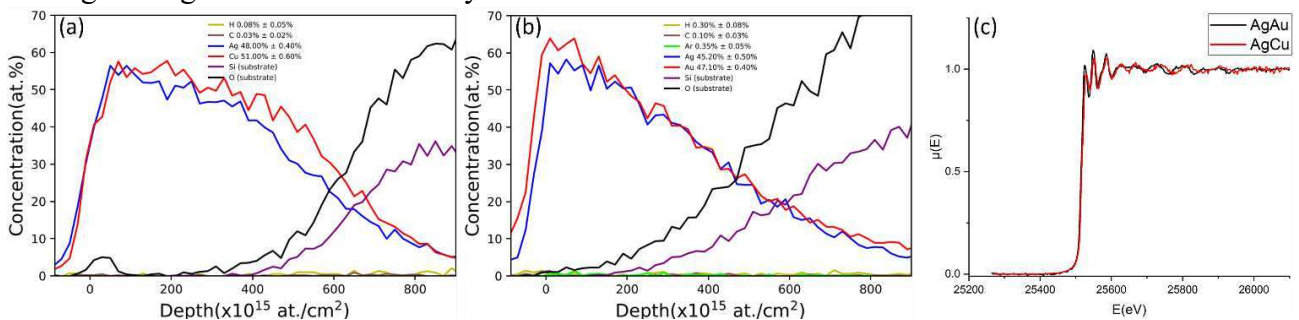


Fig. 1: (a), (b) time-of-flight elastic recoil detection analysis depth profile of 100 nm AgCu and AgAu sample, respectively, deposited on SiO₂/Si substrate using 100 alternate pulses and (c) normalized extended x-ray absorption fine structure spectra for the same samples.

[1] Method of coating a substrate so as to provide a controlled in-plane compositional modulation, PCT/EP2014/052831, granted (Inventors: K. Sarakinos and D. Magnfält).

Spurious reflections in target detection with entangled photons

Vladimir V. Kornienko¹, Matti Raasakka¹, and Ilkka Tittonen¹

¹ *Micro and Quantum Systems group, Department of Electronics and Nanoengineering, Aalto University, Espoo, Finland*

Corresponding author: vladimir.kornienko@aalto.fi

In optical detection of distant objects one can benefit from quantum light properties over those of classical light. Two-beam correlation-enhanced protocols can improve imaging or target detection even under strong background noise and in the low photon flux regime.

We demonstrate that a partially reflecting jamming object introduces noise to these protocols including quantum illumination. In contrast to background noise, the signal radiation reflected from the jammer is correlated with the corresponding idler beam. We analyze the means to mitigate this noise and introduce an indistinguishability parameter showing how efficiently the jammer can be distinguished from the target. We use quantum Chernoff bound and the density matrix orthogonalization procedure to separate the contributions from the target, the background, and the jammer.

We illustrate our findings with an experiment using optical entangled photon pairs. Our results can be applied in the design of target detection protocols and advanced imaging techniques.

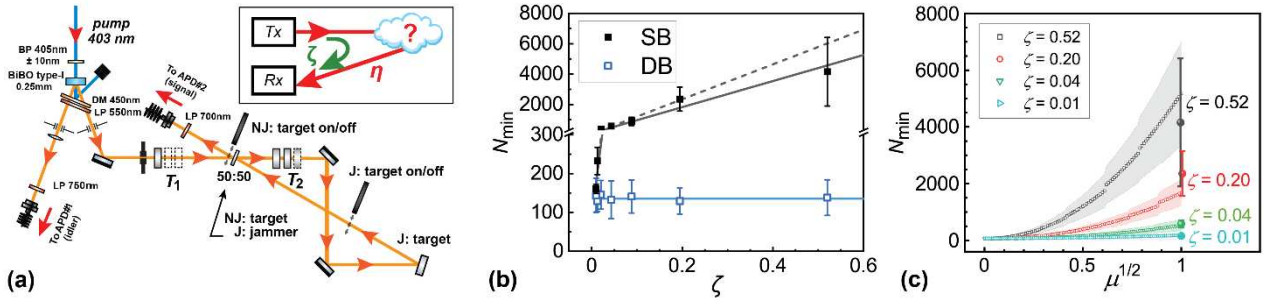


Fig. 1: (a) Experimental set-up. Filters: BP – bandpass, LP – longpass, T_1 , T_2 – neutral density. 50:50 – symmetric beam-splitter. APD – avalanche photodiode. The inset shows the modification of the target detection protocol due to the presence of a jammer. Tx – transmitter; Rx – receiver; η and ζ – target and jammer effective reflectances, respectively. “J” – jammed detection, “NJ” – non-jammed detection.

- (b) Expected value N_{\min} for minimal number of trials for single-beam (SB) and double-beam (DB) detection protocols, as a function of the jammer effective reflectance (ζ). Lines show the fit results using the exact (solid lines) and the approximate (dashed lines) equations.
- (c) DB: sweeping the indistinguishability parameter μ values by changing the bin size in processing the histogram data. SB protocol performance is shown (large closed circles) for several values of the jammer reflectance ζ .

[1] V.V. Kornienko *et al.* // *APL Quantum* (accepted for publication on 15.01.2024).

MOOCs for Versatile Physics Education

Pekka Koskinen¹ and Antti Lehtinen¹

¹*Department of Physics, University of Jyväskylä, Jyväskylä, Finland*

Corresponding author: pekka.j.koskinen@jyu.fi

Massive Open Online Courses (MOOCs) have become integral to higher education. MOOCs are fully online courses that scale well for hundreds to thousands of students and are particularly suitable for outreach, recruitment, lifelong learning and for familiarizing with a new topic. They differ from traditional university education: they serve different functions, have a more diverse audience, more straightforward assessments, and more polished material. Here, we discuss our experiences with two physics MOOCs at the University of Jyväskylä, the course *Quantum Mechanics and the Theory of Relativity for the laypeople* (Kvanttimekaniikkaa ja suhteellisuusteoriaa yleissivistävästi) that has been running for a couple of years [1] and a new course *Everyday physics* (Arjen fysiikkaa) that is still under development. We have found that MOOC development requires much work and a mindset different from teaching physics at the campus. Still, with careful planning and sufficient resource allocation, the development work is rewarding. At best, the resulting MOOCs complement traditional university courses, improve recruitment, and serve a versatile role within the physics education portfolio.

[1] <https://www.jyu.fi/fi/avoim-yliopisto/opintojaksot/kvanttimekaniikkaa-ja-suhteellisuusteoriaa-yleissivistavasti>

Physics-motivated Cell-octree Adaptive Mesh Refinement in the Vlasiator 5.3 Global Hybrid-Vlasov Code

Leo Kotipalo¹, Markus Battarbee¹, Yann Pfau-Kempf¹, Minna Palmroth^{1,2}

¹ Space Physics Group, Faculty of Science, University of Helsinki, Helsinki, Finland

² Finnish Meteorological Institute, Helsinki, Finland

Corresponding author: leo.kotipalo@helsinki.fi

Automatically adaptive grid resolution is a common way of improving simulation accuracy while keeping the computational efficiency at a manageable level. In space physics adaptive grid strategies are especially useful as simulation volumes are extreme, while the most accurate physical description is based on electron dynamics and hence requires very small grid cells and time steps. Therefore, many past global simulations encompassing e.g. the near-Earth space have made tradeoffs in terms of the physical description and used laws of magnetohydrodynamics (MHD) that require less accurate grid resolutions. Recently, using supercomputers, it has become possible to model the near-Earth space domain with an ion-hybrid scheme going beyond the MHD-based fluid dynamics. These simulations, however, must develop a new adaptive mesh strategy beyond what is used in MHD simulations.

We developed an automatically adaptive grid refinement strategy for ion-hybrid Vlasov schemes, and implemented it within the Vlasiator global solar wind - magnetosphere - ionosphere simulation Vlasiator. This method automatically adapts the resolution of the Vlasiator grid using two indices: one formed as a maximum of dimensionless gradients measuring the rate of spatial change in selected variables, and the other derived from the ratio of the current density to the magnetic field density perpendicular to the current. Both these indices can be tuned independently to reach a desired level of refinement and computational load. We test the indices independently and compare the results to a control run using static refinement.

The results show that adaptive refinement highlights relevant regions of the simulation domain and keeps the computational effort at a manageable level. We find that the refinement shows some overhead in rate of cells solved per second. This overhead can be large compared to the control run without adaptive refinement, possibly due to resource utilisation, grid complexity and issues in load balancing. These issues lay a development roadmap for future optimisations.

Sputtering of Deuterium Supersaturated tungsten surfaces: A Molecular Dynamics Simulation Approach

Kporha Faith¹, Fredric Granberg¹, and Kai Nordlund¹

¹*Accelerator Laboratory, University of Helsinki, Helsinki, Finland*

faith.kporha@helsinki.fi

Sputtering is an undesirable occurrence in a fusion plant that must be minimized to prevent the erosion of the plasma-facing wall material and ensure the overall working efficiency of the power plant. To understand the underlying sputtering process, atomistic level studies are necessary, and molecular dynamics (MD) simulation is a valuable tool for this purpose. Tungsten, a potential candidate for future nuclear power plants, has been studied under various conditions.

Experimental studies have revealed the formation of Deuterium Super-saturated layers on tungsten surfaces when exposed to Deuterium plasma [1,2]. Monte Carlo simulations have provided some insights into the impact of these layers on tungsten sputtering [3]. It revealed that there was a relationship between tungsten sputtering, supersaturation levels, incident energies and angles. However, these simulations have limitations as they do not reveal the temporal evolution of atoms and thus unable to give a comprehensive insight into the sputtering process.

By using MD simulations, we discovered that sputtering caused by lighter atoms like hydrogen, or its isotopes, is more complex than previously imagined. This arises from the fact that sputtering could happen due to diverse mechanisms, which are not observed with heavier atoms like Argon. We also discovered that in comparison to a pristine tungsten surface, deuterium decorated tungsten surfaces have a direct impact on the sputtering yields. The results obtained are significant in predicting how future nuclear power plants lifespan and plasma properties are impacted by deuterium decorated tungsten surfaces.

[1] Nishijima et al. Deuterium supersaturated surface layer in tungsten: ion energy dependence, *Nuclear Fusion* 63 (12) (2023).

[2] Gao et al. Deuterium supersaturation in low-energy plasma-loaded tungsten surfaces, *Nuclear Fusion* 57 (1) (2016).

[3] Kenmotsu et al. Effect of deuterium retention upon sputtering yield of tungsten by deuterons, *Journal of Nuclear Materials* 415 (1) (2011).

High-throughput catalyst screening for CO₂ to methanol conversion with machine-learned force-fields

Ondřej Krejčí¹, Prajwal Pisal¹ and Patrick Rinke¹

¹*Department of Applied Physics, School of Science, Aalto University, Espoo, Finland*

Corresponding author: ondrej.krejci@aalto.fi

The search for new and better catalysts is one of the key research directions in material science, as heterogeneous catalysis is essential in converting CO₂ to fuel in a closed loop carbon cycle. Approximative predictions of activity, like the Sabatier principle, have been very popular for catalytic screening. However, to take the nanostructure of real thermocatalysts into account, we need to scan the adsorption energies (AEs) for a variety of different facets and binding sites.

In this work, we will present our current workflow for obtaining the relevant AEs in CO₂ thermoreduction to methanol. We employ trained machine learning force-field from the Open Catalyst Project [1], to accelerate the search for ideal catalysts. We have calculated the surface stabilities for various facets with all Miller indices $\in \{-2, -1, 0, 1, 2\}$ and picked the most stable cuts for each facet. Subsequently, we have created all possible high symmetry binding sites on those facets and predicted AEs for the reaction key semi-products: *H, *OH, *OCHO and *OCH₃ [2]. The AE distributions for more than 100 materials are further analysed for their's activity and compared to previously reported results [3]. We fuse this computational data with reported experimental yields to overcome the gap in theoretical data and allow for ML prediction of catalytic activity in CO₂ to methanol reduction over various material classes.

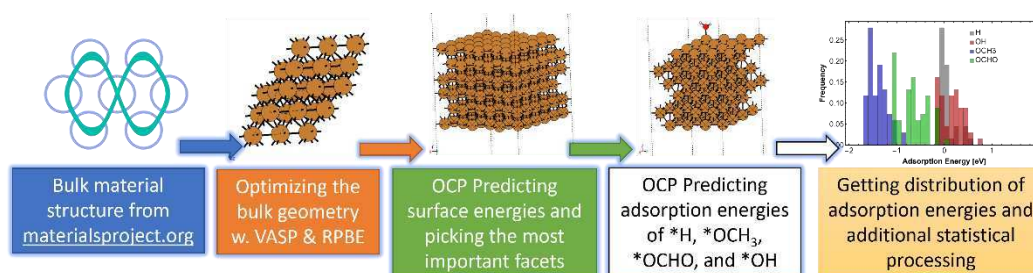


Fig. 1: Our current workflow for fast and efficient estimation adsorption energies distributions, used for more realistic description of materials activity.

[1] I L. Chanussot et al. *ACS Catal.* **11**, 6059-6072 (2021); R. Tran et al. *ACS Catal.* **13**, 3066-3084 (2023); <https://opencatalystproject.org/> .

[2] P. Amann et al. *Science* **376**, 603–608 (2022).

[3] A. J. Medford et al, *J. Catal* **328**, 36-42 (2015)

Proximity induced superconductivity in few-layer WTe₂ Josephson junction using normal Palladium contacts

Kuldeep^{*}, Richa Mitra^{*}, Pertti Hakonen and Manohar Kumar

Applied Physics Department, Aalto University, Espoo, Finland

WTe₂ is type-II Weyl semimetal with intriguing higher-order topological phases. They support helical edge states at the crystal hinges [1, 2, 3]. Interfacing these states with the superconductivity may give rise to topological superconducting, the ultimate material platform for the realization of the non-abelian anyons [4, 5]. Thus, the realization of the transparent superconducting contacts to WTe₂ is a necessary step in this direction. Palladium (Pd) which is a normal metal, diffuses latterly with tungsten (W) to form intercalated PdTe-x a superconducting compound [6]. Here we realize a highly transmissive superconducting PdTe-x contact to penta-layer WTe₂. We fabricated a proximity-induced Josephson junction. In the ultra-long junction 4.5 μm , the critical current of 0.66 μA at 450mK is one of the highest reported in the literature. The critical temperature and gap energy are in order of 1.2 K and 0.18 meV. The initial measurement indicates that the supercurrent is carried by the helical edge states. In the continuation of this work, we will fabricate the weak link in such junctions and probe the phase slips by microwave spectroscopy.

References:

- [1] Xu, Su-Yang, et al. "Electrically switchable Berry curvature dipole in the monolayer topological insulator WTe₂." *Nature Physics* 14.9 (2018): 900-906.
- [2] Li, Peng, et al. "Evidence for topological type-II Weyl semimetal WTe₂." *Nature Communications* 8.1 (2017): 2150.
- [3] Tang, Shujie, et al. "Quantum spin Hall state in monolayer 1T'-WTe₂." *Nature Physics* 13.7 (2017): 683-687.
- [4] L. Fu and C. L. Kane Phys. Rev. Lett. **100**, (2008) 096407.
- [5] Hsu, Yi-Ting, et al. "Inversion-protected higher-order topological superconductivity in monolayer WTe₂." *Physical Review Letters* 125.9 (2020): 097001.
- [6] Endres, Martin, et al. "Transparent Josephson junctions in higher-order topological insulator WTe₂ via Pd diffusion." *Physical Review Materials* 6.8 (2022): L081201.

^{*} Authors having equal contribution

Automated Structure Discovery for Scanning Tunnelling Microscopy

L. Kurki¹, N. Oinonen^{1,2}, and A. S. Foster^{1,3}

¹Department of Applied Physics, Aalto University, Finland

²Nanolayers Research Computing Ltd., London N12 0HL, United Kingdom

³WPI Nano Life Science Institute (WPI-NanoLSI), Kanazawa University, Japan

Corresponding author: lauri.l.kurki@aalto.fi

Scanning tunnelling microscopy (STM) functionalized with a CO molecule on the probe apex captures the electronic and physical structures of a sample with sub-molecular level detail [1]. While high-resolution STM is a widely adopted method in materials science, the produced images are often difficult to interpret due to the convoluted nature of the signal. In recent years, there has been rapid development in image analysis methods using machine learning, with particular impact in medical imaging. These concepts have been proven effective also in SPM in general and in particular for extracting sample properties from atomic force microscopy (AFM) images [2, 3, 4]. We build upon these models and show that we can extract atomic positions directly from STM images. We also further explore how the accuracy of these predictions varies with the use of a simultaneous AFM signal and finally establish the limits of the approach in an experimental context by predicting atomic structures from STM images of various organic molecules.

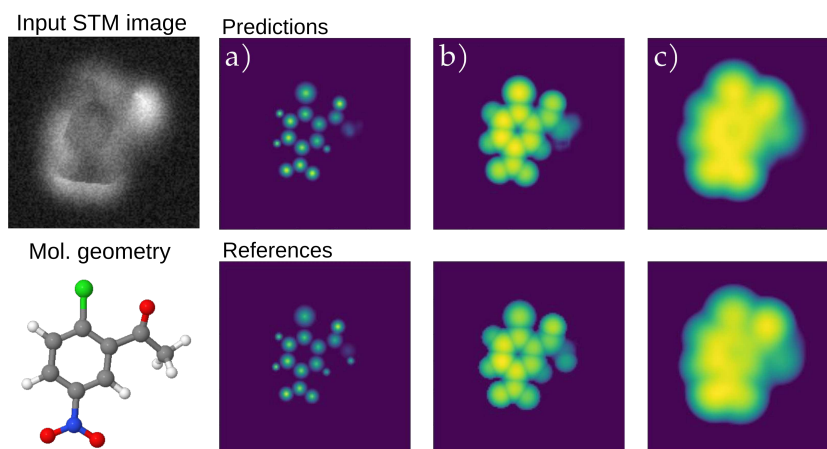


Figure 1: An example prediction of a molecular structure from a simulated STM image. We predict the (a) atomic disks, (b) vdW spheres and (c) height map descriptors [2].

[1] Cai, S., Kurki, L., Xu, C., Foster, A. S., Liljeroth, P. *J. Am. Chem. Soc.* 2022, 144, 44, 20227-20231

[2] Alldritt, B., Hapala, P., Oinonen, N., Urtev, F., Krejčí, O., Canova, F. F., Kannala, J., Schulz, F., Liljeroth, P., Foster, A. S. *Sci. Adv.* 2020, 6, eaay6913

[3] Carracedo-Cosme, J., Pérez, R. *npj Comput. Mater.* 2024, 10, 19.

[4] Kurki, L., Oinonen, N., Foster, A. S. arXiv:2312.08854 [cond-mat.mtrl-sci], 2023

High-fidelity robust qubit control by phase-modulated pulses

Marko Kuzmanović¹, Isak Björkman¹, John J. McCord¹, Shruti Dogra¹, and Gheorghe Sorin Paraoanu¹

¹ InstituteQ and QTF Centre of Excellence, Department of Applied Physics, School of Science, Aalto University, FI-00076 Aalto, Finland

Corresponding author: marko.kuzmanovic@aalto.fi

We present a set of *robust* and *high-fidelity* pulses that realize paradigmatic operations such as the transfer of the ground state population into the excited state (figure 1) and arbitrary X/Y rotations on the Bloch sphere (figure 2).

These pulses are based on the phase modulation of the control field. We provide an experimental proof-of-concept of these operations by using a transmon qubit, demonstrating resilience against deviations in the drive amplitude of more than $\approx 20\%$, and/or detuning from the qubit transition frequency in the order of 10 MHz. This modulation scheme is straightforward to implement in practice and can be deployed to any other qubit-based experimental platform.

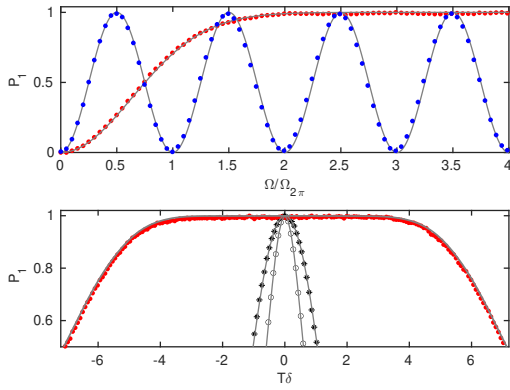


Figure 1: Top: the amplitude robustness of the population transfer pulse (red dots), compared to the usual non-modulated Rabi pulse (blue dots). Bottom: the detuning robustness of the population transfer pulse (red dots). The gray circles and stars correspond to a Rabi π ($\Omega = \Omega_{2\pi}/2$, $\Delta_{\max} = 0$) and a 3π ($\Omega = 3\Omega_{2\pi}/2$, $\Delta_{\max} = 0$) pulse respectively. The dots are experimental data, and the solid gray lines on both panels show the theoretical prediction.

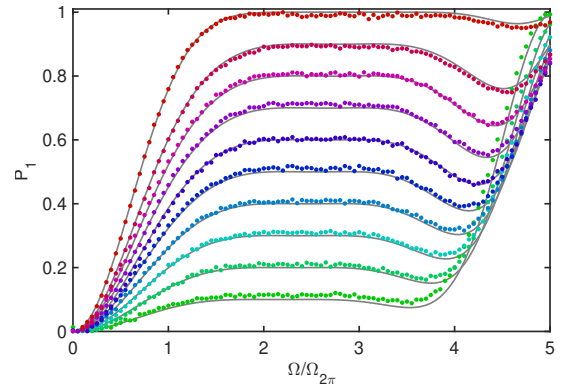


Figure 2: The experimentally measured population P_1 of the excited state (colored dots) after applying the the *amplitude robust arbitrary rotation pulse* to a qubit initialized in the ground state, designed to obtain $P_1 = \{0.1, 0.2, \dots, 1\}$. The solid gray lines show the theoretical prediction.

[1] Preprint available at <https://arxiv.org/abs/2308.13353>

Superconductivity in flat band systems with resonating valence bond pairing

Eeli Lamponen¹, Sofia Pöntys¹, Päivi Törmä¹

¹ Department of Applied Physics, Aalto University, Espoo, Finland

Corresponding author: eeli.lamponen@aalto.fi

Dispersionless Bloch bands, called flat bands, have been shown to enhance superconductivity in lattice systems; on a flat band, the movement of particles is suppressed, leading to comparatively stronger interaction effects [1, 2]. These results are obtained with conventional Bardeen-Cooper-Schrieffer (BCS) theory on the Hubbard model, where one considers a local phonon-mediated attraction between electrons on the same lattice site. For high-temperature superconductors, alternative mechanisms to explain the interaction that causes electron to form Cooper pairs are sought; among them is resonating valence bond (RVB) pairing [3] that is based on spin fluctuations. Obtained as the strongly *repulsive* limit of the Hubbard model, the RVB mechanism suggests an effective attractive interaction between electrons on neighbouring lattice sites, instead of those on the same site; see Fig. 1.

Both flat bands and the RVB interaction have been proposed as mechanisms to strengthen superconducting properties, and ultimately, to increase the critical temperature of a system. Combining the two, however, is still mostly an unexplored path. We take the RVB interaction on various lattice models that are typically used to demonstrate the desirable properties of flat bands, and study whether these properties are still present with the RVB interaction scheme. Preliminary results indicate that on multi-band lattices, flat bands and the RVB interaction can be intertwined in a non-trivial way, since the non-local nature of the RVB interaction makes the localization properties of the Bloch functions important, and the flat bands themselves are typically a result of a destructive interference pattern of the Bloch functions that suppresses particle movement.

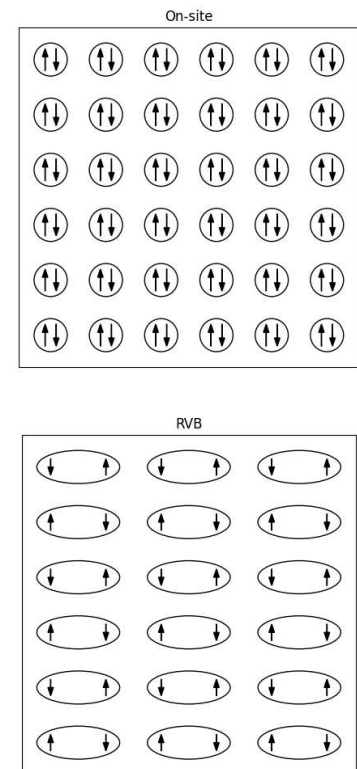


Figure 1: A schematic showing the different types of Cooper pair formation: the local, on-site interaction and the nearest-neighbour RVB interaction. The arrows represent the spin of a particle.

- [1] Peotta, Törmä, Superfluidity in topologically nontrivial flat bands, Nature Communications 6, 8944 (2015).
- [2] D. Leykam et al, Artificial flat band systems: from lattice models to experiments, Advances in Physics X 3, 1473052 (2018).
- [3] G. Baskaran, Resonating valence bond theory of superconductivity: Beyond cuprates, 2017. arXiv:1709.10070.

Attitudes towards Physics among Physics Minor Students

Katja Anniina Lauri¹ and Inkeri Kontro²

¹*Institute for Atmospheric and Earth System Research INAR / Physics, University of Helsinki, Helsinki, Finland*

²*Faculty of Engineering and Natural Sciences, Physics, Tampere University, Tampere, Finland*

Corresponding author: katja.lauri@helsinki.fi

We studied attitudes towards physics among students on a course, which has been designed to serve the needs of degree programmes whose students need at least one (but not more) university physics courses (e.g. Chemistry Eurobachelor). We studied the students on the first five times the course was given (spring 2018, 2019, 2020, 2021 and 2022). The total number of students in this study was 293 (of whom male 110 and female 181).

The course “Fysiikkaa luonnontieteilijöille” (Physics for natural scientists) is given in Finnish language and is provided by the Bachelor’s Programme in Physical Sciences at the University of Helsinki. The rough content and schedule of the course:

- Classical mechanics and relativity (2-2.5 weeks)
- Thermophysics (1-1.5 weeks)
- Electromagnetism and electrodynamics (2-2.5 weeks)
- Quantum physics (1-1.5 weeks)

Each teaching week includes six hours of contact teaching: four hours of lectures and two hours of supervised group work. “Serious calculus and algebra” like vector differentiations was used on the lectures, but the students were not expected to master it.

We used the Colorado Learning Attitudes about Science Survey (CLASS) [1] to assess the attitudes of students during the first and the last course week. The factors we used in the analysis were personal application and relation to real world (PARRW), effort and sense making (ESM), and problem solving self efficacy (PSSE) [2].

Our analysis shows that for male students, there was a statistically significant difference between the pre- and post-course CLASS results in the overall results as well as in PSSE. For female students, a statistically significant difference was seen in overall results and PARRW.

The course seemed to slightly enhance the students’ attitude towards physics, which is one of the main aims of the course.

[1] W. K. Adams, K. K. Perkins, N. S. Podolefsky, M. Dubson, N. D. Finkelstein, and C. E. Wieman, *Phys. Rev. ST Phys. Educ. Res.* **2**, 010101 (2006).

[2] I. Kontro and D. Buschhüter, *Phys. Rev. ST Phys. Educ. Res.* **16**, 020104 (2020).

Human-in-the-loop applications in Bayesian optimization for materials science

E. Lehto¹, A. Tiihonen¹, L. Filstroff², P. Mikkola³, S. Kaski^{3,4}, M. Todorović⁵, and P. Rinke¹

¹ Department of Applied Physics, Aalto University, Espoo, Finland

² ENSAI, CREST, Rennes, France

³ Department of Computer Science, Aalto University, Espoo, Finland

⁴ Department of Computer Science, University of Manchester, Manchester, United Kingdom

⁵ Department of Mechanical and Materials Engineering, University of Turku, Turku, Finland

Corresponding author: emma.lehto@aalto.fi

Bayesian optimization (BO) is a machine learning method for finding the optima of unknown functions in the fewest number of iterations possible [1]. In materials science, BO can be used for optimizing material compositions for a target property, such as the environmental stability of a perovskite material for perovskite solar cells. In this use BO can accelerate the development of next-generation energy solutions. However, machine learning methods generally struggle to meet the human ability to adapt to anomalies such as varying sample quality, which limits the use cases in automated materials optimization [2]. We address this issue by adding humans into the machine learning loop (HITL) as an additional data source for *e.g.* commenting on sample quality during the BO cycle.

We compared approaches for using HITL in simulated optimization of perovskite stability. The HITL was implemented with multitask BO using stability as the primary target and human as a secondary source. Existing experimental results [3] were used as ground truth for the stability while human expert opinion was simulated with a corresponding sample quality landscape developed based on experiments. The performance of the HITL approach was benchmarked against traditional single task BO that does not use humans as a data source. Benchmarks were implemented as 50 repetitions of 100 iterations of BO with noisy sampling. The HITL method located the global optimum location with good quality samples in an average of 10 iterations while the vanilla BO took on average 22 iterations to do the same. This indicates that our HITL approach accelerates convergence to the optima that satisfy the human guidance given during the cycle, which increases trust in the BO experiment results.

- [1] Frazier, Peter I. "Bayesian optimization." Recent advances in optimization and modeling of contemporary problems. Informs, 2018. 255-278.
- [2] Tiihonen, Armi, *et al.* "More trustworthy Bayesian optimization of materials properties by adding human into the loop." AI for Accelerated Materials Design NeurIPS 2022 Workshop. 2022.
- [3] Sun, Shijing, *et al.* "A data fusion approach to optimize compositional stability of halide perovskites." Matter 4.4 (2021): 1305-1322.

Modeling the effects of high energy ion impacts in diamond

Aleksi Leino, Chloé Nozais, and Flyura Djurabekova
Department of Physics, University of Helsinki, Helsinki, Finland
Corresponding author: aleksi.leino@helsinki.fi

Ion accelerators operating in the keV to GeV regime are central for materials characterization and modification. While theoretical understanding of ion interactions below the MeV regime is well-established, the higher energy range lacks a widely accepted predictive theory, with even the fundamentals still subject to debate. These high energy ions, also known as swift heavy ions (SHIs), interact primarily with the electrons, and electronic ground state computations no longer suffice.

There is an increasing need to understand the electronic effects for practical applications. SHIs travel in a straight path and interact with materials much like a femtosecond laser pulse but without attenuation and with a spot size of a few nanometers. This characteristic enables distinctive nanoscale modifications deep below the surface. A recent example is the production of NV centers in nitrogen-doped diamond [1]. SHIs can convert nitrogen into NV centers along their trajectories. NV centers have gained wide attention due to their potential as solid-state qubits with long coherence times. Utilizing SHI irradiation allows for the precise placement of NV centers along the trajectory, potentially resulting in, up to 1000 coupled qubits.

We present advances in modeling the effects of SHIs in diamond using the two-temperature molecular dynamics method [2]. Our simulations agree well with experimental observations and lay the foundation for progressing towards a parameter-free model.

- [1] R. E. Lake, A. Persaud, C. Christian, E. S. Barnard, E. M. Chan, A. A. Bettiol, M. Tomut, C. Trautman and T. Schenkel, *Appl. Phys. Lett.* **118**, 084002 (2021)
- [2] A. A. Leino, S. L. Daraszewicz, O. H. Pakarinen, K. Nordlund and F. Djurabekova, *EPL* **110**, 16004 (2014)

Segmentation of trabecular bone in X-ray microtomography using a workflow of elementary image processing methods

V-M. Leino¹, F. Prodam², M. F. Faienza³, and G. Brunetti⁴

¹*Department of Physics, P.O. Box 64, FI-00014 University of Helsinki, Finland*

²*Endocrinology Unit, Department of Health Sciences, Università del Piemonte Orientale, Novara, Italy*

³*Pediatric Unit, Department of Precision and Regenerative Medicine and Ionian Area, University of Bari, Bari, Italy*

⁴*Department of Biosciences, Biotechnologies and Environment, University of Bari, Bari, Italy*

Corresponding author: vesa-matti.leino@helsinki.fi

X-ray microtomography (i.e. micro-CT) imaging can be used to scan the internal structure of various types of samples at the micrometre level. The obtained 3D-image of the sample's structure can then be analysed quantitatively, provided that a segmentation of the image into its constituents, i.e., into all different regions of interest, can be accomplished. Typical samples for which the micrometre resolution of X-ray microtomography is required are bones from small animals, e.g., femurs from mice [1]. In these, regions of particular interest are the intricate 3D-network structures of trabecular bone that are found inside long bones, enclosed by – and connected to – the more compact cortical bone.

The development of a precise, reliable and preferably completely automated segmentation procedure is not a trivial task, and numerous different methods for the segmentation of X-ray microtomography images – based on varying principles – have been developed over time [2]. In recent years, the focus of the research on image segmentation has shifted to AI and machine learning methods, however, as will be demonstrated in this presentation, a relatively straightforward workflow of elementary image processing methods may still provide reasonably accurate results in comparison.

The workflow – resembling the method introduced by Herbst et al. in 2021 [2] – consists of a sequence of image processing operations that are applied to the (3D-)images consecutively. It is based mainly on morphological filtering of binary images, which are initially obtained by thresholding the original image. The filtering can be applied either as proper 3D-filtering or as fast slice-by-slice 2D-filtering.

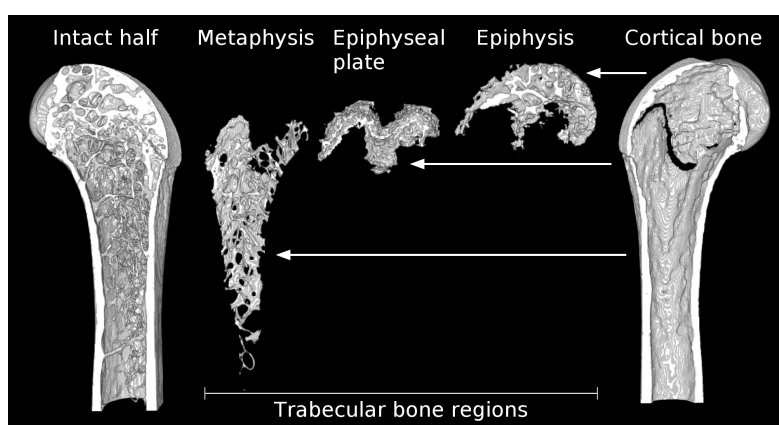


Figure 1: A 3D-visualization of a bone sample for which the segmentation has been performed. The internal structure is brought to view by first halving the initial 3D-image, and then separating – step by step – three distinct regions of trabecular bone from each other and the surrounding cortical bone. The automated segmentation workflow can distinguish the curvilinear epiphyseal plate, located between the metaphysis and the epiphysis regions, enabling a more comprehensive segmentation.

[1] G. Brunetti, et al., *J. Bone. Miner. Res.* **33**, 4 (2018).

[2] E. C. Herbst, et al., *R. Soc. Open Sci.* **8**, 8 (2021).

Radiative-transfer coherent-backscattering modelling for photometric and polarimetric phase curves of Galilean satellites

A. Leppälä¹, K. Muinonen¹, N. Kiselev², V. Rosenbush^{3,4}, L. Kolokolova⁵, A. Savushkin², and N. Karpov⁶

¹ Department of Physics, University of Helsinki, Helsinki, Finland

² Crimean Astrophysical Observatory, Nauchnij, 298409, Crimea

³ Taras Shevchenko National University of Kyiv, Astronomical Observatory, 04053 Kyiv, Ukraine

⁴ Main Astronomical Observatory of National Academy of Sciences of Ukraine, 03143 Kyiv, Ukraine

⁵ University of Maryland, College Park, MD 20742, USA

⁶ International Center for Astronomical, Medical and Ecological Research, Peak Terskol Observatory, Ukraine

Corresponding author: ari.leppala@helsinki.fi

Photometric phase curves of airless Solar System objects exhibit a distinctive opposition effect, characterized by nonlinear brightening as phase angles approach backscattering. At phase angles less than approximately 20 degrees, polarimetric phase curves predominantly display a negative degree of linear polarization. These phenomena are inadequately explained by radiative transfer (RT) models alone but incorporating coherent backscattering (CB) provides a comprehensive modelling solution.

In our study, we employed radiative-transfer coherent-backscattering (RT-CB, [1]) modelling with an ensemble-averaged scattering matrix. With this approach, parameterized phase matrix elements were utilized to replicate the observed low-phase-angle polarimetric phase curves for Io and icy moon Ganymede [2], as well as Europa [3]. We adjusted the scattering matrix until the computations closely matched the observed data, resulting in an ensemble-averaged scattering matrix for modelling both photometric and polarimetric phase curves for these satellites. Io and Europa have similar geometric albedos (A_g) 0.63 and 0.67, but negative polarization branch (NPB) shapes differ. The NPB of Ganymede ($A_g = 0.43$) is morphologically similar to that of Europa, although it is described by different parameter values for scattering function. This is likely due to the compositions of their surfaces: Europa's with H₂O ice, Ganymede's with H₂O ice and silicates, and Io's with sulfuric/silicate. Polarimetric observations show only slight or no dependence on the wavelength, indicating wide particle size distributions with different real parts of refractive index, for Europa and Ganymede ($\text{Re}(m) \sim 1.3$) and Io ($\text{Re}(m) > \sim 1.4$). Numerical computations using the RT-CB method demonstrated a match to the polarimetric observations and to the geometric albedos. For Ganymede, the single-scattering albedo ω and mean free path length $kl = 2\pi l/\lambda_{\text{eff}}$, were ≈ 0.943 and ≈ 150 , respectively, where λ_{eff} is the wavelength. For Io's regolith, $\omega \approx 0.979$ and $kl \approx 40$.

[1] K. Muinonen et. al ApJ **760**, 118 (2012)

[2] N. Kiselev et al Planet. Sci. J. **5**, 10 (2024)

[3] N. Kiselev et al Planet. Sci. J. **3**, 134 (2022)

I'd like to build and operate a fusion power plant – who will license it?

M. I. Airila¹, and T. Lindén²

¹VTT Technical Research Centre of Finland Ltd, Espoo, Finland

²Helsinki Institute of Physics, Helsinki, Finland

Corresponding author: tlinden@cc.helsinki.fi

Some countries like the USA and the UK have recently taken their position towards regulation of fusion power plants. Pressure to set up regulatory frameworks comes from political leaders and the industry, as several private companies have attracted sufficient funding to start building fusion prototypes and demonstration devices. Their investment decisions depend critically on the predictability of licensing, so these countries have launched ambitious fusion energy strategies and appropriate regulatory consultation processes to create a risk-appropriate regulatory environment. The EU is moving at a slower speed but following the developments closely. We summarize the status in these countries and speculate also how it would work in Finland - now, and later under the renewed Nuclear Energy Act [1].

[1] M. I. Airila and T. Lindén, *ATS Ydintekniikka* **52**, 25–29 (2023).

ALICE- and CMS-experiments disk storage upgrade for LHC Run 3

Roope Jukkara¹, Sami Lehti², Tomas Lindén², Mikael Myllymaki², Ville Salmela¹,
and Tommi Tervo¹

¹CSC - IT Center for Science Ltd., Espoo, Finland

²Helsinki Institute of Physics, Helsinki, Finland

Corresponding author: tlinden@cc.helsinki.fi

Helsinki Institute of Physics (HIP) participates in the Large Hadron Collider (LHC) experiments ALICE, CMS and TOTEM. HIP collaborates with CSC - IT Center for Science on providing Worldwide LHC Computing Grid (WLCG) resources. The ALICE resources are part of the Nordic distributed Tier-1 resource NDGF and the CMS resources form a CMS Tier-2 called T2_FI_HIP. The ALICE and CMS HIP disk storage hardware and software was recently upgraded and the total raw capacity of the new dCache system is 6 760 TB, which is more than three times as large as the previous system. The new storage is located about 500 km north of the location of the previous system. In the following the dCache storage upgrade and its initial performance will be discussed.

Textured grain boundaries in WMoTaNbV high entropy alloy

Anna Liski¹, Tomi Vuoriheimo¹, Marianna Kemell², Kenichiro Mizohata¹ and Filip Tuomisto¹

¹*Department of Physics, University of Helsinki, Helsinki, Finland*

²*Department of Chemistry, University of Helsinki, Helsinki, Finland*

Corresponding author: anna.liski@helsinki.fi

WMoTaNbV high-entropy alloy is a promising solid state hydrogen storage material which can absorb large quantities of hydrogen directly from the atmosphere [1]. It is a random mixture of five refractory components, of which three (Nb, V, Ta) hold negative solution energies for hydrogen in their pure form. The maximum capacity for hydrogen storage of pure metals is limited, as compared to that of hydrogen absorbing alloys and intermetallic compounds, driving the evolution of potential hydrogen storage materials towards increasing complexity. Irregularities in the lattice structure provide additional trapping sites for the small hydrogen atom to occupy, thus increasing the levels of maximum storage [2].

SEM and EDS were used to study the structure and composition of the grain boundaries in WMoTaNbV alloy. Images reveal a textured surface of the grain boundary covering the visible parts of the grain with small spherical formations. The features are likely to originate from manufacturing process and their sizescale is within the range of few hundred nanometers. The EDS measurements reveal a different elemental composition at the grain boundary, with an enrichment of V, Nb and Mo. The finding is consistent with the previous studies [3] and supports hydrogen solution results studied by ERDA.

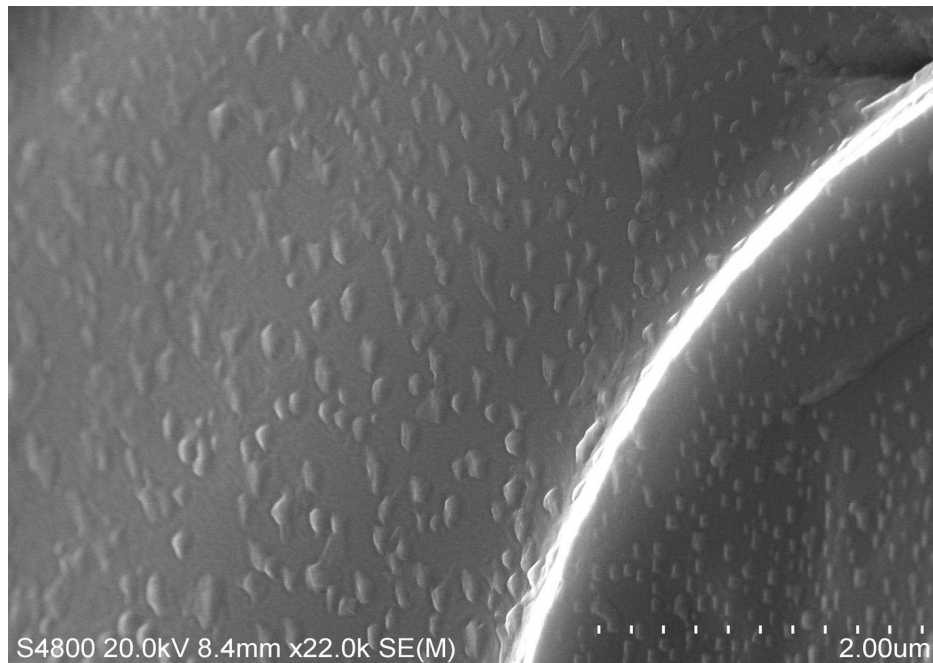


Fig. 1: SEM image of the textured grain boundary of WMoTaNbV alloy.

[1] A. Liski, et. al., *Materials*, 15 (2022), 20.

[2] M. Sahlberg, et. al., *Scientific Reports* 6 (2016) 36770.

[3] W.-H. Lee, et. al., *Metals*, 9 (2019), 12.

Mechanisms of bubble growth and blistering on metals exposed to hydrogen

Alvaro Lopez-Cazalilla¹, Catarina Serafim^{1, 2}, Sergio Calatroni², Walter Wuensch², F. Djurabekova¹

¹ Department of Physics, P.O. Box 43, FI-00014 University of Helsinki, Finland

² CERN, European Organization for Nuclear Research, 1211 Geneva 23, Switzerland

Corresponding author: alvaro.lopezcazalilla@helsinki.fi

Increasing demands of energy, along with the yet increasing concern for the development of environmentally friendly technologies, call for exploring new ways of cost-efficient energy production. Hydrogen is one of the primary candidates for this purpose, due to its abundance and diverse ways of how it can be used. Moreover, hydrogen-based technologies are carbon-neutral, and hence their use could have a major effect on slowing down the climate change. Hence, the insights on the interaction of H with metals are crucial to reach that ambitious goal.

Blistering is a process that usually takes place close to the surface of metals when they are irradiated, as can be seen in radio-frequency quadrupoles accelerating structures. This pronounced change of the surface morphology has been measured when extended irradiation is done with energetic light ions.

We use computational methods to address the fast bubble growth in Cu, associated with blistering, when exposed to H⁻ irradiation [1]. We analyze the interaction of the formed dislocation loops with the different surface orientations of copper. Furthermore, we focus on the H depth profile and vacancy distributions along low-indices crystallographic directions [2].

We find a strong correlation between the blistering and crystallographic orientations. The distance between the mean penetration depth of H and the vacancies (recoils) creation is considerably different along the considered directions, and provides an explanation of the resistance to blistering of some grain orientations. Furthermore, we introduce some successful initial tests performed with the newly developed ML potential.

- [1] Alvaro Lopez-Cazalilla, Flyura Djurabekova, Fredric Granberg, Kenichiro Mizohata, Ana Teresa Perez Fontenla, Sergio Calatroni, Walter Wuensch *Acta Materialia*, **225** 12 (2022)
- [2] Alvaro Lopez-Cazalilla, Catarina Serafim, Jyri Kimari, Milad Ghaemi, Ana Teresa Perez-Fontenla, Sergio Calatroni, Alexej Grudiev, W. Wuensch, F. Djurabekova *Acta Materialia*, **266** 119699 (2024)

A modified version of the MDRANGE software for calculations in nuclear material physics

Tetiana Malykhina¹, Andrea Sand²

¹*SCI CS Group, Aalto University, Espoo, Finland*

²*NuME Group, Aalto University, Espoo, Finland*

Corresponding author: tetiana.malykhina@aalto.fi

Computer simulation is an important component of scientific research in the field of radiation physics and materials science. Simulation makes it possible to preliminarily evaluate the results of planned nuclear physics experiments. It is important for study of material's properties, for estimation of radiation resistance of materials, and for research in the field of nanotechnology. There are a lot of programs and tools which allow us to model the interaction of particles with matter. Each software has its area of usage as well as restrictions. The MDRANGE [1] program is software that allows us to simulate the passage of ions through a substance using the molecular dynamics method.

We modified the existing version of certain program's modules to get new features.

The modified version [2] of the MDRANGE code allows us to get the following information about backscattered ions:

1. The relative number of backscattered ions normalized per 1 primary ion.
2. Energy spectra of backscattered ions.
3. Complete 3D trajectory of each backscattered ion.
4. The value of the maximum penetration depth into the matter for backscattered ions.
5. Components of the velocity vector for each segment of the trajectory of backscattered ions.
6. The contribution of various components of the total value of deposited energy, i.e., nuclear deposited energy and electronic deposited energy, for backscattered ions.

Further processing of the data allows us to obtain various levels of detail in the results.

The modified version of the MDRANGE program is adapted to work using the Triton [3] High-Performance Computing (HPC) cluster in a parallel mode. Considering the features of tasks running on the Triton HPC cluster using a job queue, some functions for calculating the initial seed of the random number generator were modified. Some scripts that we implemented in Python were used to check the uniqueness of the calculated data on ion trajectories and spectra, etc., as well as to process the results. The results of using the modified version of the MDRANGE code are presented in the report. This additional functionality of the code can be useful in material science research.

[1] K. Nordlund, *Comput. Mater. Sci.* **3**, 448 (1995).

[2] https://github.com/TetianaMalykhina/MDRANGE4_for_Triton

[3] [Triton cluster https://scicomp.aalto.fi/triton/](https://scicomp.aalto.fi/triton/)

Cloud evolution in the high-energy molecular ring λ Orionis

E. Mannfors¹ and the B-FROST collaboration

¹ Department of physics, University of Helsinki, Finland

Corresponding author: emma.mannfors@helsinki.fi

Background

High-mass stars contribute significantly to the evolution of the Galactic environment, both during their lifetime through feedback and outflows, and at their death through supernovae. Due to their short lifespans and rarity, the interaction between high-mass stars and the interstellar medium (ISM) is difficult to observe. This leads to a lack of understanding on what causes stars to form, and how the gas within galaxies evolves through time. The nearby ($d \sim 400$ pc) molecular ring λ Orionis is the perfect region to study both the effects of ongoing feedback and a recent supernova on the ISM. The λ Orionis ring surrounds the bright O8III star Meissa, and was likely formed when a binary companion of Meissa exploded as a supernova ~ 1 Myr ago [1, 2].

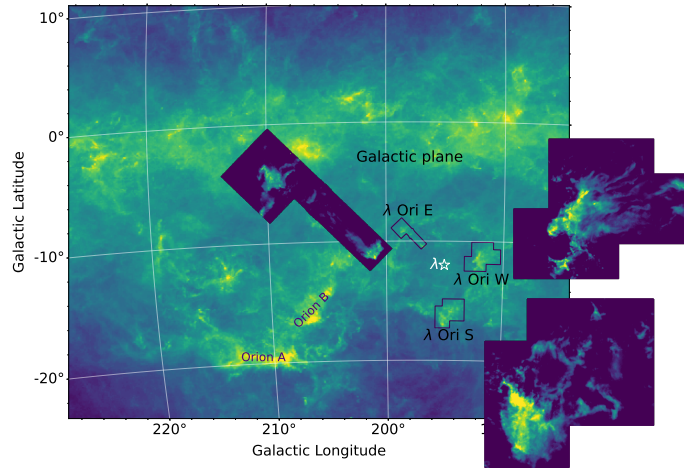


Fig. 1: The λ Orionis region. The three overlaid images show Moment 0 (integrated emission) maps of the three regions. The white star marks the location of Meissa at the center of the molecular ring.

This work

We present ^{12}CO and ^{13}CO molecular line observations of three dense regions in λ Orionis (contours in Fig. 1). These data have been observed as part of the Fields and star formation across Scales with TRA0 (B-FROST) survey (Montillaud et al., in prep.) using the 13-m TRA0 telescope located in Korea. The purpose of this survey is to explain how magnetic fields interact with molecular clouds across a wide range of environments, from quiescent regions such as MBM12 to high-energy, likely feedback-dominated regions such as λ Orionis.

We use a combination of data, including *Planck* polarization and infrared continuum observations, WISE continuum observations, and molecular lines to achieve a full picture of the λ Orionis region. We combine the data to understand how magnetic fields and stellar feedback drive cloud evolution. Catalogs of protostars from the GAIA telescope are used to study the possibility of triggered star formation in the ring. Of particular interest are the streamers visible in λ Orionis W (top-right overlay in Fig. 1), periodic structures which have perhaps been formed through turbulence between the high- and low-density ISM.

[1] Cunha, K., & Smith, V. V. (1996), *A&A*, 309, 892.

[2] Dolan, C. J., & Mathieu, R. D. (2002), *AJ*, 123, 387.

Towards a joint retrieval of aerosols and CO₂ from space-based hyperspectral imager data

A. Mikkonen¹, H. Lindqvist¹, V. Natraj², J. Nurmela¹ and J. Tamminen¹

¹ Finnish Meteorological Institute, Helsinki, Finland

²Jet Propulsion Laboratory, Pasadena, California, United States

Corresponding author: antti.mikkonen@fmi.fi

Greenhouse gas emissions from anthropogenic activities are the main driver of current global climate change. Emission monitoring is essential for the verification of emission reduction efforts and a feasible way for attaining global coverage are satellite observations. Recent developments in space-based hyperspectral cameras open up new possibilities for greenhouse gas emission monitoring also on a smaller scale.

Most of the anthropogenic greenhouse gas emissions originate from urban areas. Urban areas are also sources of co-emitted atmospheric aerosols, which decrease the local air quality and complicate the atmospheric radiative transfer. Even slight concentrations of atmospheric aerosols can cause considerable inaccuracies in space-based remote sensing observations of carbon dioxide (CO₂).

In this work, we present a novel retrieval method for a co-emitted CO₂ and aerosol emission plume content originating from a point source observed from a satellite. We plan to test the method for a joint CO₂ and aerosol retrieval and emission rate estimation from satellite-based hyperspectral imaging data, such as imagery obtained using EMIT[1] or PRISMA[2] and simulated observations from the upcoming CO2M[3] mission. The solar and viewing angle dependent radiative coupling of adjacent camera pixels and co-emission of aerosols are investigated as means to improve the CO₂ retrieval process.

As part of this work, a novel approach to solve the spectral radiative transfer equation in an inhomogeneous medium is introduced, continuing on the work presented in [4]. The GPU-based solver outputs top-of-the-atmosphere radiances in near- to shortwave-infrared wavelengths and thus enables a rapid retrieval of atmospheric constituents in a 3D atmosphere.

[1] <https://earth.jpl.nasa.gov/emit/>

[2] <https://www.asi.it/en/earth-science/prisma/>

[3] <https://www.eumetsat.int/copernicus-co2m-science-support>

[4] Mikkonen, A., Lindqvist, H., Peltoniemi, J. & Tamminen, J.: Non-Lambertian snow surface reflection models for simulated top-of-the-atmosphere radiances in the NIR and SWIR wavelengths, *Journal of Quantitative Spectroscopy and Radiative Transfer*, **315**, 2024, 108892, <https://doi.org/10.1016/j.jqsrt.2023.108892>.

Validation of the CMS Precision Proton Spectrometer data using exclusive dilepton events

A. Milieva¹ for the CMS collaboration

¹ Helsinki Institute of Physics (HIP), Helsinki, Finland

Corresponding author: anna.milieva@helsinki.fi

The CMS Precision Proton Spectrometer (PPS) consists of tracking and timing detectors installed along the Large Hadron Collider (LHC) beam line between 210 and 220 m from the interaction point on both sides of the CMS experiment. The aim of the apparatus is to measure the kinematics and Time-of-Flight (ToF) of protons which emerge intact from the proton-proton collision. The physics focus of PPS are to study high invariant mass Central Exclusive Processes (CEP), where PPS measures the intact protons and the central CMS detector the centrally produced system. The background is rejected using the kinematical matching between the protons and the centrally produced system as well as matching the longitudinal vertex position from protons ToF with the vertex reconstructed from the CMS tracker. The former however relies on a good knowledge of the LHC optics and a precise alignment of the detectors with respect to the outgoing proton beam.

To validate the PPS data from LHC Run 3, we perform a study focused on events with a lepton (a muon or an electron) pair reconstructed the CMS central detector and at least one proton measured in PPS, analogous to a similar study done with Run 2 data [1]. To remove the dominant Drell-Yan background in combination with protons from pileup events, we require dilepton invariant masses larger than 110 GeV and lepton transverse momenta larger than 20 GeV.

The key of this study is to examine the kinematics of the dilepton system which offer a precise way to calculate the fractional momentum loss of the forward proton, in the case of exclusive dilepton production. By comparing the calculated momentum loss from the dileptons and measured momentum loss from the PPS, the PPS alignment and the LHC optics used for reconstructing the proton momentum loss will be validated [2] also for the PPS Run 3 data. In addition, the motivation for searching for a doubly-charged Higgs boson decaying to two same-signed tau leptons using the CEP process with PPS will be outlined [3].

[1] CMS and TOTEM collaborations, JHEP 07 (2018) 153.

[2] CMS and TOTEM collaborations, JINST 18 (2023) P09009.

[3] A. Crivellin et al., Phys. Rev. D 99 (2019) 035004.

Detecting a gravitational wave background from early universe phase transitions with LISA

T. Minkkinen¹

¹ Department of Physics and Helsinki Institute of Physics, PL 64, FI-00014 University of Helsinki, Finland

Corresponding author: tiina.minkkinen@helsinki.fi

In the next decade or so, the first spaceborne gravitational wave observatory LISA (Laser Interferometer Space Antenna) will start probing the universe. It has the potential to observe a gravitational wave background created by early universe events, such as first order phase transitions happening right after the Big Bang. Their existence could help fill in the gaps in our current Standard Model of particle physics. Here we explore different phase transition models to see which ones give rise to gravitational wave backgrounds in LISA's sensitivity range, where there are also realistic galactic binary systems and instrument noises interfering with our observations. We use the Deviance Information Criterion to establish a range of detectable phase transition models, and see if we can use the expected annual modulation of the galactic foreground to improve phase transition detectability.

The new ALICE Fast Interaction Trigger in LHC Run 3

A. Molander^{1,2} for the ALICE collaboration

¹ Helsinki Institute of Physics (HIP), P.O. Box 64, FI-00014 University of Helsinki, Finland

²Department of Physics, University of Jyväskylä, P.O. Box 35, FI-40014 University of Jyväskylä, Finland

Corresponding author: andreas.molander@cern.ch

On the 5th of July 2022, the Large Hadron Collider (LHC) at CERN, Geneva, started the official data-taking of the current LHC run, Run 3, after a maintenance, upgrade, and commissioning period of about three and a half years. ALICE (A Large Ion Collider Experiment) has undergone many upgrades and improvements [1], one of which is the new Fast Interaction Trigger (FIT) detector [2, 3]. With its Cherenkov and scintillator arrays, FIT detects particles from proton and heavy-ion collisions in the forward regions of ALICE. It provides low-latency interaction triggers, precise interaction time, luminosity and background monitoring, and determination of multiplicity, centrality and event plane. FIT has performed well in both proton-proton and Pb-Pb collision runs: it shows excellent collision time and vertex reconstruction; provides a sophisticated interaction trigger menu; and has been giving critical feedback about luminosity and background to the LHC for online beam tuning. The performance of FIT is continuously improving thanks to upgrades to electronics, firmware and software. The installation and commissioning of FIT, its performance during the start of Run 3 and future development and outlook are presented.

- [1] W. H. Trzaska, "New ALICE detectors for Run 3 and 4 at the CERN LHC", *Nuclear Instruments and Methods in Physics Research Section A: Accelerators, Spectrometers, Detectors and Associated Equipment* **958** (2020) 162116, <https://doi.org/10.1016/j.nima.2019.04.070>.
- [2] M. Slupecki, "Fast Interaction Trigger for ALICE upgrade", *Nuclear Instruments and Methods in Physics Research Section A: Accelerators, Spectrometers, Detectors and Associated Equipment* **1039** (2022) 167021, <https://doi.org/10.1016/j.nima.2022.167021>.
- [3] W.H. Trzaska, "ALICE Fast Interaction Trigger (FIT) video" (2023), <https://videos.cern.ch/record/2298206>.
- [4] D. Finogeev, "Fully integrated digital readout for the new Fast Interaction Trigger for the ALICE upgrade", *Nuclear Instruments and Methods in Physics Research Section A: Accelerators, Spectrometers, Detectors and Associated Equipment* **952** (2020) 161920, <https://doi.org/10.1016/j.nima.2019.02.047>.



Tunable coupler for qutrit-based quantum computing

Ilya N. Moskalenko, G. S. Paraoanu

QTF Centre of Excellence, Department of Applied Physics, Aalto University School of Science,
P.O. Box 15100, 00076 Aalto, Finland

InstituteQ - The Finnish Quantum Institute, Aalto University, P.O. Box 11000, 00076 Aalto,
Finland

Corresponding author: ilya.moskalenko@aalto.fi

The last three years have witnessed an active growth in research related to the implementation of ternary logic on superconducting quantum circuits [1]. Quantum information processing using qutrits, three-level quantum systems, as a fundamental unit offers a promising alternative to conventional qubit-based architectures through larger (an exponential increase from 2^N to 3^N), more connected computational spaces. It is also worth mentioning the perspective of implementation qutrits for the simulation of the non-Hermitian dynamic of open quantum systems [2].

While theoretical studies have shown benefits for quantum compilation, simplification of a variety of algorithms [3, 4], and improved schemes for quantum error correction [5, 6], experimental implementations of qutrits have been presented on transmons via additional control of the second excited state [7, 8, 1]. These works have realized high-fidelity single qutrit operations [7], as well as effectively engineering a high-fidelity two-qutrit entanglement based on direct capacitive qutrit-qutrit coupling [8] and schemes with tunable interaction [1]. Despite the latest progress in qutrit-based systems, an essential step towards creating a multi-qutrit universal quantum processor will be the realization of scalable architectures with a large on-off ratio and canceled-out crosstalk.

In this work, we propose a modular scalable, and highly efficient two-qutrit quantum scheme with tunable coupling. We employ a tunable element with multiple degrees of freedom to achieve excellent connectivity in the nine-dimensional Hilbert space via flux-controlled interference in a three-junction superconducting quantum interference device. Crucially, the multi-mode coupler possesses an internally defined near-to-zero-coupling state that makes it particularly attractive as a modular and versatile design element for realizing fast and robust coupling in qutrit-based quantum computing and simulation applications.

- [1] R. Tanay, Phys. Rev. Appl. **19**, 6 (2023)
- [2] M. Abbasi, Phys. Rev. Lett. **128**, 16 (2022)
- [3] Y. Wang, Frontiers in Physics **8**, 2296-424X (2020)
- [4] Y.Deller, Phys. Rev. A **107**, 6 (2023)
- [5] K.C. Miao, Nat. Phys. **19**, 1745-2481 (2023)
- [6] R. Majumdar, Phys. Rev. A **97**, 5 (2018)
- [7] A. Morvan, Phys. Rev. Lett. **126**, 21 (2021)
- [8] N.Goss, Nat Commun. **13**, 1 (2022)

Generation and analysis of squeezed states in Josephson Parametric Amplifier

I. Lilja^{*,1}, E. Mukhanova^{†,1}, K. V. Petrovnin¹, M. R. Perelshtein¹, V. Vesterinen², G. S. Paroanu¹, and P. J. Hakonen¹

¹*QTF Centre of Excellence, Department of Applied Physics, Aalto University, P.O. Box 15100, FI-00076 AALTO, Finland*

²*VTT Technical Research Centre of Finland Ltd, QTF Centre of Excellence, Espoo, Finland*

The field of Quantum information offers protocols for storing, transmitting and processing information beyond what can be achieved with classical information technology. The exploitation of quantum mechanical properties can lead to quantum information protocols being significantly more efficient than their classical counterparts. Continuous-Variable (CV) states offer an attractive platform for implementing various quantum information CV protocols [1].

Unlike qubit systems based on discrete variables, CV states operate with squeezed states of the electromagnetic field. A cluster state is a multipartite entangled CV state that has a specific square lattice structure, which can be used as an ideal logical unit in quantum CV information processes [2]. However, in order to describe the internal structure of such a system, a fully quantum simulation is necessary. In this work, we demonstrate the possibility for reconstructing the real internal state of an experimentally generated system, by comparing it with fully quantum numerical simulations employing both Lindblad and Langevin equations. As an experimental reference, we use a cluster state unit cell produced inside a single resonance of a Josephson Parametric Oscillator (JPO). The entanglement properties of the experimentally generated state are entirely contained in its covariance matrix, which we compare with the results of the simulations.

The methods outlined in this work can be easily expanded to a larger cluster state network. This network can in principle be used as a universal quantum computing platform.

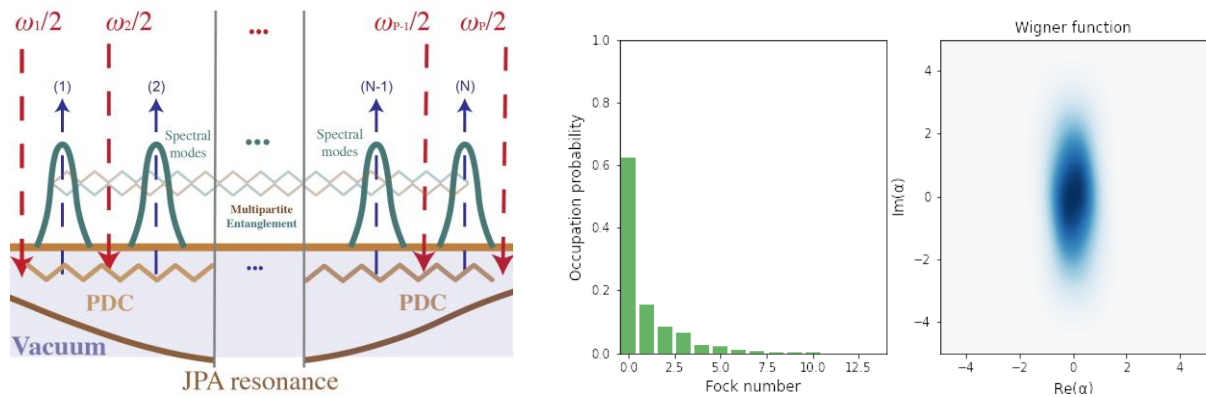


Figure 1: Illustrations on how modes are generated inside the parametric cavity (left) and a squeezed state simulation (right).

[1] M. R. Perelshtein et al. Phys. Rev. Applied 18, 024063 (2022).

[2] K. V. Petrovnin et al. Advanced Quantum Technologies 6, 2200031 (2023).

*Corresponding author: ilari.lilja@aalto.fi

†Corresponding author: ekaterina.mukhanova@aalto.fi

Personalized large-scale modeling of critical synchronization dynamics

Myrov Vladislav^{1,*}, Suleimanova Alina^{1,*}, J. Matias Palva^{1,2,3}

¹ Aalto University, Espoo, Finland

² University of Helsinki, Helsinki, Finland

³ University of Glasgow, Glasgow, United Kingdom

* Equally contributed authors

Corresponding authors: vladislav.myrov@aalto.fi, alina.suleimanova@aalto.fi

Brain activity is characterized by prominent rhythmicity in neuronal population activity, i.e., neuronal oscillations. Oscillations play mechanistic roles in regulation of neuronal activity and communication and are involved in many systems-level brain functions from sensorimotor processing to higher-level cognitive functions such as attention[1] and working memory [2]. Oscillations also serve as mathematical foundations for other types of analysis such as functional connectivity or long-range temporal correlations.

Functional connectivity refers to temporal correlations among neural activity patterns in different regions, crucial for processes like memory and attention. Measured through metrics like phase synchrony, it provides insights into brain interaction [3]. Long-range temporal correlations involve patterns in neural oscillations across time scales, indicating self-organization to criticality [4,5]. Changes in critical properties may signal conditions like epilepsy or ADHD.

Computational models can simulate neural activity with different levels of abstraction, which helps to investigate the mechanisms of brain activity generation [6]. We introduce the Myrov-Palva model - a computational model of self-synchronized oscillatory activity based on the Kuramoto model with hierarchical organization into multiple nodes with nested oscillators. We show, at first, that the model yields the most physiologically plausible dynamics in the subcritical regime. At second, we implemented a gradient-descent based fitting algorithm for synchrony and criticality to produce a whole-brain model digital-twin. Fitting the model to the real MEG data we found that it can capture individual brain dynamics with up to 70% correlation with FC and LRTC metrics.

Overall, we believe that our model can be a useful tool for simulating realistic brain-dynamics and personalized predictions.

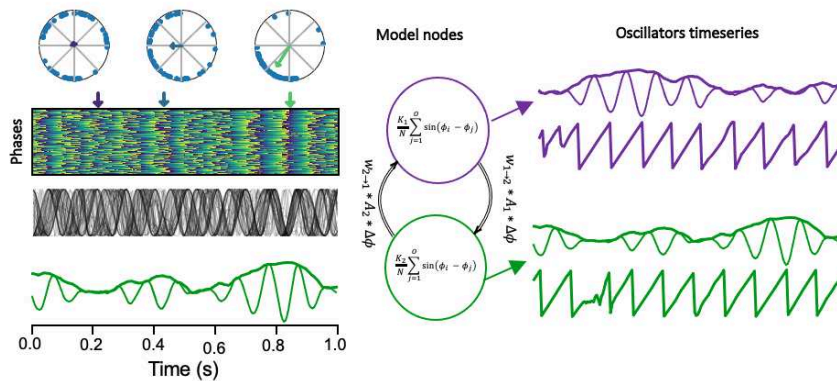


Fig. 1: Schematic representation of the Hierarchical Model implementation

1. Muriel Lobier, J. Matias Palva, Satu Palva, High-alpha band synchronization across frontal, parietal and visual cortex mediates behavioral and neuronal effects of visuospatial attention, *NeuroImage*, 2018
2. Palva & Palva et.al, Neuronal synchrony reveals working memory networks and predicts individual memory capacity, *PNAS*, 2010
3. Schmidt, B. T., Ghuman, A. S., & Huppert, T. J. (2014). Whole brain functional connectivity using phase locking measures of resting state magnetoencephalography. *Frontiers in neuroscience*, 8, 141.
4. Linkenkaer-Hansen et. al. (2001). Long-range temporal correlations and scaling behavior in human brain oscillations. *Journal of Neuroscience*, 21(4), 1370-1377
5. Beggs, J. M., & Timme, N. (2012). Being critical of criticality in the brain. *Frontiers in physiology*, 3, 163.
6. Ramezani-Panahi, M. et.al. Generative models of brain dynamics. *Front*, in *Artificial Intelligence* (2022)

Defect generation in single-layer graphene upon sputter deposition of thin metal films

Franck L. Nadji Adjim^{1,2}, Nikolaos Pliatsikas³, Olga Karabinaki⁴, John Arvanitidis³,
Dimitrios Christofilos⁴, and Kostas Sarakinos^{1,2}

¹*Department of Physics, University of Helsinki, Helsinki, Finland*

²*Department of Physics, KTH Royal Institute of Technology, Sweden*

³*Physics Department, Aristotle University of Thessaloniki, Thessaloniki, Greece*

⁴*School of Chemical Engineering & Physics Laboratory, Faculty of Engineering, Aristotle University of Thessaloniki, Thessaloniki, Greece*

email: franck.nadjiadjim@helsinki.fi

Magnetron sputtering is a vapor-based deposition process that generates ample amounts of energetic neutral and ionized species, creating defects that compromise graphene's pristine properties. It has therefore been deemed incompatible with metal film fabrication on graphene and other 2D materials. We have recently suggested [1], based on a combination of experimental and theoretical data, that defects during magnetron-sputter-deposition of Au on graphene primarily emerge from energetic species generated during neutralization and backscattering of Ar⁺ ions at the sputtering cathode.

In the present work, we study growth and defect generation in single-layer graphene (SLG) during sputter deposition of various metals (Au, Ag, Al, and Cu). Metal layers with nominal thicknesses of 20 Å are deposited on SLG/SiO₂/Si. Two different working pressures (5 and 20 mTorr) are used with the purpose of investigating the way by which the working pressure and the atomic mass of the sputtered species influence the morphology of the deposited films and the vibrational properties of the underlying SLG substrate, as probed by Scanning Electron Microscopy (SEM) and Raman spectroscopy, respectively. Metal thin films grow on SLG in the form of isolated three-dimensional islands. The shape of these islands depends on the sputtering pressure in a way that increasing pressure induces a transition from compact to dendritic islands, as observed by SEM. Raman spectra corresponding to pristine SLG exhibit three Raman bands; two relatively strong G (~1585 cm⁻¹) and 2D (~2680 cm⁻¹) peaks and a much weaker D (~1345 cm⁻¹) peak. The G band corresponds to the primary in-plane vibrational mode of SLG, while the D band is related to the distortion of the sp² hybridized structure, and hence can be associated with the presence of defects in the graphene structure. The 2D band is a second order of the D peak and its frequency shift and stronger intensity with respect to graphite reflect the two-dimensional character of graphene. The overall features of the Raman spectra seen in pristine SLG are also observed for metal/SLG/SiO₂/Si structures, although with varied intensities for the D and G bands. We find that the intensity of the D peak decreases and the intensity of the 2D peak increases with increasing pressure. We also evaluate the peak intensity (I) ratios I(D)/I(G) and I(2D)/I(G) and see a decrease in I(D)/I(G) and an increase in I(2D)/I(G) with increasing pressure. We conclude that increase in working pressure during sputter deposition induces fewer defects in SLG. Moreover, increase of the atomic mass of the target material results in more pronounced damage in the SLG, most notably at low sputtering pressures. The result of the study provides further support to the notion that energetic backscattered Ar species primarily cause damage and underscores that accurate and careful control of backscattered Ar energy and flux may allow defect-free deposition of metal layers on graphene.

- [1] N. Pliatsikas, O. Karabinaki, M. Zarshenas, G.A. Almyras, I. Shtepliuk, R. Yakimova, J. Arvanitidis, D. Christofilos, K. Sarakinos, Energetic bombardment and defect generation during magnetron-sputter-deposition of metal layers on graphene, *Appl. Surf. Sci.* 566 (2021) 150661, <https://doi.org/10.1016/j.apsusc.2021.150661>.

Micro-Alphatross: Towards High-intensity Negative Helium Beam

R. Nagy¹, T. Kalvas¹, Olli Tarvainen¹, M. Laitinen¹

¹ Department of Physics, University of Jyväskylä, P.O. Box 35, FI-40014, Jyväskylä, Finland

Corresponding author: rebekka.m.nagy@jyu.fi

Micro-Alphatross is a permanent-magnet based negative helium ion source with microwave-driven plasma production. A He^- beam in the order of $20 \mu\text{A}$ is to be reached. The negative beam is created by extracting He^+ ions from the plasma, and converting them negative by alkaline vapor (rubidium in the current prototype). The permanent-magnet configuration has several advantages compared to solenoid-based counterparts: compactness, easy maintenance and low power consumption.

The motivation for the development of the Micro-Alphatross is the vast demand for higher-intensity beams by modern technology. Ion beams with MeV energies are essential for e.g. manufacturing high-power microelectronics; they are required in implanter facilities and nanolithography, and also by several characterization methods (RBS, PIXE) to reveal the elemental and structural composition of the sample.

The device uses a 2.45 GHz magnetron to generate plasma. Power of $\sim 1 \text{ kW}$ is necessary to produce a 1 mA He^+ beam at 7 keV, which is optimal for the charge exchange using rubidium vapor. The coupling of RF power to plasma is optimized by deployment of stub tuners.

The positive ions are extracted through a non-monotonic decay of the magnetic field, which – unlike in case of a solenoid field – creates a magnetic trap leading to accumulation of charges in the extraction region. Due to this phenomenon, the extraction is susceptible to discharges, prohibiting the optimal beam transport. On-going simulations with ion optics library IBSimu suggest [1], that the trap can be avoided by changing the geometry of extraction electrodes.

In this presentation we will go through the latest endeavour towards higher intensities in negative helium beam. We will discuss especially the ion optics and the related beam transport from the plasma extraction to the charge exchange chamber.

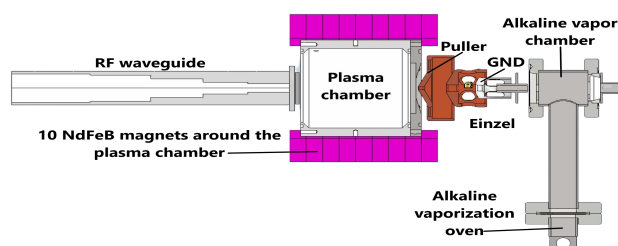


Figure 1: A simplified schematic of the negative-beam extraction of Micro-Alphatross.

- [1] T. Kalvas, O. Tarvainen, T. Ropponen, O. Steczkiewicz, J. Ärje, and H. Clark. IBSIMU: A three-dimensional simulation software for charged particle optics. *Review of Scientific Instruments*, 81(2):02B703, 02 2010.

Computing Chern numbers in two-band models with quantum circuits

Marcel Niedermeier¹, Marc Nairn², Jose L. Lado¹, and Christian Flindt¹

¹*Department of Applied Physics, Aalto University, 02150 Espoo, Finland*

²*Institut fuer Theoretische Physik, Universität Tuebingen, 72076 Tuebingen, Germany*

Corresponding author: marcel.niedermeier@aalto.fi

Quantum algorithms provide a new strategy to address problems in quantum physics, with the ultimate goal of potential deployment in real quantum computers. Specifically, a central problem in topological quantum matter is the computation of topological invariants. Topological invariants allow classifying states of matter featuring topological properties, and are a quantity of central importance in the design of topological materials. While efficient classical strategies exist to evaluate topological invariants, including the Berry phase or the Chern number in two dimensions, these schemes cannot be utilized to classify arbitrarily interacting many-body Hamiltonians. Here we present an extended quantum algorithm which allows us to calculate Chern numbers directly and requiring only a small number of ground state preparation steps [1-3]. In our calculation, we show that the Berry flux in two dimensions can be computed via a gate-based adiabatic evolution, combined with a Hadamard test scheme. We demonstrate our methodology with several paradigmatic model for topological matter, showing that our algorithm provides a faithful representation of the whole topological phase diagram.

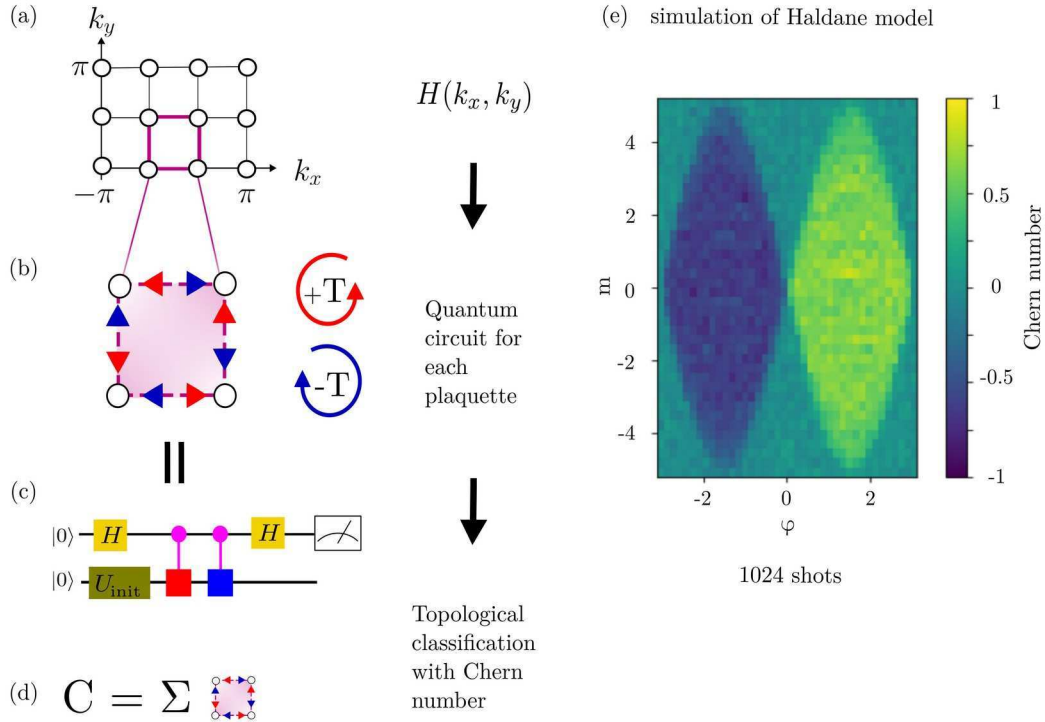


Fig. 1: Panels (a-d): Schematic representation of the quantum algorithm to calculate the Chern number. The Brillouin zone is divided into plaquettes, and the Berry flux through each plaquette is evaluated with a separate quantum circuit. To cancel spurious dynamical phases, the adiabatic evolution in (b) has to be performed in both positive and negative time. Panel (e): Topological phase diagram of the Haldane model, calculated with the Helmi device simulator (provided by IQM).

[1] M. Niedermeier, M. Nairn, J. L. Lado and C. Flindt, **in preparation (2024)**.

[2] B. Murta, G. Catarina and J. Fernández-Rossier, **Phys. Rev. A 101, 020302 (2020)**.

[3] X. Xiao, J. K. Freericks and A. F. Kemper, **Quantum 7, 987 (2023)**.

Atomistic modeling of a superconductor-transition metal dichalcogenide-superconductor Josephson junction

Jouko Nieminen¹, Wei-Chi Chiu², Xiao Xiao², Sayandip Dhara³, Michael N. Leuenberger³, Eduardo R. Mucciolo³, and Arun Bansil²

¹*Computational Physics Laboratory, Tampere University, FIN-33014, Tampere, Finland*

²*Department of Physics, Northeastern University, Boston, Massachusetts, USA*

³*Department of Physics, University of Central Florida, Orlando, Florida, USA*

Corresponding author: jouko.nieminen@tuni.fi

Using an atomistic tight-binding model, we study the characteristics of a Josephson junction (JJ) formed by monolayers of MoS₂ sandwiched between Pb superconducting electrodes. We derive and apply a Nambu-Gorkov Green's function-based (NGGF) formulation to compute the Josephson current in this system, as well as the local density of states in the junction. Our NGGF computations reveal the presence of triplet superconducting correlations in the MoS₂ monolayers and a spin-polarized subgap Andreev bound states (ABS) [1]. The methodology developed allows one to calculate NGGF of the leads and the scattering region separately, providing a feasible extension to other systems where atomistic details are needed to obtain accurate modeling of JJ physics.

We find that the contributions to the spin polarization coming from different regions of the Brillouin zone differ substantially, with the dominant one coming from states near the K and K' symmetry points where spin splitting of the valence band of MoS₂ is the strongest. Our analysis goes further and identifies a clear manifestation of the important interplay between lattice symmetry and spin-orbit coupling in establishing the intensity of this spin polarization, with monolayer systems (where mirror symmetry is present) showing stronger polarization and a richer structure of in-gap states than inversion symmetric bilayer systems. This effect appears in the amount of induced triplet superconductivity on MoS₂, markedly stronger for monolayer systems. Put together, these results point to the possibility of manipulating the spin polarization in dichalcogenide Josephson junctions by employing junction geometries that enhance the contributions from certain regions in k-space.

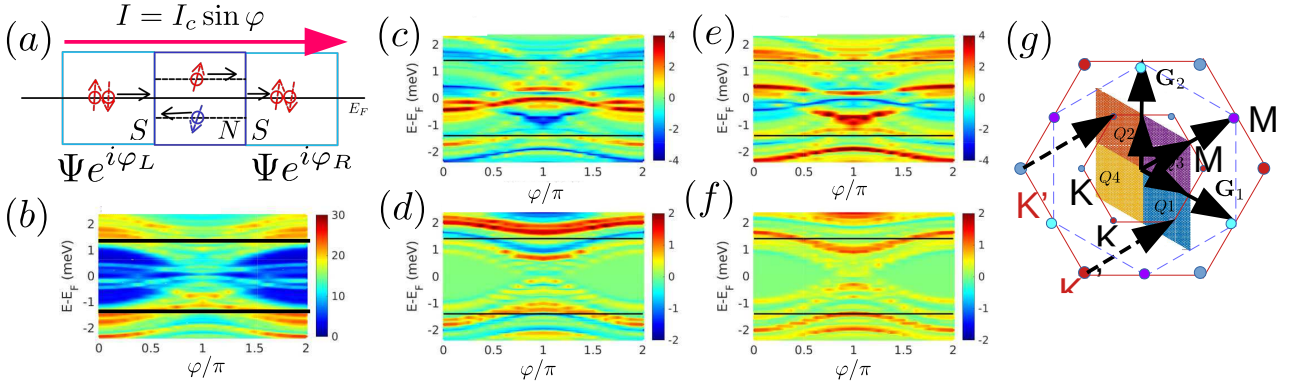


Fig. 1: Figure caption. (a) A schematic picture of Andreev reflection and supercurrent across a JJ.

(b) Local density of states (LDOS) showing ABSs for a single monolayer Pb-Mo₂-Pb JJ as a function of the phase difference. The spin polarization of the ABSs over quadrants Q1-4 of the primitive cell: (c) quadrant Q1 (blue), (d) Q2 (red), (e) Q3 (magenta), and (f) Q4 (yellow). (g) The primitive cell of reciprocal space where quadrants are indicated for spin resolved calculations.

- 1 Jouko Nieminen, Sayandip Dhara, Wei-Chi Chiu, Eduardo R. Mucciolo, Arun Bansil, Atomistic modeling of a superconductor - transition metal dichalcogenide - superconductor Josephson junction, *Physical Review B* **107**, 174524 (2023).

A Novel Method for Quantitative Assessment of Photovoltaic Material Degradation via Analysis of Color Alteration

R. Nizamov¹, A. Poskela¹, M. Hadadian¹, M. Nyberg¹, and K. Miettunen¹

¹ Solar Energy Materials and Systems, Department of Mechanical and Materials Engineering, University of Turku, Turku

Corresponding author: rustem.nizamov@utu.fi

In this study, we are introducing an enhanced method for monitoring degradation to address the critical challenges of assessing photovoltaic material durability, such as in perovskite solar cells (PSCs), and their vulnerability to environmental factors. By meticulously capturing color alterations under controlled light conditions using a custom-build photo chamber along with a digital camera (see Fig. 1), we correlate these changes into precise metrics of material stability [1]. This comprehensive approach links the colorimetric data with the performance metrics of the cells, such as the short-circuit current density J_{sc} , offering a holistic view of the impact of aging on the device's stability. Our versatile technique has also been applied in our recent studies on the stability of cellulose-based materials, specifically CNC films [2], and in the development of self-cleaning textiles with photocatalytic flower-like ZnO nanostructures [3]. Overall, this method offers a non-destructive, in situ, quick, and cost-effective means for evaluating the stability of photovoltaic materials and devices, contributing to the development of more robust and sustainable solar energy solutions.

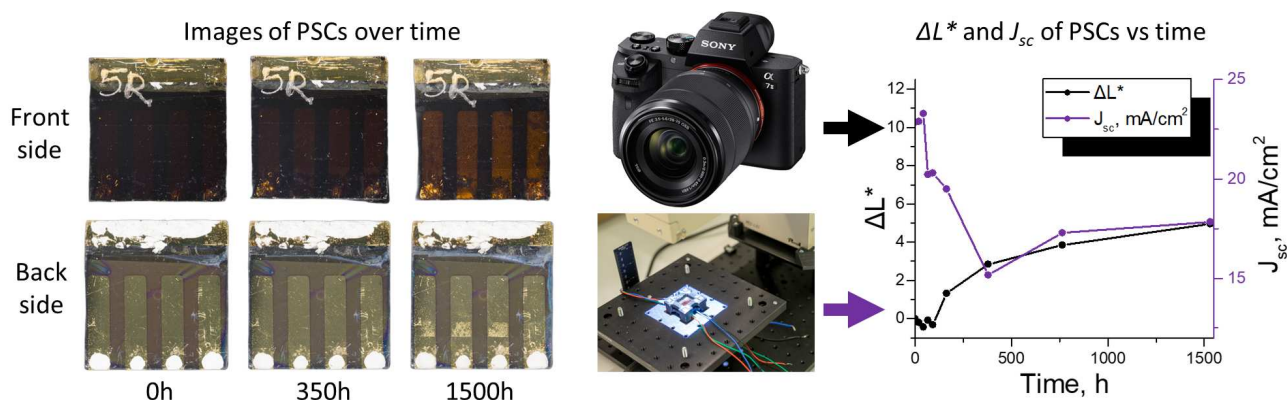


Figure 1: Periodic images of PSCs captured by a digital camera during a 1500-hour aging process, linking observed color changes (ΔL^*) to performance metrics. These metrics were obtained at specific intervals using a solar simulator and a potentiostat for cyclic voltammetry to measure J_{sc} .

[1] M. I. Asghar et al., *Solar Energy*, vol. 86, 2012

[2] T. Abitbol et al., *ACS Omega*, vol. 8, no. 24, 2023

[3] A. Lawrynowicz et al., *Journal of Photochemistry and Photobiology A: Chemistry*, vol. 450, 2024

Calculating path-dependent electronic stopping in silicon crystals using plane-wave pseudopotentials.

R. Nuñez¹, and A.E. Sand¹

¹ Department of Applied Physics - Aalto University

Corresponding author: rafael.nunez@aalto.fi

Characterizing the path-dependent effects of projectiles in silicon is relevant in several applications such as radiation damage [1] and ion implantation [2]. To provide meaningful insights into the trajectory dependence of electronic stopping in self-irradiated Si, in particular for the high-energy electronic stopping regime, we investigate electronic energy losses in silicon using the rt-TDDFT technique with plane-wave pseudopotentials [3]. We calculated electronic stopping over six main silicon channels, as shown in the figure, and three incommensurate trajectories. This allowed us to explore different electronic densities. Based on our results, we develop a model that accurately describes electronic losses along any trajectory. It includes channels and regions of higher electron density, as well as random trajectories such as those measured experimentally. The model uses the local ground state electron density and the projectile velocity to estimate an instantaneous electronic stopping power. In addition, we describe the minimum number of explicit electrons needed for the pseudopotentials in all energy ranges.

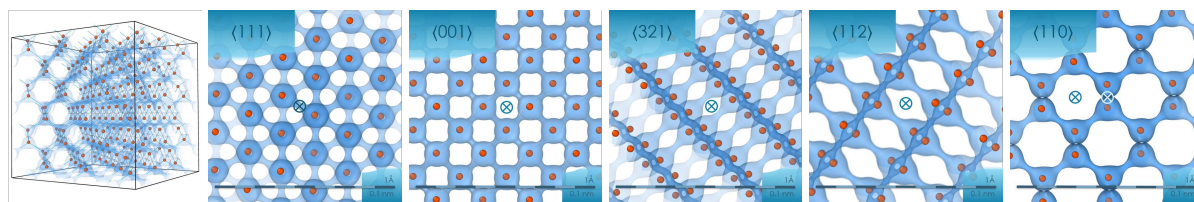


Figure: Electron density in the covalent bonding region for silicon ($\approx 0.08 e/a_0^3$). Perspective view of a 216-atom silicon diamond structure and detail on the electron density for different channeling directions. The \otimes symbol notates the position of the channeling projectile traveling perpendicular to the page.

- [1] Eva Zarkadoula, German Samolyuk, and William J Weber. Effects of the electron-phonon coupling activation in collision cascades. *Journal of Nuclear Materials*, 490:317–322, 2017.
- [2] Michael I Current. Ion implantation of advanced silicon devices: Past, present and future. *Materials Science in Semiconductor Processing*, 62:13–22, 2017.
- [3] Alfredo A. Correa. Calculating electronic stopping power in materials from first principles. *Computational Materials Science*, 150:291–303, 2018.

Computational study of cresol autoxidation: Initial steps in secondary organic aerosol formation

Aliisa Ojala, Siddharth Iyer

January 2024

Aromatic compounds, especially BTEX-compounds (benzene, toluene, ethylbenzene and xylene) and their derivatives can have an impact on the climate and human health through secondary organic aerosol (SOA) formation. They primarily originate from anthropogenic sources, such as vehicle emissions, industrial processes and solvent evaporation. These volatile organic compounds (VOCs) in the atmosphere can autoxidize, which is a sequential process of intramolecular reactions of peroxy radicals (molecules with R-O-O· structure) followed quickly by O_2 additions. This leads to low-volatility products with multiple oxygen-containing functional groups, called highly oxygenated organic molecules (HOMs). [1] These molecules can condense irreversibly to form and grow SOA, which have an impact on the climate through the scattering and absorption of sunlight and acting as seeds for cloud formation.

The oxidation process for aromatics is initiated by OH-radicals, which leads quickly to bicyclic peroxy radical (BPR) intermediates in significant yields. BPRs retain the initial 6-membered ring, but add an additional endoperoxide bridge, consisting of two oxygen atoms, connects to carbon atoms on both sides of the initiating OH-addition site. BPRs are sterically hindered, and their autoxidation is therefore slow, preferring to undergo bimolecular reactions with e.g. NO in polluted environments. Recently, a unimolecular pathway for ring-opening of BPRs was reported, leading to HOM formation in even sub-second timescales [2]. This opens up a pathway for aromatics to lead to SOA, even in non-polluted environments.

In this work, the autoxidation of cresols is studied. The cresol pathway is a major source of overall SOA for BTEX-compounds, as it is expected to account for up to 40% of toluene-related SOA formation [3]. ω B97X-D/aug-cc-pVTZ-level of theory is used for geometry optimization with single point energy calculations done at ROHF-ROCCSD(T)-F12a/cc-pVDZ-F12-level. A thorough conformer sampling is done at a lower level of theory, and multi-conformer transition state theory (MC-TST) is used for rate calculations with Eckart-tunneling correction.

For cresols, the OH-addition can happen at six different sites with different yields, leading to different chemistry. Preliminary results for ortho-cresol suggest that sites 3, 1 and 2 relative to the methyl group have the highest yields in descending order. Slow ring breakage is seen for the two highest yield addition sites, whereas fast ring breakage is seen for the BPR formed from 2-position addition. This is compatible with previous results for the ring-breaking of other substituted aromatic compounds [2]. The results of this study shed light on the SOA formation processes in the atmosphere. This will improve current models of SOA formation, which are known to have inconsistencies [1].

- [1] Nault et al. Secondary organic aerosols from anthropogenic volatile organic compounds contribute substantially to air pollution mortality, 2021.
- [2] Iyer et al. Molecular rearrangement of bicyclic peroxy radicals is a key route to aerosol from aromatics. *Nature communications*, 2023.
- [3] Schwantes et al. Formation of highly oxygenated low-volatility products from cresol oxidation. *Atmospheric Chemistry and Physics*, 17(5):3453–3474, 2017.

Recent Pomeron and Odderon Physics with TOTEM

F. Oljemark¹, for the TOTEM Collaboration

¹ Helsinki Institute of Physics, PO Box 64, FI-00014 University of Helsinki, Finland

Corresponding author: fredrik.oljemark@helsinki.fi

The TOTEM [1] experiment at the Large Hadron Collider probes the proton structure by precise measurement of elastic, inelastic and total cross-sections and comprehensive studies of diffraction. Forward-going charged particles are detected at pseudorapidities of $3.1 \leq |\eta| \leq 4.7$ and $5.3 \leq |\eta| \leq 6.5$ by the T1 and T2 telescopes, respectively, (up to 2015), and a new T2 scintillating tile telescope (covering the latter region in 2023), and leading protons by silicon detectors in Roman Pots. We have studied proton-proton (pp) elastic scattering from 0.9 TeV up to 13.6 TeV collision energy using special runs with low pileup, and acceptance down to very small values of proton momentum transfer $|t|$. The structure of the differential cross section exhibits several different regimes: at the lowest $|t|$ -values only electromagnetic (EM) scattering takes place, while above $|t| \approx 10^{-3} \text{ GeV}^2$ the nuclear interaction dominates, falling exponentially, then having a diffractive minimum ("dip") and second maximum ("bump") before falling off beyond $|t| \approx 1 \text{ GeV}^2$. Interference between nuclear and EM forces was measured with very high β^* ($\geq 1 \text{ km}$) beam optics, reaching $|t| = 6 * 10^{-4} \text{ GeV}^2$, while the dip and bump with $\beta^* = 90 \text{ m}$. Covering the complete $|t|$ range, we can evaluate the evolution of the dip and bump position and bump-to-dip cross section ratio R . The measurements between 2.76 and 13 TeV were used to extrapolate the pp cross section to the same energy as D0, who measured elastic proton-antiproton ($p\bar{p}$) scattering at 1.96 TeV. A significant difference between the pp and $p\bar{p}$ cross sections in the dip-bump region represents evidence for Odderon exchange [4]. Together with the previous evidence from the precise measurement of the ρ parameter [2], this constitutes the observation of Odderon exchange. The slope parameter of the elastic $|t|$ -distribution at 0.9 TeV will be presented for the first time.

A large part of proton-proton strong interactions is related to (non-perturbative) Pomeron exchanges, that in QCD correspond to ladder-type diagrams of gluons. Combining our forward proton measurements with the central tracking of the CMS experiment in a special run at 13 TeV and $\beta^* = 90 \text{ m}$, we recently characterized the pomeron interactions using a large sample (80 million) of central exclusively produced (CEP) charged pion pairs in the nonresonant region of the invariant mass spectrum [3]. The Pomeron form factors, cross sections, and trajectories were extracted. The parabolic minimum in the cross section as a function of the two-proton azimuthal angle difference is observed for the first time.

[1] G. Anelli et al. (TOTEM Collaboration), *JINST*, **3** S08007 (2008).

[2] G. Antchev et al. (TOTEM Collaboration), *Eur. Phys. J.*, **C 79** 785 (2019).

[3] A. Hayrapetyan et al. (CMS and TOTEM Collaborations), *arXiv:2401.14494* [hep-ex] (2024), submitted to *Phys. Rev. D*.

[4] V. M. Abazov et al. (D0 and TOTEM Collaborations), *Phys. Rev. Lett.*, **127** 062003 (2021).

Theoretical approach to inclusive semileptonic decays of heavy mesons through lattice QCD

M. Panero^{1,2}

¹ Department of Physics, University of Turin, Via Pietro Giuria 1, I-10125 Turin, Italy

² Italian Nuclear Physics Institute (INFN), Turin unit, Via Pietro Giuria 1, I-10125 Turin, Italy

Corresponding author: marco.panero@unito.it

In the Standard Model of elementary particle physics, the Cabibbo-Kobayashi-Maskawa (CKM) matrix describes the way in which weak interactions can induce transitions between different quark flavors (and, hence, trigger decays of heavy hadrons). This matrix plays a particularly important rôle in the search for physics beyond the Standard Model, since its elements are sensitive to the latter, and may even reveal the existence of new particles with masses beyond the reach of present accelerators. Recent experimental results about CKM matrix elements exhibit some tension with Standard Model predictions, but also a puzzling discrepancy between exclusive and inclusive channels.

In this contribution, mainly based on ref. [1], I will discuss a new way to derive theoretical predictions for the inclusive semileptonic decays of heavy mesons from *ab initio* calculations in the non-perturbative regularization of quantum chromodynamics (QCD) on a Euclidean lattice, which is amenable to Monte Carlo simulation on supercomputers. The approach is based on a numerical reconstruction (carried out by means of a variant of the Backus-Gilbert method) of spectral distributions, starting from a set of four-point Euclidean correlation functions computed on the lattice.

I will present results for differential decay rates of heavy mesons obtained from different ensembles of lattice QCD configurations, comparing them with analytical predictions from the operator-product expansion. Finally, I will comment on ongoing and future work in this research program.

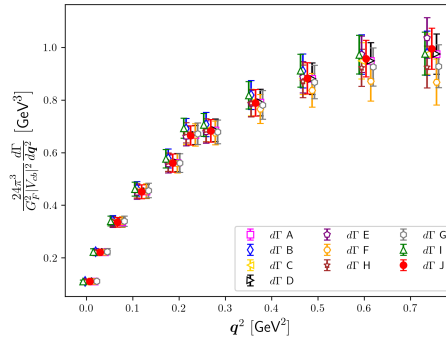


Figure 1: Theoretical prediction for the differential rate associated with inclusive semileptonic decays of a B_s -like meson, as a function of the squared transferred momentum. The figure shows results for different choices of the parameters in our analysis, denoted by symbols of different colors (their mutual consistency being a non-trivial check of the robustness of the calculation).

[1] P. Gambino, S. Hashimoto, S. Mächler, M. Panero, F. Sanfilippo, S. Simula, A. Smecca, and N. Tantalo, JHEP **07** (2022), 083.

Ilmastonmuutoksen luonnontieteellisten perusteiden opettaminen osana Ilmastoasiantuntijan erikoistumiskoulutusta

Kenneth Peltokangas¹, Tiina Nygård², Taina Ruuskanen¹, ja Laura Riuttanen¹

¹*Ilmakehätieteiden keskus (INAR), Helsingin yliopisto, Helsinki, Finland*

²*Ilmatieteen laitos, Helsinki, Finland*

Corresponding author: kenneth.peltokangas@helsinki.fi

Uusi ilmastoasiantuntijan erikoistumiskoulutus pyrkii vastaamaan kasvaneeseen ilmasto-osaamisen tarpeeseen ja kehittämään ilmasto-osaamista yli toimialarajojen. Koulutusohjelma on kehitetty yhteistyössä Helsingin yliopiston, Itä-Suomen yliopiston, Ilmatieteen laitoksen sekä Climate University -verkoston ja Climate Leadership Coalition kanssa. Koulutuksen aikana opiskelijat perehtyvät ilmastonmuutoksen fysikaalisiin näkökulmiin, kasvihuonekaasujen dynamiikkaan ja ilmastonmuutoksen laajempiin vaikutuksiin ekosysteemeissä. Luonnontieteellisten näkökulmien lisäksi koulutus tarjoaa myös taloudellisia ja oikeustieteellisiä näkökulmia, joiden tunteminen on tärkeä osa ilmastotyötä. Koulutus on kaksivuotinen ja sisältää sekä pakollisia että valinnaisia opintojaksoja (laajuus 60 opintopistettä). Opintojen aikana opiskelijat työskentelevät itsenäisesti, vertaisryhmissä sekä yhdessä eri alojen asiantuntijoiden kanssa.

Koulutuksessa aloittaa 42 opiskelijaa maaliskuussa 2024. Opiskelijoiden tiedot ja taidot ilmastonmuutoksesta ja sen luonnontieteellisistä perusteista vaihtelevat suuresti. Yksi koulutuksen haasteista tuleekin olemaan miten ottaa huomioon opiskelijoiden erilaiset lähtötasot. Toisaalta ei ole aivan selvää mitä ilmasto-osaaminen eri aloilla oikeastaan tarkoittaa. Ilmastoasiantuntijan erikoistumiskoulutuksen tarkoituksena onkin yhtä lailla paneutua siihen mitä ilmasto-osaaminen on kuin mikä on paras tapa opettaa ilmasto-osaamista. Opetusta on tarkoitus kehittää opiskelijälähtöisesti ja tutkimuspohjaisesti, jotta opiskelijat saavuttavat riittävät tiedot ja taidot ilmastonmuutoksen luonnontieteellisten perusteiden ymmärtämiseksi riippumatta heidän lähtötasostaan. Tämän esityksen tarkoitus on esitellä alustavia tuloksia ja kokemuksia erikoistumiskoulutuksen kehittämisestä.

Mean-field theory and dynamical mean-field theory studies on flat band superconductivity from two to three dimensions

R. Penttilä¹, and P. Törmä¹

¹ Department of Applied Physics, Aalto University School of Science, Aalto, FI-00076, Finland

R. Penttilä: reko.penttila@aalto.fi

Superconductivity in flat-band lattices, i.e. lattices that have an energy band with no momentum dependence, has gathered great interest. BCS theory predicts that in systems with small interaction strengths critical temperature of superconductivity is enhanced in flat bands in comparison to dispersive bands [1]. Most of the past theoretical studies on flat-band superconductivity have been done for two or one-dimensional lattices [2, 3]. In this talk, I present results on the effect of the transition from two to three dimensions on the superconducting characteristics in flat-band lattices.

We study three different three-dimensional extensions of the Lieb and dice lattices called the stacked, extended, and twice-extended lattices. At the mean-field level, we find that the critical temperatures of order parameters and superfluid weights for the extended Lieb and dice lattices are maximized in the quasi-2D regime, i.e. with weak coupling between the two-dimensional planes. We also perform dynamical mean-field theory (DMFT) calculations to include the quantum fluctuations inside the unit cells. We find that the critical temperature obtained from the order parameters is no longer maximized in the quasi-2D region. Rather, the change in critical temperature is connected to the ratio given by the number of flat bands to the number of orbitals in the unit cell.

- [1] N. B. Kopnin, T. T. Heikkilä, and G. E. Volovik, “High-temperature surface superconductivity in topological flat-band systems,” *Physical Review B*, vol. 83, no. 22, 2011.
- [2] A. Julku, S. Peotta, T. I. Vanhala, D.-H. Kim, and P. Törmä, “Geometric origin of superfluidity in the Lieb-lattice flat band,” *Physical Review Letters*, vol. 117, no. 4, p. 045303, 2016.
- [3] F. Hébert, V. Iglovikov, B. Grémaud, G. Batrouni, and R. Scalettar, “Superconducting transitions in flat-band systems,” *Physical Review B: Condensed Matter and Materials Physics (1998-2015)*, vol. 90, no. 9, 2014.

Non-Hermitian topological modes from local loss engineering in photonic arrays

Elizabeth Pereira¹, Hongwei Li², Andrea Blanco-Redondo³, and Jose L. Lado¹

¹ Department of Applied Physics, Aalto University, 02150 Espoo, Finland

² Nokia Bell Labs, 21 JJ Thomson Avenue, Cambridge, CB3 0FA, UK

³CREOL, The College of Optics and Photonics, University of Central Florida, Orlando, FL 32816, USA

Corresponding author: elizabeth.pereira@aalto.fi

Non-Hermitian systems have risen as a powerful strategy to engineer new forms of topological excitations. Photonic devices allow creating a whole variety of new artificial lattices challenging to emulate in conventional materials, opening up possibilities to realize new forms of topological matter. Beyond conventional photonic topological states in closed quantum systems, photonic devices provide a flexible platform to harvest non-Hermitian topology, and in particular, robust topological modes by exploiting engineered gains and losses. Here [1] we present a family of photonic models relying on the real-space modulation of photonic losses giving rise to non-Hermitian topological excitations. We demonstrate that the non-Hermitian topological modes survive spatial fluctuations in the loss and couplings of the system, and we also discuss the localization transition associated with this model in the quasicrystalline limit which has a correspondence in the analogous Hermitian model. Our results provide a realistic strategy to create topological modes in photonic systems from real-space loss engineering.

[1] E. L. Pereira, H. Li, A. Blanco-Redondo, and J. L. Lado, “Non-hermitian topology and criticality in photonic arrays with engineered losses”, arXiv preprint arXiv:2311.09959 (2023)

Solar Energy and Recycling: A Rapidly Approaching Challenge

Aapo Poskela¹, Simon Jech², Mahboubeh Hadadian¹, Elena Akulenko¹, Annukka Santasalo-Aarnio², and Kati Miettunen¹

¹*Solar Energy Materials and Systems, Faculty of Technology, University of Turku, Turku, Finland*

²*Department of Mechanical Engineering, School of Engineering, Aalto University, Espoo, Finland*

Corresponding author: aapo.poskela@utu.fi

The industry standard for silicon solar panel lifetime is 25 to 30 years [1]. Combined with the fact that installed photovoltaic (PV) capacity has increased from 9.2 GW in 2007 to 1500 GW in 2023 [2], we will face an unprecedented increase in PV waste as the newly installed panels start to reach their end-of-life.

It is naturally desirable that most of the PV waste can be handled through recycling methods, especially since silicon solar panels include valuable silver, and their aluminum frame and front glass account for a notable share of the value of the panels. However, a definite method for recycling solar panels does not yet exist. Plausible recycling methods range from revival of the recycled product by replacing degraded components to reusing components from recycled products in newly assembled panels and recovering pure elements from the waste (**Fig. 1**). Each of the methods come with their own advantages, drawbacks and energy costs [3].

Discussion of recycling does not only involve what is done after a solar panel reaches its end-of-life, but can also be used to inform the design of new types of solar panels [4], [5]. Design choices that directly impact recycling include the choice of materials (rarity, cost, ease of recovery) and structure (ease of disassembly).

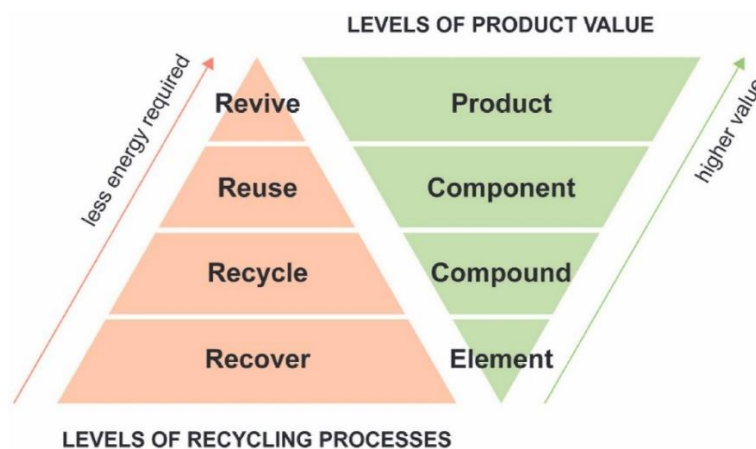


Fig. 1: An illustration of different recycling levels and their corresponding value in terms of recovered product [3].

- [1] M. S. Chowdhury *et al.*, “An overview of solar photovoltaic panels’ end-of-life material recycling,” *Energy Strategy Reviews*, vol. 27, p. 100431, Jan. 2020, doi: 10.1016/J.ESR.2019.100431.
- [2] “Executive summary – Renewables 2023 – Analysis - IEA.” Accessed: Jan. 23, 2024. [Online]. Available: <https://www.iea.org/reports/renewables-2023/executive-summary>
- [3] K. Miettunen and A. Santasalo-Aarnio, “Eco-design for dye solar cells: From hazardous waste to profitable recovery,” *J Clean Prod*, vol. 320, Oct. 2021, doi: 10.1016/j.jclepro.2021.128743.
- [4] S. Jech, N. Garg, K. Miettunen, and A. Santasalo-Aarnio, “COMPARISON OF EXPERIMENTAL SEPARATION METHODS FOR SILICON SOLAR PANELS”, doi: 10.4229/EUPVSEC2023/5DV.2.37.
- [5] E. S. Akulenko, M. Hadadian, A. Santasalo-Aarnio, and K. Miettunen, “Eco-design for perovskite solar cells to address future waste challenges and recover valuable materials,” *cell.com*, 2023, doi: 10.1016/j.heliyon.2023.e13584.

Defects in aluminum-rich silicon-doped AlGaN

I. Prozheev¹, F. Mehnke², M. Schilling², T. Wernicke², M. Kneissl², R. Bès¹,
I. Makkonen¹, and F. Tuomisto¹

¹*Department of Physics and Helsinki Institute of Physics, University of Helsinki, P.O. Box 43, FI-00014
HELSINKI, FINLAND*

²*Technische Universität Berlin, Institute of Solid State Physics, Hardenbergstr. 36, D-10623 BERLIN, GERMANY*
Corresponding author: firstname.lastname@helsinki.fi

We study defects in Si-doped Al_{0.90}Ga_{0.10}N layers with Doppler broadening of positron annihilation radiation and x-ray absorption spectroscopy. The samples were grown by metal-organic vapor phase epitaxy on AlN/sapphire substrates. The Si doping was varied in the range from $9 \times 10^{17} \text{ cm}^{-3}$ to $1.7 \times 10^{19} \text{ cm}^{-3}$. Two growth regimes were applied: a low V/III ratio of 200 at a reactor pressure of 50 mbar (series H) and for a high V/III ratio of 700 and a growth pressure of 200 mbar (series L). In series L, (high V/III ratio of 700 and a growth pressure of 200 mbar) we observe positron saturation trapping at cation vacancy defects present above $5.0 \times 10^{18} \text{ cm}^{-3}$ for all studied Si doping levels. We observe high V_{III} concentration probably due to low formation energy in these samples with low carbon content. Interestingly, when Si content approaches 10^{19} cm^{-3} positron data shows a transition for the dominant positron trap from V_{III} to another defect, which we interpret as a high density of Si-DX centres. In series H, the positron data show the cation vacancy concentration increasing with the Si concentration from $<1 \times 10^{16} \text{ cm}^{-3}$ to $>2.0 \times 10^{18} \text{ cm}^{-3}$. The reason for the lower V_{III} content is an order of magnitude higher level of C acceptors, which is shifting the Fermi level away from the conduction band edge and increasing the formation energy of V_{III}. In samples with three highest Si levels above 10^{19} cm^{-3} , negatively charged non-open volume defect appears with concentrations similar to the Si concentration as data points move closer to AlN lattice point similar to behaviour observed in L series with highest Si content.

In order to assess the short-range ordering of Si atoms we apply x-ray absorption spectroscopy method. Data show, that in the H series samples with low/moderate Si content, the Si is in more GaN-like surroundings. When this is the case, resistivity decreases with increasing Si content. In the samples with moderate/high Si content, the Si is in more AlN-like surroundings. In these samples, resistivity increases with increasing Si content. Local environment of Si in 90%-AlN AlGaN changes from GaN- to AlN-like with increase of Si doping.

- [1] F. Tuomisto, and I. Makkonen, *Rev Mod Phys*, **85**(4), 1583 (2013).
- [2] G. Kusch, *et al.*, *Semicond Sci Technol*, **32**, 035020 (2017).
- [3] F. Mehnke, *et al.*, *App Phys Lett*, **103**(21), 212109 (2013).
- [4] I. Prozheev, *et al.*, *App Phys Lett*, **117**, 142103 (2020).

All-optical switching at the two-photon limit with interference-localized states

Ville A. J. Pyykkönen¹, Grazia Salerno¹, Jaakko Kähärä^{1,2} and Päivi Törmä¹

¹ Department of Applied Physics, Aalto University School of Science, Espoo, Finland

²Institute for Atmospheric and Earth System Research/Physics, Faculty of Science, University of Helsinki, Helsinki, Finland

Corresponding author: ville.pyykkonen@aalto.fi

In a recent publication [1], we propose a single-photon-by-single-photon all-optical switch concept based on interference-localized states on lattices and their delocalization by interaction. In the talk, I will present the switch concept and the main findings of the article. In its “open” operation, the switch stops single photons while allows photon pairs to pass the switch. Alternatively, in the “closed” operation, the switch geometrically separates single-photon and two-photon states. The concept is demonstrated using a three-site Stub unit cell and the diamond chain. The systems are modeled by Bose-Hubbard Hamiltonians, and the dynamics is solved by exact diagonalization with Lindblad master equation. I will also discuss realization of the switch using photonic lattices with nonlinearities, superconductive qubit arrays, and ultracold atoms. Particularly, the switch allows arbitrary “ON”/“OFF” contrast while achieving picosecond switching time at the single-photon switching energy with contemporary photonic materials.

[1] V. A. J. Pyykkönen, G. Salerno, J. Kähärä, and P. Törmä, Phys. Rev. Research **5**, 043259 (2023)

Comparing resource requirements of noisy quantum simulation algorithms for the Tavis–Cummings model

A. Haukisalmi¹, M. Raasakka¹, and I. Tittoinen¹

¹ Micro and Quantum Systems group, Department of Electronics and Nanoengineering, School of Electrical Engineering, Aalto University, Espoo, Finland

Corresponding author: matti.raasakka@aalto.fi

Fault-tolerant quantum computers could facilitate the simulation of quantum systems unfeasible for classical computation via Trotterization, a systematic way of implementing time-evolution operators of qubit Hamiltonians as quantum circuits [1]. Pre-fault-tolerance, however, one must make do with noisy intermediate-scale quantum (NISQ) devices, which cannot by themselves manage the deep circuits required by Trotterization [2]. The utilisation of NISQ devices then calls for the use of additional strategies, which include quantum error mitigation (QEM) for alleviating device noise, and variational quantum algorithms (VQAs) which combine classical optimization with short-depth, parameterized quantum circuits.

This work compares two such methods: zero-noise extrapolation (ZNE) with noise amplification by circuit folding [3, 4], and incremental structural learning (ISL) [5], a type of circuit recompiling VQA. These are applied to Trotterized time-evolution of the Tavis-Cummings model (TCM) under a noise simulation. Since both methods add circuit evaluation overhead, it is of interest to see how they compare both in the accuracy of the dynamics they produce, and in terms of the quantum resources used. Additionally, noisy recompilation of time-evolution circuits with ISL has not previously been explored. The comparison is done for various simulation parameters, such as the TCM system size.

We find that while ISL achieves lower error than ZNE for smaller system sizes, it fails to produce correct dynamics for 4 qubits, where ZNE is superior. Diverging resource requirements for ISL and ZNE are observed, with ISL achieving low circuit depths at the cost of a large number of circuit evaluations. These results highlight the importance of considering the performance of VQAs under noisy conditions as well. To our knowledge, recursive recompilation of Trotter circuits with ISL, where the circuits are run with noise during the optimization itself has not been reported on previously, and the challenges that ISL faced here with small systems of 4 qubits show that there is much room for improvement.

- [1] S. Lloyd, “Universal quantum simulators”, *Science* **273**, 1073 (1996).
- [2] L. Bassman, M. Urbanek, M. Metcalf, J. Carter, A. F. Kemper, and W. A. de Jong, “Simulating quantum materials with digital quantum computers,” *Quantum Sci. Technol.* **6**, 043002 (2021).
- [3] Y. Li and S. C. Benjamin, “Efficient Variational Quantum Simulator Incorporating Active Error Minimization”, *Phys. Rev. X* **7**, 021050 (2017).
- [4] K. Temme, S. Bravyi, and J. M. Gambetta, “Error Mitigation for Short-Depth Quantum Circuits”, *Phys. Rev. Lett.* **119**, 180509 (2017).
- [5] B. Jaderberg, A. Agarwal, K. Leonhardt, M. Kiffner, D. Jaksch, “Minimum Hardware Requirements for Hybrid Quantum-Classical DMFT”, *Quantum Sci. Technol.* **5** 034015 (2020).

GLA enhances the transmittance and electrical conductivity of ALD Al-doped ZnO for thermoelectric and TCO applications.

Tomi Koskinen¹, Ramesh Raju¹, Christoffer Kauppinen², Ilkka Tittonen¹

¹*Department of Electronics and Nanoengineering, Aalto University, P.O. Box 13500, Aalto 00076, Finland*

²*VTT Technical Research Centre of Finland Ltd, Tietotie 3, Espoo, FI-02044 VTT, Finland*

Corresponding author: Tomi.koskinen@canatu.fi, ramesh.raju@aalto.fi

Transparent thermoelectric materials enable the integration of sensing and energy harvesting devices on various surfaces such as windows and user interfaces. A key constraint for device performance in such applications is the available surface area from which the thermoelectric power should be harvested without compromising the optical properties. Here, we demonstrate atomic layer deposition (ALD) of aluminum doped zinc oxide (AZO), the most prominent n-type thermoelectric material, on grass-like alumina (GLA), a high-performance, low-cost antireflective coating. The conformal nature of the ALD process enables the AZO growth to closely follow the topography of the underlying GLA film, therefore providing an increased effective surface area compared to a reference AZO film grown directly on plain glass. The films grown on GLA show an improved electrical conductivity attributed to additional doping by the GLA. The effect is pronounced at lower AZO thicknesses, resulting in a 228% increase in the electrical conductivity and an 80% increase in the thermoelectric power factor of 32 nm thick films. Moreover, the GLA-AZO films partly inherit the antireflective behavior of the GLA film, thus showing improved optical transparency compared to the reference AZO film on glass. Our results promote transparent thermoelectric devices with improved transparency and thermoelectric performance.

[1] *T.koskinen, R.Raju, C.Kauppinen, I.Tittonen, Grass-like alumina enhances transmittance and electrical conductivity of atomic layer deposited Al-doped ZnO for thermoelectric and TCO applications. Appl. Phys. Lett. 123, 011902 (2023) ;*

Diamond timing detectors of the CMS Precision Proton Spectrometer

M.-M. Rantanen¹, F. Garcia¹, P. Koponen¹, R. Turpeinen¹, and K. Österberg^{1,2}
for the CMS collaboration

¹ Helsinki Institute of Physics, Helsinki, Finland

²Department of Physics, University of Helsinki, Helsinki, Finland

Corresponding author: milla-maarit.rantanen@helsinki.fi

The CMS Precision Proton Spectrometer (PPS) detector system measures the time-of-flight (ToF) and position of protons that remain intact in the collisions in the very forward region at the Large Hadron Collider (LHC). The detector system consists of movable tracking and timing stations about 200 m from on both sides of the interaction point of CMS. The detectors can be moved to few millimetres from the circulating beam. At this distance from the beam the particle flux is high and precise measurements of particle ToFs is needed for good quality reconstruction of particle tracks. Due to the location close to the beam the detectors are exposed to high and highly non-uniform irradiation, which is why the timing detectors, in addition to good timing resolution, need to have good radiation tolerance to be able to operate in this harsh environment.

Single crystal diamond detectors are well suited for ToF measurements in harsh radiation conditions thanks to their excellent radiation tolerance and fast signals. For the LHC Run 3 (2022-2025) the PPS timing stations were upgraded with the goal of improving the radiation tolerance and reaching a timing resolution of less than 30 ps. In the upgrade the stations were equipped with 500 μm thick single crystal CVD diamond detectors in double-diamond configuration. In the double-diamond configuration diamond detectors with the same electrode pattern are aligned on both sides of the readout board. Before installation in the PPS, the diamond detectors were tested and their quality checked. The testing was done at different stages of the fabrication through visual inspection with microscope techniques and electrical measurements, including leakage current and signal amplitude measurements. The timing detectors have been used for data taking in Run 3. This contribution will present the PPS timing detectors and the procedure used to test the diamond detectors. The detector performance in Run 3 will be discussed.

Nanoscale Roughness Characterization of LPCVD-Fabricated SiN Thin Films on Silicon Wafers Using AFM

K.A.C Rathnathilaka^{1,2}, Tuomas Vaimala², and Alberto Ronzani²

¹ Department of Computational Engineering, LUT University, Lappeenranta, Finland

²VTT Technical Research Centre of Finland, Espoo, Finland

Corresponding author: achini.rathnathilaka@vtt.fi

This study explores the nanoscale surface roughness of Low Pressure Chemical Vapor Deposition (LPCVD) silicon nitride (SiN) thin films with varying nominal thicknesses (1 nm, 2 nm, 5 nm, 10 nm, 20 nm, and 50 nm) on silicon wafers. The roughness measurements were obtained using Atomic Force Microscopy (AFM) at four different points on each wafer and a polished silicon wafer is included as a reference substrate. Five wafers are examined for each thickness category, ensuring the statistical strength and reliability of the obtained data. The determined median roughness values for the SiN thin films are: 0.281 ± 0.039 nm (50 nm), 0.263 ± 0.033 nm (20 nm), 0.284 ± 0.031 nm (10 nm), 0.246 ± 0.032 nm (5 nm), 0.257 ± 0.028 nm (2 nm), and 0.159 ± 0.016 nm (1 nm). These values are slightly higher than the corresponding roughness value for the polished silicon wafer (0.178 ± 0.004 nm). The trend observed in Fig. 1 reveals a gradual decrease in roughness with decreasing film thickness. Specifically, roughness values for 50 nm, 20 nm, 10 nm, 5 nm, and 2 nm SiN films exhibit a consistent downward trend, varying from approximately 0.30 nm to 0.25 nm. This research contributes to the fundamental understanding of nanoscale surface characteristics in LPCVD-fabricated SiN thin films, with potential implications for optimising thin film deposition processes in microelectronic and nanotechnology applications. The findings provide valuable insights into the relationship between film thickness and surface roughness, guiding the development of advanced materials for future technological advancements.

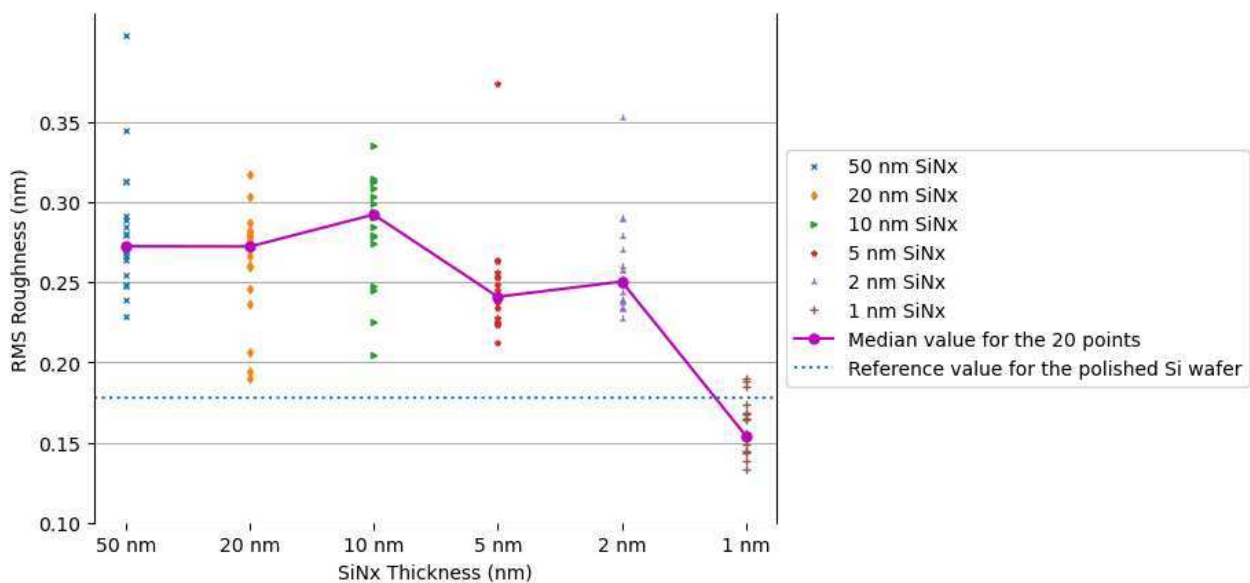


Figure 1: Roughness Variation for Different SiNx Nominal Thickness Values

Towards gravity detection using optomechanics with mass-loaded resonators

Ewa Rej¹, Richa E. Cutting¹, Joe Depellette¹, Matthew Herbst¹, Yulong Liu², and Mika S. Sillanpää¹

¹*Department of Applied Physics, Aalto University, FI-00076 Aalto, Finland*

²*Beijing Academy of Quantum Information Sciences, Beijing 100193, China*

Corresponding author: Mika.Sillanpaa@aalto.fi

The interface between quantum mechanics and gravity remains an open question. While indirect measurements studying gravity originating from source masses in quantum states could probe this interface, experiments are challenging due to the small masses that need to be utilized to retain quantum coherence and the correspondingly small gravitational force. Micromechanical oscillators, already demonstrated as sensors with high force sensitivity and routinely prepared in their motional ground state, are an ideal platform for realizing these experiments.

Here we detail an optomechanical setup with gold spheres weighing a few mg on silicon nitride membranes coupled to three-dimensional microwave cavities. These mass loaded membranes vibrate at 2 kHz in the drum mode. Following implementation of vibration isolation, we show thermalization of these massive oscillators to mK temperatures, and optomechanical feedback cooling in the bad-cavity limit by three orders of magnitude, with the goal to prepare the oscillators in their ground state.

In the measurement scheme, this mass loaded resonator is placed near a strongly piezo-actuated source mass, and the resulting time-dependent classical gravitational force between the two masses is sensed making use of resonant enhancement. Two mass loaded oscillators in close proximity pave the way for measurements of gravity between milligram masses in quantum states [1].

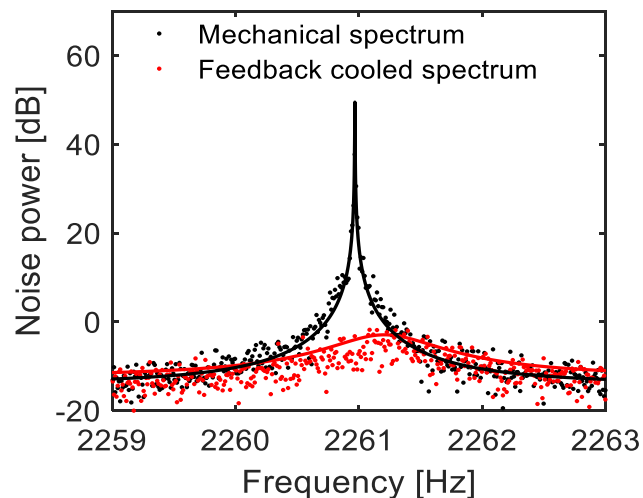
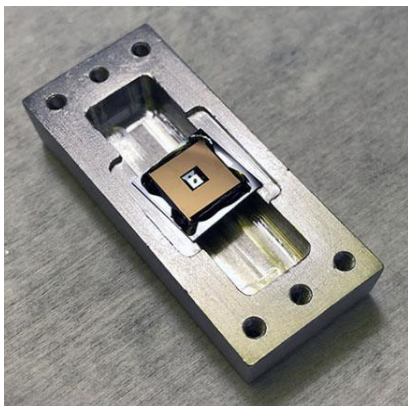


Fig. 1: Left: Photo of a representative optomechanical device, showing a mass-loaded SiN membrane inside a 3D cavity. Right: Mechanical noise spectrum of the SiN membrane with (red) and without (black) feedback cooling. Through feedback cooling we apply a viscous force that cools the mechanical oscillator, in this case by three orders of magnitude. Solid lines are Lorentzian fits.

- [1] Yulong Liu, Jay Mummery, Jingwei Zhou, and Mika A. Sillanpää, ‘Gravitational Forces Between Nonclassical Mechanical Oscillators’, *Physical review applied* 15, 034004 (2021).

Intermittency in interplanetary coronal mass ejections observed by Parker Solar Probe and Solar Orbiter

Julia Ruohotie, Simon Good, and Emilia Kilpua
Department of Physics, University of Helsinki, Helsinki, Finland
Corresponding author: julia.ruohotie@helsinki.fi

Interplanetary coronal mass ejections (ICMEs), massive plasma clouds originating from the Sun, are often observed as large-scale flux ropes. While they usually have smoothly varying magnetic fields, fluctuations at smaller scales are also observed. A well-known feature of solar wind plasma is that, when moving from large to small scales, distributions of fluctuation amplitudes become more non-Gaussian due to increasingly uneven spatial distribution of energy with decreasing scale. This phenomenon is called intermittency. While intermittency has been extensively studied in the solar wind, its properties within ICMEs remain unclear.

This presentation introduces a statistical study of intermittency within ICMEs observed by Parker Solar Probe and Solar Orbiter at varying heliospheric distances from the Sun. Employing structure functions with kurtosis as the main measure of intermittency, we study magnetic field fluctuations within ICMEs and their sheath regions, as well as in the upstream and downstream solar wind. Additionally, the analysis examines the connection between intermittency and heliospheric distance, cross-helicity, and residual energy.

Double-beta decay Q-value measurements with the JYFLTRAP Penning trap

J. Ruotsalainen¹ T. Eronen, A. Kankainen, M. Mougeot, E. Kauppinen

¹ Department of Physics, University of Jyväskylä, Jyväskylä, Finland

Corresponding author: jouni.k.a.ruotsalainen@jyu.fi

The observation of double beta decays and double-electron captures have become an important tool in the search for physics beyond the Standard Model (SM). In these rare decays, an isotope which energetically cannot undergo a single beta or electron capture decay, can decay via double decay to a more stable isobar. These decays can either emit two neutrinos (2ν) or no neutrinos (0ν). While several isotopes have been observed undergoing the 2ν double beta decay [1], allowed by the SM, the search for the neutrinoless decay mode is still ongoing. The neutrinoless decay mode requires the neutrino to be its own antiparticle (a Majorana particle), which would be a violation of the SM.

In the search for the neutrinoless double beta decay, the energy released in the decay (Q-value) needs to be known precisely. Firstly, the Q-value is used to calculate the half-life of the branch, indicating the feasibility of observing the decay in the isotope, as the half-lives are in the order of $\geq 10^{25}$ a [1]. Secondly, the Q-value is used to confirm the observation of the decay and a precise value is needed to separate the decay signal from noise [1].

In three recent measurements at the Ion Guide Isotope Separator On-Line (IGISOL) facility [2] in the University of Jyväskylä, the JYFLTRAP double Penning trap [3] was used to determine the $Q_{\beta\beta^-}$ of ^{104}Ru , ^{122}Sn , ^{142}Ce and ^{148}Nd , and Q_{EDEC} of ^{120}Te . In addition, the precisely known Q_{EDEC} of ^{102}Pd and ^{150}Nd , and $Q_{\beta\beta^-}$ of ^{124}Sn were re-measured. The Q-values were determined by measuring the mass difference of ions of the mother and daughter isotopes. A precision of ~ 100 eVs or better was reached for the Q-values. While most of our measurements are in agreement with their currently accepted values in the Atomic Mass Evaluation [4], the Q_{EDEC} of ^{120}Te was found to differ by 20 keV from the accepted value of 1735.6(18) keV. By using the microscopic interacting boson model (IBM-2) [5], half-lives will be calculated for the 0ν and 2ν decay modes for these isotopes. So far, half-lives have been calculated for the branches of ^{104}Ru . In this case, half-life of the 2ν decay mode was found to be short enough to be observed. In my contribution, I will present the JYFLTRAP measurement setup, the Phase Imaging Ion Cyclotron Resonance (PI-ICR) measurement technique [6] used to measure the Q-values and initial results of our measurements.

[1] M. J. Dolinski et. al, Annu. Rev. Nucl. Part. Sci. **69** 219 (2019)

[2] I. Moore et. al, Nucl. Instrum. Methods Phys. Res. B **317** 208 (2013)

[3] T. Eronen et. al, Eur. Phys. J. A. **48** 46 (2012)

[4] M. Wang et. al, Chinese Phys. C **45** 030003 (2021)

[5] F. Iachello and A. Arima, The Interacting Boson Model (1987), Cambridge University Press.

[6] S. Eliseev et. al, Phys. Rev. Lett. **110** 082501 (2013)

Peculiarities in scattering and extinction of dielectrically active particles

A. Sihvola¹, P. Ylä-Oijala¹, and H. Wallén¹

¹ Department of Electronics and Nanoengineering, Aalto University, Espoo, Finland

Corresponding author: ari.sihvola@aalto.fi

Wave scattering by spherical particles is a classical problem in electromagnetics and optics. The solution by L.V. Lorenz and G. Mie consisting of expansions on the harmonic wave components have been used numerous times during the past hundred years for analysis of wave phenomena, synthesis of scattering structures, and materials modeling. Despite the apparent simplicity of the forward problem (single-frequency electromagnetic wave hitting a spherical homogeneous structure with given dielectric and magnetic properties), the variety in the behavior of the scattering, absorption, and extinction properties forms a multi-dimensional domain with still unexplored parametric spaces.

In this talk, we will discuss our recent discoveries ([1]) and on-going studies on scattering by *active* dielectric spheres and other shapes. The object being active means that it is neither dissipative (lossy) nor lossless, thus having a negative absorption cross section. Among the interesting phenomena observed are enhancement in backscattering, unexpected resonances, and negative extinction.

[1] A. Sihvola, H. Wallén, P. Ylä-Oijala, and R. Parveen, J. Opt. Soc. Am., B, **40**, 194–205 (2023).

Statistical Study on Turbulent Energy Transfer in Coronal Mass Ejection Sheaths at 1 au

Juska Soljento, Simon Good, and Emilia Kilpua

Department of Physics, University of Helsinki

Corresponding author: juska.soljento@helsinki.fi

Turbulence is a fundamental process that transfers energy from large energy-injection scales to successively smaller scales through a cascade of eddies, until a scale is reached where energy is lost to particle heating. Coronal mass ejections (CMEs), which are spectacular eruptions of magnetic field and plasma from the Sun, can act as a local source of turbulence in the solar wind, injecting energy as they decelerate and expand in interplanetary space. The rate at which energy is being transferred by turbulence in plasmas can be quantified by using the Politano–Pouquet law [2].

Fast CMEs drive shock waves that compress the surrounding solar wind and accelerate particles to high speeds, causing them to stream far ahead of the shock. The region of compressed plasma between the shock and the CME ejecta is known as the sheath region. Recent case studies have applied the Politano–Pouquet law in CME-driven sheaths [1, 3]. Their findings suggest that the rate of turbulent energy transfer in sheaths is enhanced compared to the ejecta and the solar wind in general. We conduct a statistical study on a set of CME-driven sheaths observed by the Wind spacecraft at 1 au to investigate if this trend holds more generally.

- [1] R. Márquez Rodríguez, L. Sorriso-Valvo, and E. Yordanova (2023), “Turbulence, intermittency, and cross-scale energy transfer in an interplanetary coronal mass ejection,” *SoPh*, **298**, 54.
- [2] H. Politano and A. Pouquet (1998), “Dynamical length scales for turbulent magnetized flows,” *GeoRL*, **25**, 273-276.
- [3] L. Sorriso-Valvo, E. Yordanova, A. P. Dimmock, and D. Telloni (2021), “Turbulent cascade and energy transfer rate in a solar coronal mass ejection,” *ApJL*, **919**, L30.

Computational modelling of magnetic colloidal particle self-organization and pattern formation at multiple length scales

Emil Stråka^{1,2}, Max Holl^{1,2}, Alberto Scacchi^{1,2,3}, Mikko Haataja⁴, Jaakko Timonen^{2,3} and Maria Sammalkorpi^{1,2}

¹ Department of Chemistry and Materials Science, Aalto University, Finland

² Center of Excellence in Life Inspired Hybrid Materials (LIBER), Aalto University, Finland
<https://www.libercentre.fi/>

³ Department of Applied Physics, Aalto University, Finland

⁴ Department of Mechanical and Aerospace Engineering, Princeton University, USA

Corresponding author: emil.straka@aalto.fi

Magnetic colloidal particles (MCPs) refer to particles ranging in diameter from a few nanometers to several micrometers that can be manipulated with magnetic fields. The magnetic response and assembly of MCPs finds use in numerous advanced materials applications. We have examined MCP assembly and pattern formation in external magnetic field both on solid substrates, and in magnetic fluids where the MCPs are suspended in a suitable carrier fluid. Such fluids are known as ferrofluids. Here, we focus on our theoretical and computational approaches to gain insight into the behavior of MCPs in our experiments.

We focus on two different systems with different modelling description scales. In the first system, micron sized MCPs under an applied external magnetic field, show the formation of pillar-like assemblies with field and time-dependent retention response [1]. Via particle-based computational modelling approaches, we shed light to the memory and hysteresis effects and discuss the kinetic control with regards to total current able to pass through the sample. The modelling highlights the significant role of the surface roughness of MCPs in the observed jamming and memory effects, suggesting the potential for tunable magnetic remanence based on surface characteristics [1]. In the second system, we explore governing factors in guiding the instabilities and pattern formation at a diffuse interface between a ferrofluid and a non-magnetic fluid.. The modelled system connects with our prior experimental work on such diffuse, non-conventional ferrofluid interfaces [2,3]. Via analytical and semi-analytical methods, we study the linear stability of the interface and the onset of magnetic field-driven pattern formation.. Our results reveal that the onset of instability gets shifted towards higher magnetic fields and wavelengths as a function of the diffuse interface width. This in turn counteracts the effect of the vanishing effective interfacial tension often associated with such diffuse interfaces. Together, our computational and theory work on these MCP systems combined with our experimental characterization reveals guidelines for designing and controlling the patterns and understanding how they arise.

[1] X. Liu, H. Tan, E. Stråka, X. Hu, M. Chen, S. van Dijken, A. Scacchi, M. Sammalkorpi, O. Ikkala, B. Peng, Bioinspired trainable magnetic sensory responses using magnetic colloidal assemblies, submitted (2024).

[2] C. Rigoni, G. Beaune, B. Harnist, F. Sohrabi, and J. V. I. Timonen. Ferrofluidic aqueous two-phase system with ultralow interfacial tension and micro-pattern formation. *Communications Materials*, 3(1), 2022.

[3] T. Cherian, F. Sohrabi, C. Rigoni, O. Ikkala, J. V. I. Timonen. Electroferrofluids with nonequilibrium voltage-controlled magnetism, diffuse interfaces, and patterns. *Science Advances* 7(52):eabi8990 2021.

Coexistence of ergodic and non-ergodic behaviour in one-dimensional toy model of a flat-band superconductor

Koushik Swaminathan^{*1}, Meri Teeriaho², Ville-Vertti Linho² Sebastiano Peotta^{†1}

1. Department of Applied Physics, Aalto University School of Science

2. Department of Physics, University of Helsinki

We further analyse the Hamiltonian of the projected dice lattice [1] where the coexistence of ergodic and non-ergodic behaviour of quasiparticles was found to be a consequence of the presence of flat bands. We study the two body and three body interactions of this Hamiltonian on a 1D chain, and the effect of these interactions on transmission through the model. We investigate the level spacing statistics of this Hamiltonian and gauge the impact of the different types of interactions present within the system on the integrability of the model through the use of tuneable parameters. We determine the conditions for which the model shows integrable and chaotic behaviour.

References

[1] Koushik Swaminathan, Poula Tadros, and Sebastiano Peotta. **Phys. Rev. Research** 5, 043215 (2023)

[2] Koushik Swaminathan, Meri Teeriaho, Ville-Vertti Linho, and Sebastiano Peotta. *Article in Progress*

*Corresponding author: koushik.swaminathan@aalto.fi

†Corresponding author: sebastiano.peotta@aalto.fi

Evolution of structure functions at NLO without PDFs

T. Lappi^{1,2}, H. Mäntysaari^{1,2}, H. Paukkunen^{1,2}, and M. Tevio^{1,2}

¹ Department of Physics, University of Jyväskylä, Jyväskylä, Finland

²Helsinki Institute of Physics, University of Helsinki, Helsinki, Finland

Corresponding author: mirja.h.tevio@jyu.fi

The increasingly precise experimental data from LHC have led to global extractions of parton distribution functions with significantly improved accuracy. While there are ways to approximate some theoretical uncertainties like those arising from the choices of the factorization scale, alternative approaches to tame the remaining theoretical uncertainties may eventually be needed for precision phenomenology and searches for new physics. An option advocated here is to formulate the global analysis of QCD entirely in terms of Deep Inelastic Scattering (DIS) structure functions instead of PDFs. In this talk, we show how to write down the Q^2 dependence of DIS structure functions at NLO with three active quark flavours, what are the novel features with respect to the leading-order case discussed in Ref. [1], and how the independence of the factorization scale and scheme arises in practice. The steps towards the first PDF-free global analysis of QCD including LHC data are outlined.

[1] T. Lappi, H. Mäntysaari, H. Paukkunen, and M. Tevio, *Evolution of structure functions in momentum space*, *Eur. Phys. J. C* 84.1 (2024) [arXiv:2304.06998 [hep-ph]]

Ultra-fast photochemistry in the strong light-matter coupling regime

Arpan Dutta^{1,4}, Ville Tiainen¹, Luís Duarte³, Nemanja Markešević¹, Dmitry Morozov², Hassan A. Qureshi^{1,4}, Gerrit Groenhof², J. Jussi Toppari¹

¹*Nanoscience Center and Department of Physics, University of Jyväskylä, P.O. Box 35, Jyväskylä, 40014, Finland.*

²*Nanoscience Center and Department of Chemistry, University of Jyväskylä, P.O. Box 35, Jyväskylä, 40014, Finland.*

³*Present address: Department of Chemistry, University of Helsinki, P.O. Box 55, Helsinki, 00014, Finland.*

⁴*Present address: Department of Mechanical and Materials Engineering, University of Turku, Turku, 20014, Finland.*

Corresponding author: j.jussi.toppari@jyu.fi

Strong coupling between molecules and confined light modes of optical cavities forming polaritons can alter photochemistry, but the origin of this effect remains largely unknown [1]. While theoretical models suggest a suppression of photochemistry due to the formation of new polaritonic potential energy surfaces [2], many of these models do not account for the energetic disorder among the molecules, which is unavoidable at the ambient conditions [3,4]. Here, we combine experiments and simulations to show that for an ultra-fast photochemical proton transfer reaction of 10-hydroxybenzo[h]quinoline (HBQ) such thermal disorder prevents the modification of the potential energy surface and that suppression is due to radiative decay of the lossy cavity modes. We studied HBQ-doped low-Q all-metal Fabry-Pérot microcavities with identical geometry having differing HBQ concentration, and thus differing coupling strengths. We demonstrate that by increasing the coupling strength we can reduce the radiative losses and enhance reactivity of the strongly coupled system, in contrast to the theoretical paradigm, which would predict stronger suppression. We also show that the excitation spectrum under strong coupling is a product of the excitation spectrum of the "bare" molecules and the absorption spectrum of the molecule-cavity system, suggesting that polaritons can act as gateways for channeling an excitation into a molecule, which then reacts "normally". The extent of this excitation leak from polaritons to the bare molecules is determined by the spectral overlap between the bright polaritonic states and the molecular absorption. Our results therefore imply that strong coupling provides a means to tune the action spectrum of a molecule, rather than to change the reaction.

[1] Garcia-Vidal, F. J., Ciuti, C. Ebbesen, T. W. *Science*, **373**, eabd0336 (2021)

[2] J. Galego, et al., *Nat. Commun.* **7**, 13841 (2016).

[3] G. Groenhof, et al., *J. Phys. Chem. Lett.* **10**, 5476 (2019).

[4] Mony, J., Climent, C., Petersen, A. et al., *Adv. Funct. Mater.* Photoisomerization efficiency of a solar thermal fuel in the strong coupling regime. **31**, 2010737 (2021)

Poisoning of a thin-film ALD TiO₂ photocatalyst by thermal ion diffusion from microscopy glass substrate

Tuomas Tinus¹, Harri Ali-Löytty^{1,2}, and Mika Valden¹

¹Surface Science Laboratory, Tampere University, Tampere, Finland

²Liquid Sun Oy, Tampere, Finland

Corresponding author: tuomas.tinus@tuni.fi

Titanium dioxide (TiO₂) is a commonly used photocatalyst, with decades of high-quality research work to support further investigation of its properties. Since plain titanium dioxide only has moderate efficiency towards photocatalytic reactions of interest – water and carbon dioxide splitting, etc., owing to its large bandgap, decoration with nanoparticles has been recently utilized to enhance it. Noble metal nanoparticles (e.g. Ag, Au) absorb light through the phenomenon of surface plasmon resonance, transferring the energy to the catalyst and improving its activity [1]. Magnetic nanoparticles (e.g. FeOx) enhance the local fields. The heterojunction between nanoparticles and TiO₂ can improve separation of charges brought about by light absorption, improving activity through reducing recombination [2]. Understanding the interaction between photocatalyst and decorating nanoparticles as well as their synergistic properties is crucial to implementing such materials and ensuring maximum efficiency. Creating a model photocatalyst allows for isolating interactions of interest and approaching research into aforementioned properties in a systematic manner.

In this work, a light is shone on key aspects of creating a model photocatalyst material to enable research into interactions between decorating nanoparticles and supporting photocatalyst. Important considerations for a model catalyst – uniformity, reproducibility, repeatability – are addressed by utilizing a thin film deposition technique with unmatched control over thin film material properties, namely Atomic Layer Deposition (ALD). Impact of deposition parameters, such as deposition temperature, is discussed. Finally, ALD TiO₂ requires post-deposition annealing in order to produce the crystal structure with highest photocatalytic activity – which in turn can result in diffusion of ions from the underlying substrate and poisoning of the catalyst (Fig.1) [3]. Through this lens substrates are evaluated and based on the results an optimal model photocatalyst was selected for our research [4].

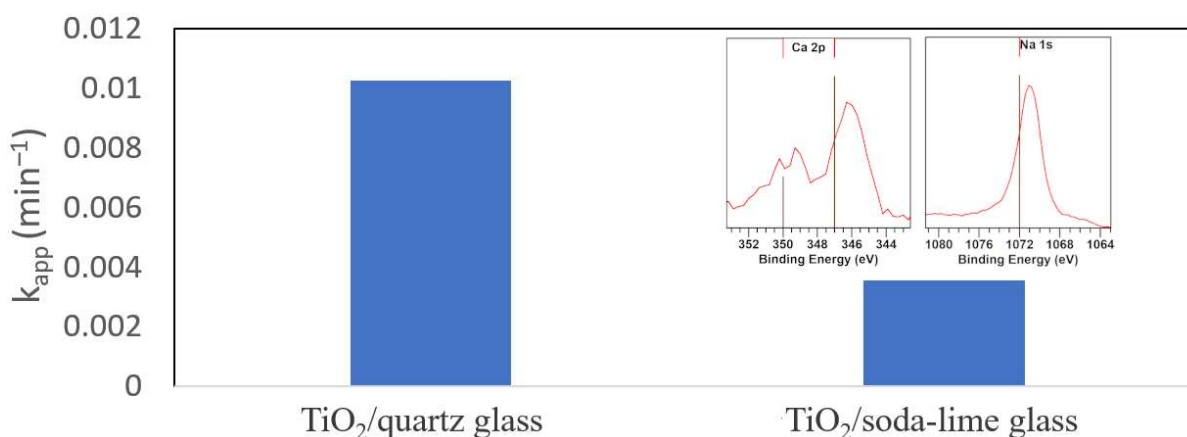


Fig. 1: Rate of photocatalytic degradation of methylene blue by ALD TiO₂ thin film photocatalyst on quartz glass and soda-lime glass substrates. Inset: XPS spectra of ALD TiO₂ on soda-lime glass following post-deposition annealing.

- [1] Bhuskute, B. D., et al. *Nanoscale Adv.* **4**, 4335–4343 (2022).
- [2] Hu, C. et al. *Angew. Chem. Int. Ed.* **60**, 16309–16328 (2021).
- [3] Paz, Y., Heller, A. *Journal of Materials Research* **12**, 2759–2766 (1997).
- [4] Sorvali, M.; Tinus, T.; Thamby, J.; Honkanen, M.; Ali-Löytty, H.; Charmforoushan, A.; Valden, M.; Saarinen, J.; Mäkelä, J. M. Pre-print <https://doi.org/10.2139/ssrn.4654514>.

Influence of an External Static Magnetic Field on the Dynamics of Vacuum Arc Initiation

Marzhan Toktaganova^{1,*}, Roni Koitermaa², Flyura Djurabekova¹, Andreas Kyritsakis², Tauno Tiirats² and Veronika Zadin²

¹*Department of Physics, University of Helsinki, Helsinki, Finland*

²*Institute of Technology, University of Tartu, Tartu, Estonia*

* Corresponding author: marzhan.toktaganova@helsinki.fi

The significance of the magnetic field in vacuum arcing has often been overlooked in various experimental and computational investigations, despite its relevance in numerous applications. Advanced technologies like muon colliders and vacuum interrupters in future accelerators generate substantial magnetic fields, which have the potential to impact the plasma initiation dynamics of vacuum arcing by focusing the initial electron beam. In this study, we employ concurrently coupled FEMOCS approach, integrating particle-in-cell, emission, and heating, to explore the impact of introducing an external magnetic field, oriented parallel and perpendicular to the electric field, on the heating characteristics of both the cathode and anode.

Scanning Droplet Adhesion Microscope for accurate surface characterization

Valtteri Turkki^{1,2}, Maja Vuckovac^{1,2}, Zoran Cenev^{1,2}, Jaakko V.I. Timonen^{1,2}, Robin H.A. Ras^{1,2}

¹ Department of Applied Physics, Aalto University, P.O. Box 15100, 02150 Espoo, Finland

² Center of Excellence in Life-Inspired Hybrid Materials (LIBER), Aalto University, P.O. Box 15100, 02150 Espoo, Finland

Corresponding author: valtteri.turkki@aalto.fi

Studying wetting of surfaces is important in many scientific and engineering applications, such as microfluidics or paint industry. Contact angle goniometry (CAG) is the gold standard method for studying wetting and it is by far the most used method. As surfaces and coatings improve, the optical limitations of CAG become an issue. This is especially true with superhydrophobic surfaces, where the errors of CAG are significant and comparing samples reliably becomes nearly impossible. [1] Thus, alternative methods that measure the interaction forces directly are needed.

Scanning Droplet Adhesion Microscope (SDAM) is an instrument design for measuring the wetting force and adhesion force, which are measured when the sample surface is brought in contact with the droplet probe and when the droplet probe is separated from the sample again, respectively. The SDAM droplet probe consists of a force sensor that has a hydrophilic disk on which a roughly $1.5 \mu\text{l}$ droplet is attached to, as seen in Figure 1. The scanning property of SDAM enables studying the sample with high spatial resolution and detecting defects. By measuring the wetting forces directly SDAM can surpass any other wetting characterization method in resolution.



Figure 1: SDAM droplet probe in contact with a superhydrophobic micropillar array surface.

However, measuring the most superhydrophobic surfaces is still a challenge as the wetting forces go below the commercial force sensor resolution of approx. 5 nN. [2] Here we introduce a cantilever-type force sensor that has optimized geometry so that it can hold a droplet of $15 \mu\text{N}$ and be robust while having an unmatched resolution down to 1 nN. [3] Furthermore, the manufacturing process of the cantilever allows for flexible probe design. Thus, with the new force sensor SDAM could be used to study topics like adhesion between two soft materials, such as tissues, by replacing the droplet with a tissue. This opens up many applications for SDAM beyond just wetting for which the instrument was originally developed and makes it a highly interesting tool for many branches of materials science research.

- [1] M. Vuckovac, M. Latikka, K. Liu, T. Huhtamäki, and R. H. Ras, “Uncertainties in contact angle goniometry,” *Soft Matter*, vol. 15, no. 35, pp. 7089–7096, 2019.
- [2] V. Liimatainen, M. Vuckovac, V. Jokinen, *et al.*, “Mapping microscale wetting variations on biological and synthetic water-repellent surfaces,” *Nature communications*, vol. 8, no. 1, p. 1798, 2017.
- [3] V. Turkki, “Force sensor design for scanning droplet adhesion microscope,” M.S. thesis, Aalto University School of Science, Espoo, Dec. 2023.

Nuclear lifetime analysis using the Advanced Plunger-Particle detector Array device (APPA plunger)

Eetu Uusikylä¹

¹ Department of Physics, University of Jyväskylä, Finland

Corresponding author: eetu.j.e.uusikyla@jyu.fi

Abstract

The APPA plunger (Advanced Plunger-Particle detector Array) is a new device designed for measuring the lifetimes of nuclear excited states in exotic nuclei close to the $N = Z$ line. It comprises a target foil and a degrader foil, facilitating the use of the Recoil Distance Doppler Shift (RDDS) method, based on the Doppler effect. A Doppler shift in the energy of a gamma ray occurs when it is emitted from a moving nucleus. This shift's magnitude is directly proportional to the velocity of the emitting nucleus and to the detection angle of the gamma ray. The degrader foil in the plunger is used to manipulate the recoil velocity. Consequently, the gamma-ray intensity is divided into two peaks corresponding to the shifted (emission after target) or degraded (emission after degrader) components. The intensity ratio of these peaks is dependent on the distance between the foils and the lifetime of the excited state under measurement. Typically, measurement is performed at different target-to-degrader distances ranging from few μm to 100's μm to minimize the systematic uncertainty in the lifetime analysis.

The APPA plunger was commissioned using the $^{40}\text{Ca} + ^{24}\text{Mg}$ reaction to measure the 2^+ state lifetime in ^{62}Zn , which is known from previous measurements. Following this validation of APPA, it was used to measure the 2^+ state lifetime in $N = Z$ nucleus ^{66}As . The lifetime of an excited state can be used to determine the $B(E2)$ value, which can be used to investigate nucleus's collectivity and deformation, namely, its deviation from a spherical shape. The goal of this research is to understand the systematics of the $B(E2; 2^+ \rightarrow 0^+)$ values along the $N = Z$ line in the mass $A = 60\text{--}80$ region. Although, several $B(E2; 2^+ \rightarrow 0^+)$ values have become available in this region over the past few years, the missing $B(E2; 2^+ \rightarrow 0^+)$ value for ^{66}As motivates this research.

Heat transport in a superconducting qubit-resonator chain with weak coupling to two thermal baths

Antti Vaaranta^{1,2}, Marco Cattaneo^{1,2}, Paolo Muratore-Ginanneschi^{1,2}, and Jukka Pekola²

¹ QTF Centre of Excellence, Department of Physics, University of Helsinki, P.O. Box 43, FI-00014 Helsinki, Finland

²QTF Centre of Excellence, Department of Applied Physics, School of Science, Aalto University, FI-00076 Aalto, Finland

Corresponding author: antti.vaaranta@helsinki.fi

Study of heat transport in superconducting devices is a rapidly growing field of research, aiming to shed light on the connection between quantum mechanics and thermodynamics [1, 2, 3, 4]. Here we study a superconducting quantum system comprised of capacitively coupled qubit-resonator chain with edges coupled to two resistors acting as thermal baths, as shown in figure 1. We derive a Hamiltonian of the circuit and from there obtain a master equation describing the open quantum system behaviour of the qubit-resonator chain. We study how the couplings within the system affect the overall dynamics and compare to each other the so-called local and global descriptions of the master equation. From the obtained master equations we can compute the steady state heat transfer through the qubit-resonator chain, when the baths are at different temperatures. It is shown that this kind of design can be made to act as a quantum heat valve, like in [1] by suitably choosing the inner system couplings. In the valve the heat flow through the system can be controlled by controlling the frequencies of the qubits and resonators.

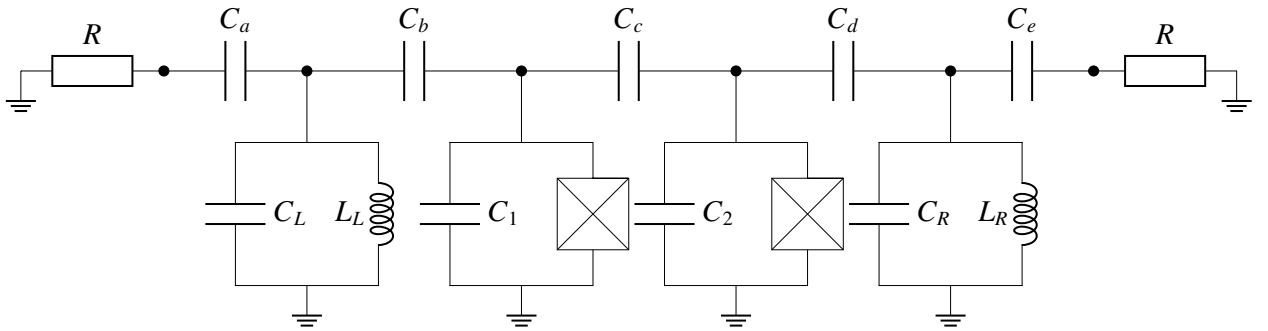


Figure 1: The superconducting qubit-resonator chain with coupling to two resistors at its edges, which act as thermal baths, introducing dissipation to the system.

- [1] A. Ronzani *et al.*, Nat. Phys. **10** 991-995, 2018
- [2] B. Karimi *et al.*, Quantum Sci. Technol. **2** 044007, (2017)
- [3] B. Karimi *et al.*, Phys. Rev. B **94** 184503, (2016)
- [4] C. D. Satrya *et al.*, J. Physics Commun. **7** 015005, (2023)

Challenges and opportunities of using cellulose substrates in photovoltaics

J. Valdez Garcia¹, J. J. Kaschuck², T. Abitbol³, K. Miettunen¹

¹ Solar Energy Materials and Systems, Department of Mechanical and Materials Engineering, University of Turku, Turku, Finland

² Physical Chemistry and Soft Matter group, Department of Agrotechnology and Food Sciences, Wageningen University & Research, Wageningen, Netherlands

³ Sustainable Materials Laboratory, Institute of Materials, Swiss Federal Institute of Technology in Lausanne (EPFL), Lausanne, Switzerland

Corresponding author: jvagar@utu.fi

Solar energy increasing importance necessitates the production of more and more devices. In the near future, their recycling will start drawing attention due to its inherent difficulty. Perovskite solar cells (PSCs) are fabricated on glass, and this makes the recovery of valuable materials difficult at the end of the device lifetime. One solution is to substitute glass with a flexible and burnable substrate. Nanocellulose has surged as a promising material to replace synthetic polymeric substrates such as PET and PEN. In contrast to these, cellulose is plant-sourced and has a lesser environmental impact than oil-based polymers [1]. Cellulose, while having a lot of potential, still has some challenges that need to be tackled. In this work we discuss the both the pros and cons of cellulose used as a substrate for solar cells, and how processing affects its properties [2].

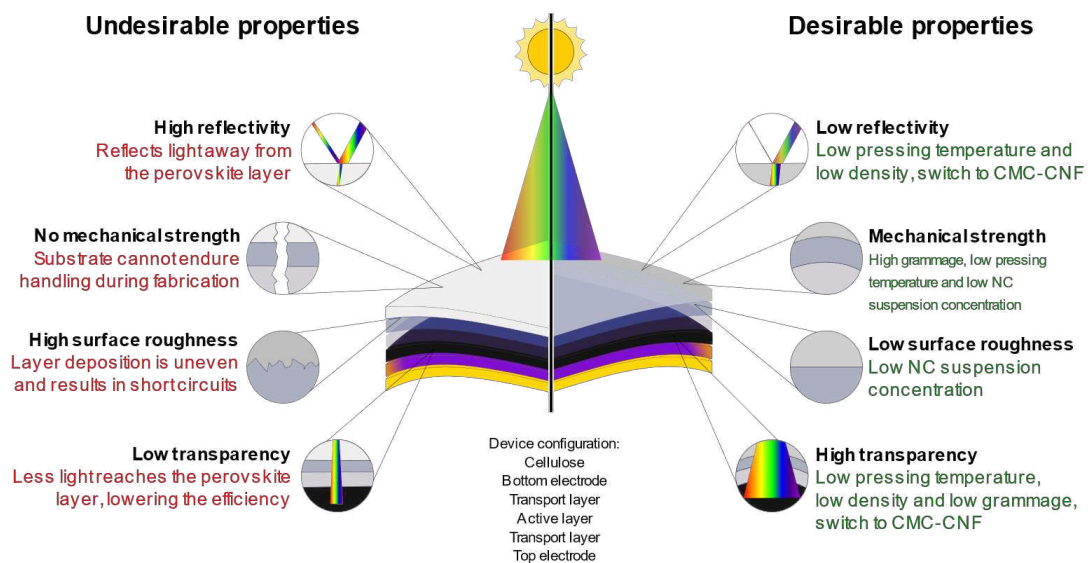


Figure 1 Diagram explaining showing different properties of cellulose as a substrate for PSCs and how they can be modified during processing. Nanocellulose (NC), Carboxymethylated cellulose (CMC), Cellulose nanofibrils (CNF)

[1] Bio-based materials for solar cells, K. Miettunen et al., *Wires Energy and Environment*, accepted waiting to be published, 2023

[2] Processing factors affecting roughness, optical and mechanical properties of nanocellulose films for optoelectronics, J. J. Kaschuck et al., *Carbohydrate Polymers*, accepted waiting to be published, 2024

CodeRefinery - supporting your research software development journey

Aurélie Vancraeyenest¹, Samantha Wittke¹, and Radovan Bast²

¹*CSC – IT Center for Science Ltd., P.O. Box 405 FI-02101 Espoo, Finland*

²*UiT The Arctic University of Norway, N-9037 Tromsø, Norway*

Corresponding author: aurelie.vancraeyenest@csc.fi

Reproducibility and openness are becoming of ever more crucial importance in any research ecosystem. In physics as in many other domains, research often relies on software written as a by-product, and it is an essential part of the research workflow. However, software is often overlooked from the reproducibility point of view. This can come from many reasons, like the focus being on research publications and data rather than software. It can also originate from researchers not being adequately prepared to write reusable and sustainable software. The CodeRefinery project (<https://coderefinery.org/>) aims at supporting researchers to write reproducible and sustainable research code no matter their domain or career stage.

Come and hear how the CodeRefinery workshops can help you get started with tools and practices that will enhance the reusability and sustainability of your software, such as version control, documenting and sharing code, modular code development, automating testing, etc. The workshops are held twice a year online, are free of charge and open to all researchers regardless of their field, background, or experience in developing software.

Finally, CodeRefinery is not just workshops, it also is a community of people that enjoy helping others write better code and use computing resources efficiently. The community is tightly knit to Nordic-RSE (<https://nordic-rse.org/>), an association of Research Software Engineers in the Nordics and Baltics. So, if you care about software and are curious to hear what Nordic-RSE and CodeRefinery are up to, come and talk to us.

Quantum Phase Transitions in Fermionic Chains with a Lee-Yang Method

Pascal M. Vecsei¹, Jose L. Lado¹, and Christian Flindt¹

¹*Department of Applied Physics, Aalto University, Konemiehentie 1, 02150 Espoo, Finland*

Corresponding author: pascal.vecsei@aalto.fi

Predicting the phase diagram of interacting quantum many-body systems is a central problem in condensed matter physics. A variety of quantum many-body systems, ranging from unconventional superconductors to spin liquids, exhibit complex competing phases whose theoretical description has been the focus of intense efforts. We have shown that neural network quantum states and matrix product states can be combined with a Lee-Yang method to investigate quantum phase transitions in spin systems and predict their critical points [1,2]. Here, we extend our method to fermionic chains[3], whose ground states we obtain using tensor networks. Specifically, we implement our approach for quantum phase transitions in a fermionic chain with dimerized hopping and nearest and next-to-nearest neighbor repulsion at different fillings to detect transitions into charge density wave ordered phases. We show that the Lee-Yang method combined with tensor networks allows predicting critical points of interacting fermionic systems. As such, our results provide a starting point for determining the phase diagram of more complex quantum many-body systems, potentially including frustrated Heisenberg models and two-dimensional Hubbard models.

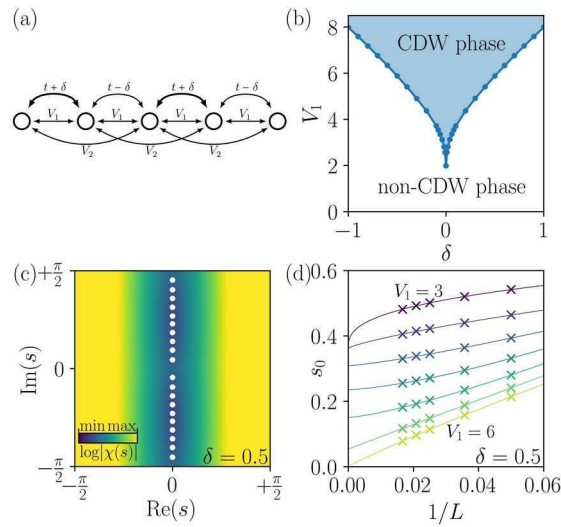


Fig. 1: Lee-Yang method for fermion chains: Panel (a) shows a sketch of the model we study, panel (b) depicts the location of the Lee-Yang zeros in the complex plane of the counting field s , the zeros are the white dots on the imaginary axis. Panel (d) depicts the scaling of the nearest Lee-Yang zero to the origin of the complex plane with system size, as function of the parameter V_1 . Panel (b) shows the resulting phase diagram.

- [1] Pascal M. Vecsei, J. L. Lado, C. Flindt, Phys. Rev. B **106**, 054402 (2022)
- [2] Pascal M. Vecsei, C. Flindt, J. L. Lado, Phys. Rev. Research **5**, 033116 (2023)
- [3] Pascal M. Vecsei, J. L. Lado, C. Flindt (in preparation)

Curiosity over the Lines – Open Data in Interdisciplinary Learning

Peitsa Veteli¹

¹ *Helsinki Institute of Physics, Helsinki, Finland*

Correspondence: peitsa.veteli@helsinki.fi

Our world is a dynamic collection of complex systems, interactions and uncertainties. For an observer with a well-developed scientific worldview, this can feel both daunting and beautiful, while students of all ages tend to struggle with the mental transition from iron-clad facts to understanding models and scientific thinking in general. Cognitively, our human minds tend to focus on individual topics. We attach previously attained skills in problem solving to examples of those topics, while rising above this novice state requires metacognitive competence to see beyond specific case contexts and into the larger structures of scientific reasoning underneath [1]. The educational challenge of fostering such competencies over subject lines is an important part of supporting the kind of scientific literacy for all espoused by, for example, the Finnish national secondary level curricula. This is compounded by the trend seen all over the traditionally developed countries, where younger students, in particular, gain some societal appreciation of natural sciences over their teenage years (“it is important and somebody should do it”), but simultaneously lose personal interest in pursuing related careers and deeper understanding of the nature of science [2].

How can we better encourage students to see the benefits of this mindset, where knowledge is not to be found in mere acquisition of facts but created through the process of striving for them?

The Education and Open Data –project at HIP proposes one avenue into that discourse through openly accessible materials from modern cutting-edge research institutions and authentic, meaningful programming integrated into everyday teaching. Our focus is primarily on using digital tools, such as computational essays [3], when needed in service of the wider topic being taught on any given lesson, rather than on the computer science itself. Since 2016, we have provided training, materials and hands-on help for in-service and upcoming secondary level teachers as well as their students willing to take the leap, both around Finland and at CERN. Beginning with particle physics, the project has since expanded into a broad variety of topics such as air quality, atmospheric radiation, aerosol production and climate change. A serendipitous mix of expert interactions from the research world (such as the CMS experiment, Hyytiälä SMEAR II station or ICOS collaboration), the contemporary nature of the questions asked and the open-ended, inquiring nature of working with real world data produce a learning experience that should combine multiple beneficial aspects of various educational approaches. This is supported by feedback gathered from hundreds of participants, with consistently high (>75%) student responses on learning more about the methods of science and willingness to use similar tools again in their studies. The contextual flexibility of open materials in education, as well as their high suitability as springboards for further discussions on the nature of data collection, presentation and veracity, open a crucially important opportunity for civic education beyond the subject-specific learning goals themselves [4,5].

- [1] Dockett, J. & Mestre, J. Synthesis of discipline-based education research in physics. *Phys. Rev. ST Phys. Educ. Res.* **10**, 020119 (2014).
- [2] Schriebl, D., Müller, A. & Robin, N. Modelling Authenticity in Science Education. *Sci & Educ* **32**, 1021–1048 (2023).
- [3] Odden, T. O., Silvia, D. W. & Malthe-Sørensen, A. Using computational essays to foster disciplinary epistemic agency in undergraduate science. *J. Res. Sci. Teaching* 1-41 (2022).
- [4] Vrtič, M. P. Teaching science & technology: components of scientific literacy and insight into the steps of research. *Int. J. Sci. Edu.*, **44:12**, 1916-1931 (2022).
- [5] Miller, E., Manz, E., Russ, R., Stroupe, D. & Berland, L. Addressing the epistemic elephant in the room: Epistemic agency and the next generation science standards. *J. Res. Sci. Teaching* 00: 1-23 (2018).

Modeling the fragmentation dynamics and valence photoelectron spectra of aminobenzoic acid

Onni Veteläinen¹, Minna Patanen¹, Matti Alatalo¹, and Sergio Díaz-Tendero²

¹ 1 NANOMO, University of Oulu, Oulu, Finland

² Departamento de Química, Universidad Autónoma de Madrid, Madrid, Spain

Corresponding author: onni.vetelainen@oulu.fi

Keywords: molecular dynamics, hydrogen migration, photoionization, theoretical spectroscopy

The fragmentation of dicationic aminobenzoic acid ($C_7H_7NO_2^{2+}$) has been investigated using extended Lagrangian molecular dynamics. The orto-, meta- and para-isomers were considered, including the two rotational isomers for the orto- and meta species. The Franck-Condon approximation was applied and an estimated excess internal energy was randomly distributed among the nuclear degrees of freedom at the beginning of each trajectory. This computational approach has been successful in studying hydrogen migration processes in the past [1]. A thousand trajectories were calculated for each isomer and internal energy estimate, and propagated for 250 fs. The formation of hydronium H_3O^+ as a fragmentation product following Auger decay of orto- and meta-aminobenzoic acid was experimentally observed in a previous study [2]. In particular, the rate of H_3O^+ production was much higher for the orto-isomer. The molecular dynamics provide a clear mechanism for hydronium production; a combination of hydrogen migration, neutral water emission and roaming, and a partial explanation for the production rate discrepancy between the two isomers. The specific excited states leading to the relevant fragmentation channels are investigated using the equation-of-motion coupled cluster method.

Adapting the computational scheme of [3], vibrationally resolved valence photoelectron spectra are calculated using the time-dependent adiabatic Hessian Frank-Condon method, with the ground and excited states optimised using density functional theory and time-dependent density functional theory, respectively. The (0-0) transition energies are fixed using vertical ionization potentials obtained from the GW approximation in many-body perturbation theory. Comparison of theoretical and experimental photoelectron spectra are hoped to provide insight into the relative abundancies of the rotational isomers.

- [1] Kling, N.G., Díaz-Tendero, S., Obaid, R. et al. Time-resolved molecular dynamics of single and double hydrogen migration in ethanol. *Nat Commun* **10**, 2813 (2019).
- [2] Abdul Rahman Abid, Onni Veteläinen, Nacer Boudjemia, Eetu Pelimanni, Antti Kivimäki, Matti Alatalo, Marko Huttula, Olle Björneholm, and Minna Patanen, Forming Bonds While Breaking Old Ones: Isomer-Dependent Formation of H_3O^+ from Aminobenzoic Acid During X-ray-Induced Fragmentation, *The Journal of Physical Chemistry A* **2022**, 127(6), 1395-1401.
- [3] Lukas Gallandi and Thomas Körzdörfer, Long-Range Corrected DFT Meets GW: Vibrationally Resolved Photoelectron Spectra from First Principles, *Journal of Chemical Theory and Computation* **2015**, 11(11), 5391-5400

Refractive index of Mercury analog particles from light scattering measurements

M. Vuori¹, A. Penttilä¹, and K. Muinonen¹

¹ Department of Physics, University of Helsinki, Helsinki, Finland

Corresponding author: mikko.vuori@helsinki.fi

Sample properties such as shape and size can be studied via light scattering, if the material complex refractive index is known. An inverse light scattering method for deriving the complex refractive index of a mm-sized single particle in a specific wavelength using laboratory measurements is presented. Laboratory measurements were done using the 4π scatterometer [1], which measures Mueller matrix elements of a particle suspended in air using acoustic levitation as a function of scattering angle. The measured samples were fragments of silicate glass, created as Mercury surface analogs by Carli et al. [2]. To obtain the complex refractive index of a glass sample, measurements were compared to simulations from a newly modified SIRIS4 Fixed Orientation (SIRIS4 FO) geometric optics code [3].

The 4π scatterometer is a unique instrument which measures the intensity of polarized light scattered from a particle using linear polarizers and a detector rotating around the particle on a rotational stage. Mueller matrix elements can be calculated for the particle from the polarization measurements. The scatterometer uses an acoustic levitator as a sample holder, which provides nondestructive measurements and full orientation control of the sample.

To compare the measurement results to simulations, the SIRIS4 single-particle geometric optics code was modified to handle particles in a fixed orientation. The modified SIRIS4 FO calculates the Mueller matrix elements over the full solid angle around the particle, as functions of the two angles, which give the direction of observation of the scattered wave compared to the direction of the incident wave. A 3D model of the shape of the measured particle was constructed using X-ray microtomography and was transported to SIRIS4 FO.

The complex refractive index was obtained with a nonlinear least squares analysis by minimizing the sum of squared residuals between the Mueller matrix elements from measurements and simulations with varying refractive index values. The obtained real part of the refractive index was $n = 1.59$ and the imaginary part $k = 2.05 \times 10^{-5}$. Previous values of the refractive index derived by the manufacturers of the glass support our findings.

[1] Helander et al., APL 116, 19 (2020)

[2] Carli et al., Icarus 266, 267 (2016)

[3] Vuori, Master's Thesis, University of Helsinki <https://helda.helsinki.fi/items/acd24b00-b8aa-4349-995c-ffe133c7a739> (2023)

Defect stabilization effect in fusion reactor plasma-facing materials

T. Vuoriheimo¹, A. Liski¹, P. Jalkanen¹, K. Mizohata¹, T. Ahlgren¹, K. Heinola², and J. Räisänen¹

¹*Accelerator laboratory, Department of Physics, University of Helsinki, Helsinki, Finland*

²*International Atomic Energy Agency IAEA, Vienna International Centre, Vienna, Austria*

Corresponding author: tomi.vuoriheimo@helsinki.fi

Hydrogen isotopes deuterium (D) and tritium (T) are used as fuel in future fusion reactors. The atoms are in ionized state, and they are magnetically confined within the vacuum vessel of the reactor. During operation of fusion reactors, energetic hydrogen plasma particles interact with the in-vessel components as ions and charge-exchange neutrals (CXN), and can damage the vessel first wall. These ions are either steered along the magnetic field lines to the divertor, or have escaped the magnetic confinement. Ions have energies ranging from a few electronvolts up to several keV during plasma edge-localized modes (ELMs) or other transient events. The energetic ions and CXNs cause defect formation in the first wall materials altering their properties. Vacancies, self-interstitials, and clusters of them formed in the material can function as trap sites for radioactive T. Understanding of defect formation is essential when considering new methods to reduce T retention and to understand the first wall materials behavior in the course of fusion reactor operation.

We investigated defect production and D trapping in tungsten (W) by implanting D ions into W with ELM-relevant energies: 100 eV and 5 keV that have been observed in JET [1] during inter-ELM and intra-ELM phases, respectively, and 100 eV and 20 keV that may take place in ITER [2] during ELMy operation. In this work, ion fluence was chosen based on JET data for a single ELM event [1]. D ions were implanted sequentially as follows: i) high-energy implantation followed by low energy, and ii) low-energy implantation followed by high energy. Also, samples with only one implantation energy were prepared as references. All samples were analyzed with Elastic Recoil Detection Analysis (ERDA) to observe trapped D depth profile within the first 400 nm from the sample surface.

Sequential implantations of high-energy – low-energy showed increased trapping compared to mono-energy implantations. This is due to trap production by the high energy ions, where the subsequent low-energy ions were easily retained. In the sequence of low-energy – high-energy implantation, trapping was also increased but assumedly by so-called defect stabilization effect. In defect stabilization effect, hydrogen isotopes present in the metal lattice increase irradiation damage formed by subsequent energetic ions. In our experiment, the increased retention was therefore due to the retained low-energy ions from the first implantation of the sequence. Defect stabilization has been studied previously by high energy self-irradiation of W [3,4] and is stated to happen by hindering movement of interstitial W atoms and therefore reducing Frenkel pair annihilation [5]. Our results show that defect stabilization is happening also with D ions only and can give new information for the defect stabilization effect that may need to be taken into account when calculating damage and lifetime estimates for nuclear reactor components. Defect stabilization effect may increase T retention in W more than single energy laboratory experiments suggest.

[1] Brezinsek S, Wiesen S, Harting D, et al., Phys. Scr. T167 (2016) 14076

[2] Guillemaut C, Jardin A, Horacek J, et al., Phys. Scr. T167 (2016) 14005

[3] Markelj S, Schwarz-Selinger T, et al., Nucl. Mater. Energy. 12 (2017) 169–174

[4] Schwarz-Selinger T, Bauer J, et al., Nucl. Mater. Energy. 17 (2018) 228–234

[5] M. Pečovnik M, Hodille E A, et al., Nucl. Fusion 60 (2020) 036024

Design and construction of a modular 3D scanner for semiconductor devices

M. Väänänen^{1,2}, M. Kalliokoski², R. Turpeinen², J. Aaltonen², P. Luukka¹, A. Karjalainen¹, A. Karadzhinova-Ferrer¹

¹ Department of Physics, LUT University, Lappeenranta, Finland

²Helsinki Institute of Physics, Helsinki, Finland

Corresponding author: mika.vaananen@lut.fi

We have designed and built a modular 3D scanner for analyzing semiconductor device samples using commercial off-the-shelf (COTS) components. Current commercial solutions offer great spatial resolution, but have limited sample holding capacity and can be prohibitively expensive. Our design includes a modular sample holder allowing scanning of samples from 1cm² through 13cm diameter full silicon wafers. We present proof-of-concept results of first scans done with the system.

The base of the scanner is a Genmitsu 4040 Pro desktop CNC milling machine, modified by replacing the spindle and tool holder with a sample holder and fixing a light source and a camera below and above the sample holder respectively. In the current version, the light source is an infrared LED, which allows us to scan silicon devices. The camera is held in place with a laboratory stand.

In upcoming versions, the light source will be a collimated LED panel. This will eliminate the effects of stray light, and enables changing out the whole light panel for using different wavelengths for different materials.

Flux Rope Extraction Scheme for Solar Magnetic Field Simulations

Andreas Wagner^{1,2}, Daniel Price¹, Emilia Kilpua¹, Slava Bourgeois^{3,4}, Jens Pomoell¹, Stefaan Poedts^{2,5}

¹*Space Physics Research Group, University of Helsinki, Helsinki, Finland*

²*Centre for mathematical Plasma-Astrophysics (CmPA), KU Leuven, Leuven, Belgium*

³*Instituto de Astrofísica e Ciências do Espaço, University of Coimbra, Coimbra, Portugal*

⁴*Solar Physics and Space Plasma Research Centre (SP2RC), University of Sheffield, Sheffield, United Kingdom*

⁵*Institute of Physics, University of Maria Curie-Skłodowska, Lublin, Poland*

Corresponding author: andreas.wagner@helsinki.fi

Analyzing the early-stage behavior of eruptive magnetic flux ropes in the solar corona may give us insights about its destabilization, leading to a solar eruption and its potential impacts at Earth. However, observations and measurements of the magnetic field topology in the lower solar corona are limited. For this reason, modelling the magnetic field in these regions of the solar atmosphere is crucial in understanding the physical evolution of these eruptions.

A subsequent challenge is to derive the magnetic field lines from the simulation data that pertain to the flux rope. Therefore, we develop a semi-automatic flux rope extraction and tracking scheme, which makes use of both common flux rope proxies (like the twist number) and mathematical morphology algorithms. Furthermore, this new method is wrapped into a user-friendly GUI called GUITAR (GUI for Tracking and Analyzing flux Ropes). Finally, we use GUITAR to extract and track the flux rope of a time-dependent data-driven magnetofrictional simulation [1] of active region AR12473 and analyze the early-stage properties and evolution of the resulting set of field lines.

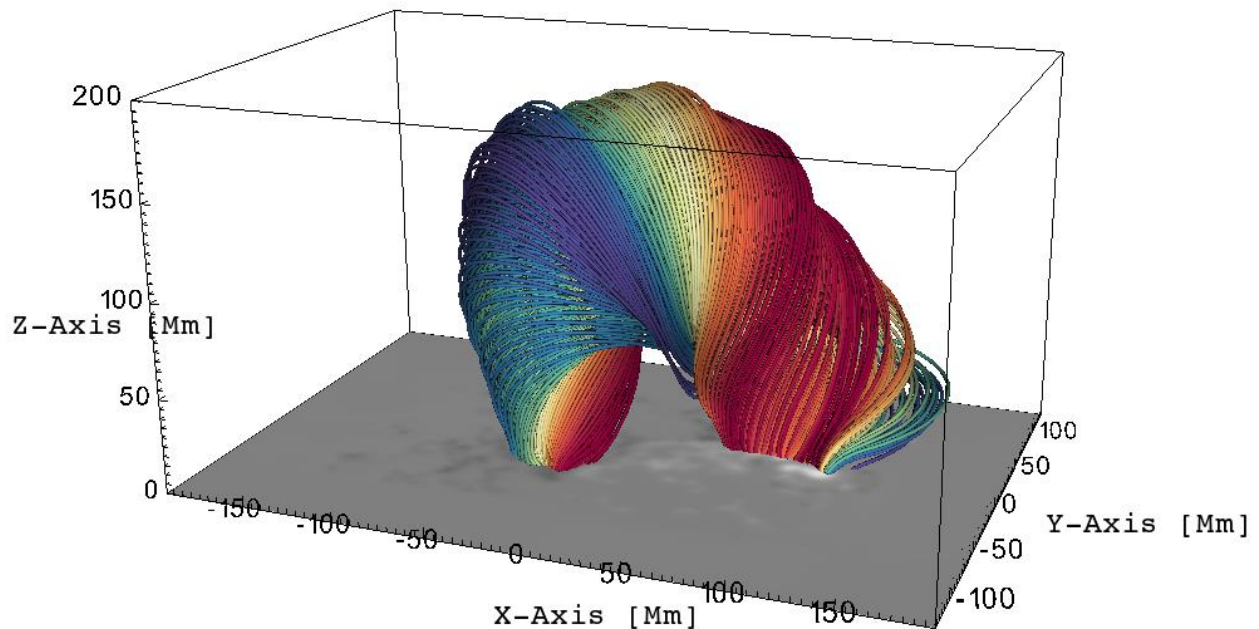


Fig. 1: Extracted Flux Rope of Modelling of Active Region AR12473 (adapted from [2]).

[1] J. Pomoell et al., *Sol. Phys.*, **294**, 41 (2019)

[2] A. Wagner et al., *A&A*, in production (2024)

Insights into the mechanism of nano Ni_3TeO_6 calcination via in situ synchrotron X-ray diffraction

Shubo Wang¹, Javier Fernández-Catalá^{1,2}, Qifeng Shu³, Marko Huttula¹, Wei Cao¹, Harishchandra Singh¹

¹Nano and Molecular Systems Research Unit, University of Oulu, FIN-90014, Oulu, Finland

²Materials Institute and Inorganic Chemistry Department, University of Alicante, Ap. 99, E-03080 Alicante, Spain

³Process Metallurgy Research Unit, University of Oulu, FI-90014 Oulu, Finland

Corresponding author: shubo.wang@oulu.fi; harishchandra.singh@oulu.fi

The versatility of metal tellurate chemistry enables the creation of unique structures with tailored properties, opening avenues for advancements in a wide range of applications [1]. Controllable nanoengineering of a Ni_3TeO_6 among all Ni tellurates with a broad variety of, like electric, magnetic, photocatalytic and multiferroic properties, relies on a thorough understanding of the synthesis process controlled by experimental parameters [2][3]. Common synthesis process of Ni_3TeO_6 involves mixing Ni source and Te source in a stoichiometric ratio (Ni : Te = 3:1) mechanically mainly in solid state approach or wet-chemically for sol-gel and hydrothermal approach, following by calcination [2-4].

In this work, we answered a question that *how nano-sized Ni_3TeO_6 forms from its complex hydrothermal precursors*. The work starts with exploration of the phase transitions during calcination of the hydrothermal precursors, and then complemented by post-mortem morphology characterization by TEM and chemical state determination by XPS, and thermal analysis. The obtained results provide a detailed *reaction sequence*, beginning with the dehydration and dehydroxylation of a stoichiometric Ni/Te oxyhydroxide coordinated by Te with a schematically pseudo formula of $(3\text{Ni}/\text{Te})(\text{OOH})_4\cdot\text{H}_2\text{O}$, and culminating in the preferred nucleation of trigonal Ni_3TeO_6 . Further calcination after full crystallization of Ni_3TeO_6 results in the formation of impurity phase (Fig. 1). These findings clarify the reactions occurring during calcination of Ni/Te mixed precursors, which have frequently been inferred from empirical and post-mortem reports but not confirmed via comprehensive and in situ guided explorations.

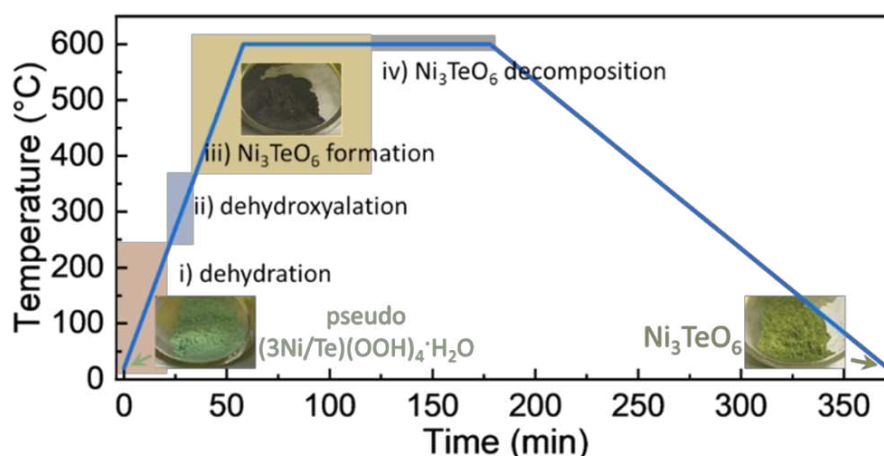


Fig. 1: Calcination of a hydrothermally mixed precursor to obtain Ni_3TeO_6 is a complex multistage process.

- [1] A. Yamuna, et al, J. Hazard. Mater. **435**, 128988 (2022).
- [2] J. Fernández-Catalá, et al, npj 2D Mater. Appl. **7**, 48 (2023).
- [3] J. Fernández-Catalá, et al, ACS Appl. Nano Mater. **6**, 4887 (2023).
- [4] L. Xu, et al, Mater. Lett. **184**, 1 (2016).

Effective Interactions and Density of States in Plasmonic Bose-Einstein Condensation

Pelin Yildirim^{*1}, Jani M. Taskinen^{1,2}, Päivi Törmä¹

¹ Department of Applied Physics, School of Science, Aalto University, Espoo, Finland

²VTT Technical Research Centre of Finland Ltd, Espoo, Finland

*Corresponding author: pelin.yildirim@aalto.fi

Bose-Einstein condensates (BEC) are typically formed by atomic gases cooled to ultracold temperatures to ensure that the particles are lowered to the ground state. One way to overcome the low temperature condition is to use metallic nanoparticle arrays that are coupled to dye molecules either in weak [1] or strong [2] coupling regimes. The electromagnetic modes called surface lattice resonances (SLRs) created in plasmonic lattices act as bosonic particles to form the condensate at room temperature. Strong coupling BEC experiences blue-shift in the condensate energy as an indicator of the effective interactions present in the lattice.

The objective of this work is to observe the effective interactions by monitoring the condensate energy of lattices with different density of states (DOS) values. The change in DOS is achieved by altering the nanoparticle geometry, namely by changing the length of the gold rectangular nanoparticle. Transmission experiments are conducted to calculate DOS of the array, and the condensation experiments are conducted to observe the condensate energy. The findings of the work indicate a positive relation between DOS and effective interactions in plasmonic BEC.

[1] Hakala, T.K., Moilanen, A.J., Väkeväinen, A.I. et al. Bose-Einstein condensation in a plasmonic lattice. *Nature Phys* **14**, 739-744 (2018). <https://doi.org/10.1038/s41567-018-0109-9>

[2] Väkeväinen, A.I., Moilanen, A.J., Nečada, M. et al. Sub-picosecond thermalization dynamics in condensation of strongly coupled lattice plasmons. *Nat Commun* **11**, 3139 (2020). <https://doi.org/10.1038/s41467-020-16906-1>

Quantum computing algorithm for an inverse travel time problem

J. Ilmavirta¹, M. Lassas², J. Lu², L. Oksanen², L. Ylinen³

¹ University of Jyväskylä, Finland

² University of Helsinki, Finland

³ Aalto University, Finland

Corresponding author: Lauri.Ylinen@aalto.fi

In the inverse travel time problem in seismic imaging one tries to reconstruct the interior structure of Earth from the travel times of seismic waves between different points on the surface of Earth. An analogous (in a mathematical sense) problem appears in medical imaging. The mathematical idealization of this problem is the so-called boundary rigidity problem studied in Riemannian geometry. Here we consider an inverse travel time problem on a graph, which is a discrete version of the above (continuous) inverse travel time problem. We consider the computational complexity of the problem and show that the discrete inverse problem is computationally intractable (a so-called NP-complete problem).

We also consider quantum algorithms for the discrete inverse travel time problem. Quantum computing is a technology that utilizes quantum mechanical phenomena to do computation faster than is believed to be possible with classical computers. It is a rapidly developing and interdisciplinary field comprising physics, computer science, and mathematics. It is predicted that in the future quantum computers will enable scientists to solve problems outside the capabilities of classical computers in many fields such as molecular simulations in drug discovery and complex combinatorics problems.

We present a quantum algorithm for the discrete inverse travel time problem which has a quadratic improvement in computational cost when compared with the standard classical algorithm.

This talk is based on the paper [1].

[1] J. Ilmavirta, M. Lassas, J. Lu, L. Oksanen, and L. Ylinen. “Quantum computing algorithms for inverse problems on graphs and an NP-complete inverse problem”, arXiv 2306.05253 (2023)

Dimuon production in neutrino-nucleus collisions - the SIDIS approach

I. Helenius^{1,2}, H. Paukkunen^{1,2}, and S. Yrjänheikki^{1,2}

¹ Department of Physics, University of Jyväskylä, Jyväskylä, Finland

²Helsinki Institute of Physics, University of Helsinki Helsinki, Finland

Corresponding author: sami.a.yrjanheikki@jyu.fi

We present a next-to-leading order perturbative QCD calculation of dimuon production in neutrino-nucleus collisions. This process is vital in the determination of the strange and anti-strange quark distributions in global PDF analyses. It is usually calculated by assuming factorization to the inclusive DIS charm production cross section, with a multiplicative acceptance correction to account for the energy cut on the outgoing muons and an effective semileptonic branching ratio of charmed hadrons. We instead compute this process directly using semi-inclusive DIS cross sections and charmed-hadron fragmentation functions. As a part of this calculation, we implement the decay of the charmed hadrons to a muon by utilizing available e^+e^- data. We compare our predictions with NuTeV and CCFR data using the EPPS21, nCTEQ15HQ, and nNNPDF3.0 nuclear PDF sets, assess the uncertainties in our approach, and estimate the impact of next-to-leading power NNLO corrections. We find our results to be in good agreement with the experimental data. Additionally, we compute effective multiplicative acceptance and nuclear modification corrections. Our results for the acceptance correction show some disagreement with values used in the literature. The nuclear correction factor has a significant uncertainty arising from the nuclear PDFs.

Focused ultrasound in combined magnetic resonance imaging and magnetoencephalography system

Koos Zevenhoven¹, Gösta Ehnholm¹, Emi Iizuka¹ and Risto J. Ilmoniemi¹

¹*Department of Neuroscience and Biomedical Engineering, Aalto University, Finland*

Corresponding author: koos.zevenhoven@aalto.fi

In magnetoencephalography (MEG), the electric currents due to neuronal activity in the brain are measured via extremely sensitive magnetic field measurements around the head. The reconstruction of source location is usually done with the help of magnetic resonance imaging (MRI), which produces structural images based on signals arising from nuclear spins due to applied magnetic fields. At Aalto University, we have built the first full-scale imaging system capable of both MEG and MRI in the same device [1]. The MRI implementation is unconventional, measured in an ultra-low magnetic field in the microtesla range, allowing the same superconducting quantum interference devices (SQUIDs) to be used for detecting both MEG and MRI. In addition to detection, we use superconductivity in a pulsed polarizing magnet that polarizes the spins before measurement.

Further combining the imaging of brain activity with brain stimulation creates new opportunities for brain research and medical applications. Applying low-intensity focused ultrasound to stimulate or modulate brain activity has recently received increasing interest because of observed excitatory and inhibitory effects in animals and humans [2]. However, focusing ultrasound in the brain without opening up the skull poses a challenge because of aberration of the ultrasonic waves by the skull. Therefore, the method greatly benefits both from imaging the shape of the skull and of detecting the ultrasound focus itself, both of which can be done with MRI. Another challenge, however, is posed by the compatibility of the ultrasound system with the sensitive imaging device.

In this work, we combine our MEG-MRI system with focused ultrasound and a setup for imaging the location of the ultrasound focus using SQUID-detected MRI. A piezo-based ultrasound transducer was attached to a lens to achieve a focus inside an adjacent cylindrical agarose gel sample. The sample and transducer are positioned inside the imaging volume. The ultrasound setup was carefully designed to minimize electromagnetic disturbances that could harm the sensitive SQUID measurement. For detecting the ultrasound focus via MRI, we apply a novel technique with a localized gradient coil made by winding 1-mm copper wire onto a frame 3D-printed from ASA plastic.

We describe our combination device and present the first results regarding the effect of the ultrasound setup on the SQUID measurement noise as well as the detection of the ultrasound focus via MRI. This work is expected to serve as a basis for future human MEG measurements of the effects of ultrasound stimulation and to pave the way for advanced brain research and medical applications.

[1] K. Zevenhoven, “Unconventional MRI scanner technology and intelligent dynamics” doctoral thesis, Aalto University (2023).

[2] G. Darmani et al., *Clinical Neurophysiology* 135, 51 (2022).

Machine Learning Optimization of Thermally Activated Nylon Actuator Coils

Yuhao Zhang¹, Maija Vaara², Azin Alesafar², Bach Ngyen², Matthias Stosiek¹, Joakim Löfgren¹,
Jaana Vapaavuori², Patrick Rinke¹

1: Department of Applied Physics, Aalto University, Espoo, Finland

2: Department of Chemistry and Materials Science, Aalto University, Espoo, Finland

Yuhao Zhang: yuhao.zhang@aalto.fi

As smart textiles thermally activated polymers offer higher strain at lower cost compared to other actuation mechanisms for shape memory polymers (SMPs) [1]. The optimization of thermal SMP actuation in terms of processing conditions is aggravated by the fact that traditional design of experimental methods struggle with high dimensional optimization spaces while conventional machine learning-based optimization approaches suffer from a lack of sufficient experimental data. To overcome these problems, we apply an active learning approach using Bayesian optimization [2].

We focus on nylon SMPs with the objective to maximise actuation in terms of the three design variables consisting of number of plies, twisting and coiling weights used for producing the coils prior to curing. Since the experimental parameters are all discrete and not continuous as in conventional Bayesian optimization, we developed a discrete Bayesian optimization approach in our Bayesian Optimization Structure Search (BOSS) code [3]. In this presentation, I will illustrate the BOSS active learning workflow, which is also depicted in Figure 1. BOSS fits a surrogate model (here a Gaussian process) to the available nylon SMP data. With the exploration lower confidence bounds (ELCB) acquisition function, we then determine from this surrogate model and its uncertainty where to best acquire new data. At those conditions, a new nylon coil is prepared and tested. The experimental data is fed back into the data pool and a new surrogate model is fitted. The process continues iteratively, until maximal actuation is found.

After sampling 33 data points, we achieve a maximal actuation strain of 1.066. The corresponding design variables are 1 ply with a twisting and coiling weight of 1288g. Inspection of the surrogate model reveals that actuation strain correlates most strongly with number of plies followed by twisting and coiling weight. Future work will focus on optimizing other polymer types with transfer learning.

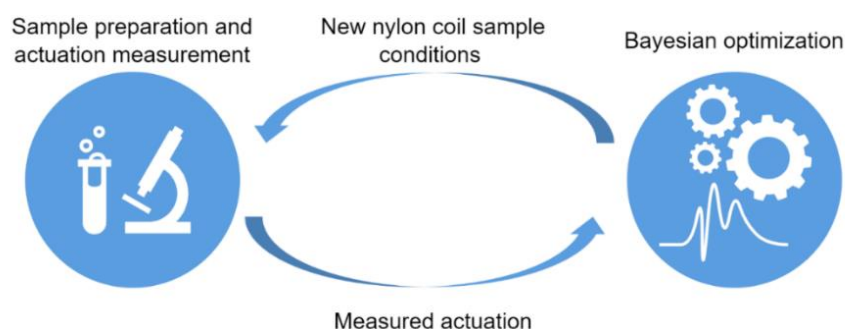


Fig. 1: Active learning workflow loop for thermal actuation optimization of nylon coils. 4 Samples are generated and fed back into the model at each iteration.

- [1] Kongahage, D. & Foroughi, J. Actuator materials: Review on recent advances and future outlook for smart textiles. *Fibers* **7**, 21 (2019). DOI: 10.3390/fib7030021
- [2] Löfgren J, Tarasov D, Koitto T, Rinke, P Balakshin M, Todorović. Machine Learning Optimization of Lignin Properties in Green Biorefineries. *ACS Sustainable Chemistry & Engineering*. **10**, 29, (2022). DOI: 10.1021/acssuschemeng.2c01895
- [3] Todorović, M., Gutmann, M.U., Corander, J. *et al.* Bayesian inference of atomistic structure in functional materials. *npj Comput Mater* **5**, 35 (2019). <https://doi.org/10.1038/s41524-019-0175-2>

Vacancy defects in Si doped β -(Al,Ga)₂O₃

Iuliia Zhelezova^{1*}, Ilja Makkonen¹, Zbigniew Galazka², and Filip Tuomisto¹

¹*Department of Physics and Helsinki Institute of Physics, University of Helsinki, Finland*

²*Leibniz-Institut für Kristallzüchtung, Berlin, Germany*

*email: iuliia.zhelezova@helsinki.fi

While n-type doping is routinely achieved for β -Ga₂O₃, it is not a straightforward question for its wider band gap alloys. Cation vacancies are archetypical compensating defects for n-type dopants in compound semiconductors. In this work, we study their formation in Si-doped single crystals of β -(Al,Ga)₂O₃ [1] with positron annihilation spectroscopy [2]. We present results obtained in 8 different (16 pieces) Czochralski-grown β -(Al,Ga)₂O₃ single crystals with Al content 0, 10, 20, and 25%, in both undoped and n-type doped form [1]. The unintentional Si content in the undoped crystals is $2\text{-}3 \times 10^{17} \text{ cm}^{-3}$, and in the doped crystals, the Si content is $3\text{-}6 \times 10^{18} \text{ cm}^{-3}$ as measured by SIMS. Hall measurements show that the undoped crystals are n-type for all Al mole fractions with the carrier concentration roughly matching the unintentional Si content, but in the Si doped crystals the doping efficiency is reduced at higher Al content, and the doped 25% alloy is electrically insulating [2].

We present results obtained with both room-temperature 3D Doppler broadening spectroscopy [3] and temperature-dependent positron lifetime spectroscopy. The undoped samples show the unusually high anisotropy observed in β -Ga₂O₃ for all Al contents (Fig. 1). In contrast, the Si doped samples exhibit significantly smaller anisotropy irrespective of the Al content. There is a similar clear distinction between the two groups of samples (undoped vs. Si-doped) seen in Fig. 2 that shows the average positron lifetime in the temperature range 40-600 K. The positron lifetime is significantly longer (190-220 ps) in the Si doped samples than in the undoped samples. In the undoped samples, the positron lifetimes are in the same range (170-195 ps) with those obtained earlier in Sn doped, Fe doped, and Mg doped crystals [4]. Importantly, there is no difference between the Si doped samples with Al content 10-25 %. The presence of Al in the crystals causes the emergence of negatively charged defects with no or very little open volume as seen at the low temperature range in the data.

The results indicate that Si doping generates unrelaxed Ga vacancy related defects in all the samples, as opposed to the split Ga vacancies that typically dominate the positron annihilation signals in β -Ga₂O₃ [3-5]. However, these unrelaxed Ga vacancies do not appear to be the key to understanding to the sudden strong passivation of the Si dopants at higher Al content, as there appear to be no significant differences between the Si doped samples across the Al content range in our experiments. Similarly, the negative ion-like defects are also independent of the Al content. Further work is required to resolve this issue.

[1] Z. Galazka, et al., J. Appl. Phys. 133, 035702 (2023).

[2] F. Tuomisto, I. Makkonen, Rev. Mod. Phys. 85, 1583 (2013).

[3] A. Karjalainen, et al., Phys. Rev. B. 102, 195207 (2020).

[4] A. Karjalainen, et al., Appl. Phys. Lett. 118, 072104 (2021).

[5] A. Karjalainen, et al., J. Appl. Phys. 129, 165702 (2021).

Two-dimensional noble gas clusters in a graphene sandwich

Manuel Längle¹, Kenichiro Mizohata², Clemens Mangler¹, Alberto Trentino¹, Kimmo Mustonen¹, E. Harriet Åhlgren^{1,2}, Jani Kotakoski²

¹Physics of Nanostructured Materials, *University of Vienna, Vienna, Austria*

²Accelerator Laboratory, *University of Helsinki, Helsinki, Finland*

Corresponding author: harriet.ahlgren@helsinki.fi

Two-dimensional materials offer an intriguing solid state frame for controlled nanostructures. Here, we use two graphene sheets as a platform for encapsulation. The atomically thin carbon layers support the formation of two-dimensional solid state structures in the van der Waals gap at room temperature. Moreover, the frame also allows their direct observation via high resolution transmission electron microscopy.

We present results on Kr and Xe clusters in between two suspended graphene layers, and uncover their atomic structure [1]. We show that small crystals ($N < 9$) arrange on the basis of the simple non-directional van der Waals interaction. Larger crystals show some deviations, possibly enabled by defects in the encapsulating frame. We further discuss the dynamics of the clusters within the graphene sandwich by performing extensive molecular dynamics simulations. Depending on the size of the cluster, we also observe occasional fluid clusters under the pressure of approx 0.3 GPa.

Our results open a way for the so-far unexplored frontier of encapsulated two-dimensional van der Waals solids with exciting possibilities for fundamental condensed-matter physics research and possible applications in quantum information technology.

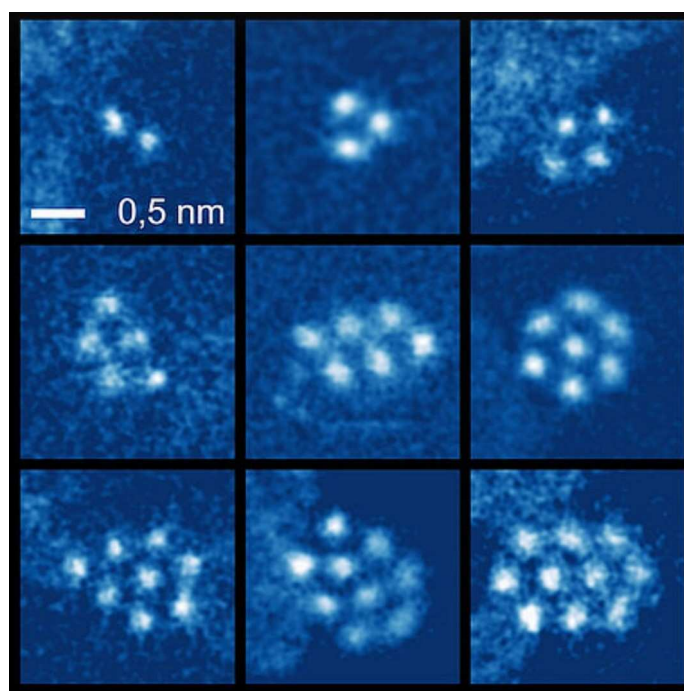


Fig. 1: Solid two-dimensional xenon nanoclusters imaged by scanning transmission electron microscopy. The clusters are confined between two graphene sheets (filtered out of the image) and vary from two atoms (top left) to ten atoms (bottom right) in size.

[1] Längle, M., Mizohata, K., Mangler, C., Trentino, A., Mustonen, K., Åhlgren, H., Kotakoski, J., Two-dimensional few-atom noble gas clusters in a graphene sandwich. *Nature Materials*, 2024.

Latest results on multiplicity-dependent flow, testing the lower limit of flow in small systems with ALICE

Anna Önnerstad on behalf of ALICE¹

¹*University of Jyväskylä, Helsinki, Finland*

Corresponding author: anna.b.s.onnerstad@jyu.fi

It is known that in ultrarelativistic heavy-ion collisions, such as Pb–Pb at the LHC, long-range correlations are a collective flow effect of the quark-gluon plasma. However, similar effects have also been observed in smaller collision systems, e.g. p–Pb and pp. The origin of these long-range correlations in small systems and whether it is the same as in large collision systems still need to be understood. The non-flow effects, such as jets, get larger in small systems, making the flow measurements more difficult. Therefore, it is important to examine the methods where the non-flow effects are properly subtracted.

This talk will present the results from long-range correlations of charged particle pairs with two-particle angular correlations in pp and p–Pb collisions. The results will include the extracted flow amplitudes using the low-multiplicity template fit method, which allows for the subtraction of the enhanced away-side jet yields. These results set a lower limit of event multiplicity on the flow signal. Additionally, we will present a comparison of our results to viscous hydrodynamical models.